Department for Nanobiotechnology
Institute for Biological Inspired Material
University for Natural Resources and life science, Vienna

MASTER THESIS

OPTIMIZATIONS OF THE SOLID PHASE SUBMONOMER SYNTHESIS OF AMPHIPHILIC POLYPEPTOID HELICES

For the award of the academic degree
Dipl. Ing.

Practical work: 03.09.2018 – 06.03.2019

Author
Paul Erik Gailit, B.Sc.
Matriculation Number
01241643

First Supervisor:
Univ.-Prof. Dr. Phil. Tekn. Lic. Civ. Ing. Erik Reimhult, BBA, MSc

Co-Supervisor:
DI Ronald Zirbs

Vienna, Feburary 2020

Suggestions for affidavits

I hereby declare that I am the sole author of this work; no assistance other than that permitted has been used and all quotes and concepts taken from unpublished sources, published literature or the internet in wording or in basic content have been identified by footnotes or with precise source citations.

- Paul Erik Gailit

Acknowledgement

First, I want to thank my supervisor Prof. Erik Reimhult for offering me the opportunity to fulfill my practical work for the thesis in his group. With a personal office space and an own lab-bench, it was very easy to focus on the work. Secondly, I want to thank DI Ronald Zirbs for the continuous help during the practical and theoretical work. Thank you for all the input and the chemical knowledge which expedited the jobs in the lab but also with the improvements in my writing skills. My work in the lab would not been as flawless without Martina Schroffenegger, who patiently answered every question with her best knowledge and conscience and offered her help without hesitation in every situation. Of course, thank you Max Willinger for recommending me to work in this wonderful group at the Department for Nanobiotechnology the great atmosphere in the lab.

Index

1. Abstract

Antibiotic resistance is an important topic since the golden era of antibiotics in 1940. Increasing cases of mortality are recorded due to the ineffectiveness of antibiotics against multiresistant bacteria. The problem of bacteria adapting to organic active substances and thereby counteracting antibiotics is on the rise. The innate immune system of many organisms has successfully combatted bacterial infections for hundreds of millions of years. A significant part of the innate immune system of many organisms are membrane-active antimicrobial peptides. The amphiphilic polypeptide melittin, the main component of bee venom, which is known to form pores in eukaryotic cell membranes, can be taken as a model also for the action of antimicrobial peptides. This peptide can be imitated by a peptoid. Polypeptoids are polymers consisting of N-substituted glycine units with the ability to form secondary structures. These internally ordered structures are proven to be more thermally stable in comparison to polypeptides and, most importantly, resistant to proteolytic degradation by microorganisms. A polypeptoid analog specifically designed to attack prokaryotic cells could provide a prototype of a new class of antibiotics, against which microorganisms cannot develop antibiotic resistance. We showed that it is possible to synthesize polypeptoids with alternating hydrophobic and hydrophilic monomers in sufficient yields via solid-phase submonomer synthesis. MALDI-TOF-MS data proved that with step-by-step solid-phase synthesis, tetramers of alternated R-α-methylbenzylamine and 4-bromo-R-α-methylbenzylamine respectively were created. The synthesis itself was optimized to balance incubation time, concentration and product yield. Based on that, modifications of the hydrophobic and hydrophilic groups can be conducted to increase the difference in polarity of the sidechains within the molecule. The possibility to form amphiphilic polypeptoids allows further experiments on the synthesis of longer helical polypeptoids and the effect of such polypeptoids on microorganisms. The aim is to design a new class of antibiotics that is minimally prone to developing antibiotic resistance.

Antibiotikum Resistenz ist ein wichtiges Thema seit der goldenen Ära der Antibiotika 1940. Immer mehr Todesfälle werden verzeichnet, bei denen jegliche Art von Antibiotika wirkungslos bei betroffenen Patienten sind. Das Problem, dass Bakterien sich immer neu an alle Arten von Wirkstoffen anpassen und diese effektiv bekämpfen wird immer prominenter. Das angeborene Immunsystem neutralisiert seit Jahrmillionen erfolgreich unerwünschte bakterielle Eindringlinge. Eine Klasse des angeborenen Immunsystems vieler Organismen sind membranaktive antimikrobielle Proteine. Das amphiphile Polypeptid Melittin, die Hauptkomponente des Bienengifts, ist bekannt dafür, Poren in eukaryotische Zellmembranen zu bilden. Der Wirkungsmechanismus kann auch für antimikrobielle Peptide als Model herangezogen werden. Dieses Peptid könnte von einem Peptoid imitiert werden. Polypeptoide bestehen aus N-substituierten Glycin Einheiten, welche ebenfalls Sekundärstrukturen ausbilden können. Diese Strukturen weisen höhere Thermostabilitäten gegenüber Peptiden und eine Resistenz gegen mikrobiellen Abbau auf. Ein analoges Polypeptoid welches speziell konstruiert wird Lyse bei Prokaryonten herbeizuführen würde eine neue Klasse an Antibiotika hervorbringen, wogegen Mikroorganismen womöglich keine Resistenzen ausbilden können. Wir haben gezeigt, dass es möglich ist mit Submonomer Festphasen Synthese, Polypeptoide mit abwechselnd hydrophoben und hydrophilen Monomeren zu synthetisieren. MALDI-TOF-MS Analysen beweisen, dass mittels step-by-step Festphasen Synthese Tetramere von abwechselnd R-α-Methylbenzylamine und 4-Bromo-R-α-Methylbenzylamine hergestellt wurden. Weiters wurde die Synthese optimiert und eine Balance zwischen Inkubationszeit, Konzentration, und Ausbeute gefunden. Auf dieser Grundlage können Modifikationen der hydrophilen- und der hydrophoben Gruppen durchgeführt werden, um den Unterschied der Polarität der Seitengruppen innerhalb des Moleküls zu erhöhen. Die Möglichkeit amphiphile Polypeptoide herstellen zu können, erlaubt weitere Experimente, wie die Synthese längerer, helikale Polypeptoide und die Auswirkungen auf Mikroorganismen. Das Ziel ist es, eine neue Klasse an Antibiotika zu formulieren, welche nicht der Gefahr der Antibiotikum Resistenz zum Opfer fällt.

ABBREVIATIONS

^{1}H-NMR	Nuclear magnetic resonance spectroscopy
2-CTC	2-chlorotrityl chloride
aa	Amino acid
ACN	Acetonitrile
ACH	α-cyano-4-hydroxycinnamic acid
AmR_{mba}	4-amino-R-α-methylbenzylamine
ATT	6-aza-2-thiothymine
AzR_{mba}	4-azido-R-α-methylbenzylamine
BrHAc	2-bromoacetic acid
BrR_{mba}	4-bromo-R-α-methylbenzylamine
$CDCl_3$	Deuterium chloroform
Cl_3CH	Chloroform
CuBr	Copper bromide
D_2O	Deuterium oxide
DCM	Dichloromethane
DHB	2,5-dihydroxybenzoic acid
DEE	Diethyl ether
DIC	N,N'-diisopropylcarbodiimide
DIPE	Diisopropyl ether
DIPEA	N,N-diisopropylethylamine
DMF	N,N-dimethylformamide
EtOH	Ethanol

Fmoc	fluorenylmethyloxycarbonyl protecting group
HFIP	1,1,1,3,3,3 - hexafluoro-2-propanol
HPLC	High performance liquid chromatography
MALDI-TOF-MS	Matrix Assisted Laser Desorption Ionization - Time of Flight - Mass Spectrometry
MeOH	Methanol
NaN_3	Sodium azide
NaHAc	Sodium acetate
$NaSO_4$	Sodium sulfate
R_{mba}	R-α-methylbenzylamine
S_N^2	Nucleophilic substitution type II
TLC	Thin layer chromatography

2. Introduction

2.1. Antibiotics & resistance

With the discovery of Penicillin in 1928[1], humanity announced the fight against bacteria and its derived diseases. Humans thought they had a perfect treatment against deadly infections over the following years. Soon they learned that prokaryotes adapt and gain resistance against antibiotics during the golden age of antibiotics.[2] Since then, different kinds of strategies have been developed to attack bacteria. However, the targeted organisms continue to evolve to survive the drugs they are treated with. Due to irresponsible abuse of antibiotics over the last decades, more and more examples of bacteria developing multi-resistance against every known antibiotic on the market appear. [3] New ways must be found for treating bacteria effectively without cultivating multi-resistant germs. The innate immune system of many organisms consists of various ways to attack prokaryotic intruders. One of those ways are membrane active peptides which incorporate into cell-membranes and induce lysis of the victim. Models for these kinds of active ingredients already exist in nature.

2.2. Melittin, a model for cell-lysing compounds

A prominent cell-lysing peptide is melittin, a 26 amino acid long helical oligopeptide, the main component of bee venom.[4] A specialty of this molecule is its amphiphilic nature, which means that the peptide consists of a hydrophobic and a hydrophilic area.

| (A1) | (A2) | (B1) | (B2) | (C1) | (C2) |
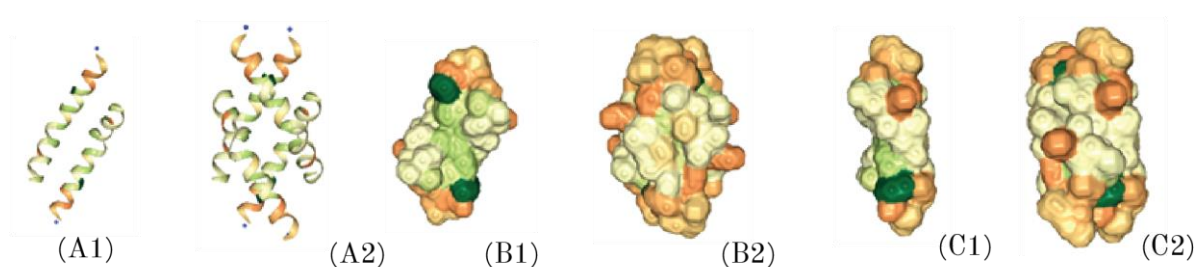
Fig. 1: Melittin displayed as: (A1) ribbon structure asymmetric unit, (A2) ribbon structure bio assembly, (B1) surface map asymmetric unit, (B2) surface map bioassembly, (C1) surface map asymmetric unit 90° angle, (B2) surface map bioassembly 90° angle. Green: Hydrophobic; Yellow: Hydrophilic | Pictures taken from PDB "2mlt"

In nature proteins occur in bio assemblies which consist of asymmetric units.[5] In the case of Melittin, two asymmetric units form the bio assembly. Fig. 1 (A1 – C2) depicts the hydrophobicity map of the peptide melittin. Green parts display hydrophobic regions,

yellow & orange parts display hydrophilic regions while Fig. 1 (A1) shows the asymmetric unit (consisting of two helices) and Fig. 1 (A2) the bio assembly (consisting of two asymmetric units). When looking at the ribbon-style Fig. 1 (A1 & A2) one can observe not only the radial but also the axial amphiphilic behavior in the alpha helix. Fig. 1 (B1) shows the surface map of the peptide showcasing that the hydrophobic regions are covered when assembled and the Fig. 1 (C1 & C2) shows the same peptide rotated 90°. In the assembly of melittin in a biological system, the hydrophobic regions of two asymmetric units point towards each other due to hydrophobic interactions, while displaying the hydrophilic regions towards the outside of the molecule. With a eukaryotic cell membrane present [*Fig.* 2 (A)] and high concentrations, the asymmetric unit points its hydrophobic residues towards the hydrophobic lipid layer and incorporates itself into the cell membrane [*Fig.* 2 (B)]. The self-assembly proceeds and the helices organize themselves so that the hydrophilic parts point towards each other, resulting in pore formation.[6] [*Fig.* 2 (C)]
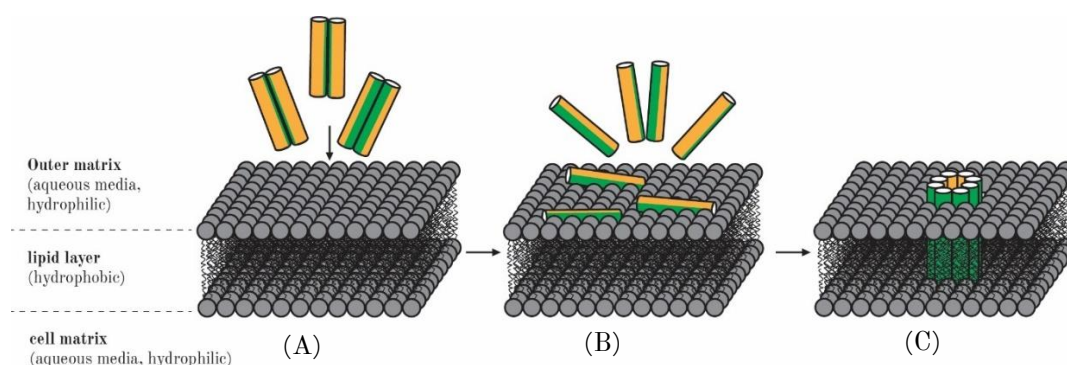
Fig. 2: Mode of action of pore formation in the cell membrane | Green: hydrophobic, Orange: Hydrophilic

This membrane interaction is the result of the amphiphilic nature of the molecule. The hydrophobic parts are oriented towards the lipid-layer while the hydrophilic parts point to the inside of the pore. The cell dies due to cell lysis.

This mode of action could be exploited to design helices that target prokaryotes instead of eukaryotes. However, peptides aren't viable candidates for sustainable antibiotics, because bacteria recognize especially organic compounds and develop mechanisms to counteract these kinds of active ingredient. There are many enzymes that efficiently degrade peptides, rendering their actionable life-time short. A solution to this issue could be polypeptoids, which combine similar physicochemical properties to peptides with stability to enzymatic degradation.

2.3. Differences between polypeptides and polypeptoids

Polypeptides are omnipresent in nature and are organic polymers consisting of amino acids, ranging from a few monomers to large chains. Polypeptides consist of a backbone and sidechains. The backbone contains a secondary amine with a hydrogen-atom able to form hydrogen-bonds. On the α-carbon (C_α) of the backbone various side groups (sidechains) are attached [**Fehler! Verweisquelle konnte nicht gefunden werden.**], which play a fundamental role in the function of the peptide. Polypeptides form secondary structures mostly because of sidechain-sidechain interaction due to hydrogen- or disulfide-bonding, hydrophobic- and electrostatic interactions of the sidechains and/or size exclusion[7]. The most common secondary structures are α-helices and β-sheets. These motifs arrange into more complex tertiary structures. The quaternary structure consists of the assemblies of several tertiary structures to obtain fully functional proteins.[8]
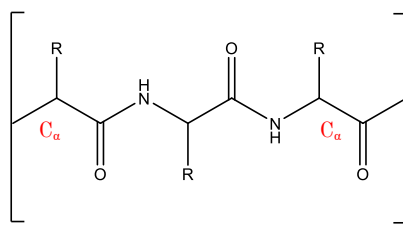
Fig. 3: Polypeptide Backbone

Polypeptoids (*N*-substituted glycines) don't exist in nature. The principal difference with respect to *polypeptides* is the location of the residue (the sidechain), which is attached to the nitrogen instead of the alpha-carbon [**Fehler! Verweisquelle konnte nicht gefunden werden.**]. This translocation results in the loss of the hydrogen bond-forming hydrogen. Nonetheless, polypeptoids also tend to form secondary structures due to sidechain-sidechain interaction and steric exclusions. Nanosheets[9] and Helices[10] have been observed for specific monomer-sequences. Polypeptoids are more thermo-resistant[11] in comparison to polypeptides and proteolytically stable[12].
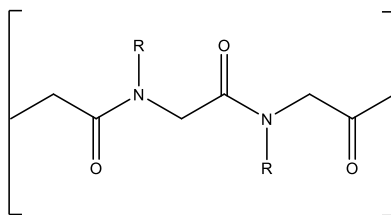
Fig. 4: Polypeptoid backbone

12

Cell-walls of bacteria could be attacked by imitating the amphiphilic helical structure of melittin, by choosing a specific sequence of peptoid-monomers to form polypeptoids with similarities to melittin. For successive incorporation, the exact length of the polypeptoid chain that corresponds to the membrane thickness must be known. Another crucial factor is the hydrophobicity, which determines the interaction with the membrane. While melittin attacks eukaryotic cells, synthetic polypeptoids can be engineered to specifically target prokaryotic cells. This is possible due to differences in the composition and the thickness of the cell membrane. The helix must be precisely as large as the thickness of the cell-wall.[13] These structures are candidates for sustainable antibiotics not prone to the risk of antibiotic resistance and the lack of biodegration by microorganisms.

2.4. Aim

The mode of action of the cell-lysing polypeptide helices of melittin is promising for creating a new class of antibiotics. However, peptides are prone to enzymatic degradation by the immune system of the bacteria. For this reason, the peptide must be imitated by a compound which cannot be recognized and broken down by the prokaryotic organism. Polypeptoids, which consist of *N*-substituted glycines, are not only immune to enzymatic degradation, but are also more thermally stable than peptides. Our ultimate goal is to reconstruct the peptide melittin by synthesizing amphiphilic polypeptoid helices and design them to target prokaryotic instead of eukaryotic cell-membranes. With sequence-specific synthesis of polypeptoids still in its infancy, a critical first aim is to characterize and optimize the synthesis of helix-forming and amphiphilic peptoids obtained by sequence-controlled solid-phase synthesis. The synthesis must be optimized to obtain a sufficient yield of the defined product.

A further aim is to establish analytic protocols to evaluate the effect of various parameters on the synthetic approach. The product can be determined with the help of matrix assisted laser desorption ionization time of flight mass spectrometry (MALDI-ToF-MS), but the results of MALDI-ToF-MS are affected by the matrix used for the desorption and ionization. By comparing various MALDI matrices commonly used for peptide or peptoid analysis, possible interactions of the matrices with the product must be tested. Obtaining a pure product is important for further analysis and modification. The possibility of the separation of various chain lengths can be tested with RP-HPLC.

13

In the course of this thesis, the following investigations were conducted:

(a) Optimization of the chain elongation with one monomer up to 5 blocks

(b) Chain elongation with one monomer up to 12 blocks

(c) Chain elongation with a hydrophobic and a hydrophilic monomer

(d) Defining the product with MALDI-TOF-MS

(e) Optimization of MALDI-TOF-MS analysis and matrix usage

(f) RP-HPLC analysis of the increase in hydrophobicity with an increasing chain length of hydrophobic monomers

(g) The impact on the product yield of reactivating the resin

2.5. Synthesis of polypeptoids

Today two ways to synthesize polypeptoids are known. The solution technique "ring opening polymerization" (ROP)[14] uses amino acid *N*-carboxyanhydrides which are cyclic polypeptoid monomers. It is possible to form polymer structures with controlled length. Despite the advantage of the fast and simple polymerization, this technique is not practicable due to the lack of control over the sequence of a co-polymer. At the second technique "Solid Phase Submonomer Synthesis" (SPSS)[9] one monomer at a time is added onto a resin. This way, precise control over the length and the sequence of the polypeptoid can be obtained. The method for the synthesis of oligo-peptoids is the two-step elongation: Acetylation and monomer adding. Which monomer is used for the elongation process defines the function and the assembly of the peptoid and must be carefully chosen.

2.6. Monomers

Choosing a suitable sequence and type of monomers is crucial for achieving a polypeptoid with a specific secondary structure. (R)-(+)-α-methylbenzylamine (R_{mba}) [**Fehler! Verweisquelle konnte nicht gefunden werden.**] is one example of a helix-forming monomer.[15] It is possible to observe the helical nature of a trimer of R_{mba} using circular dichroism. This observation suggests that using R_{mba}, the length of one turn of the helix is approximately three monomers long.[15] The enantiomeric excess of the monomer is crucial. Racemic mixtures form random coils rather than organized helical structures.[10]
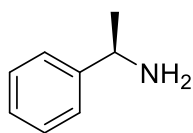
Fig. 5: (R)-(+)-α-methylbenzylamine

The additional binding of further side-groups will be necessary to obtain the targeted hydrophobicity gradients in the polypeptoid. This can be achieved by a wide range of different coupling and "click" reactions. The azido group is known for being a starting group for these reactions. The para-substituted azido derivate [Fig. 6 (B)] must be synthesized from a precursor because it is not commercially available. With a one-step S_N^2-reaction a para-substituted halogen derivate like 4-bromo-(R)-(+)-α-methylbenzylamine [Fig. 6 (A)] can be converted into 4-azido(R)-(+)-α-methylbenzylamine (AzRmba). [Fig. 6 (B)]
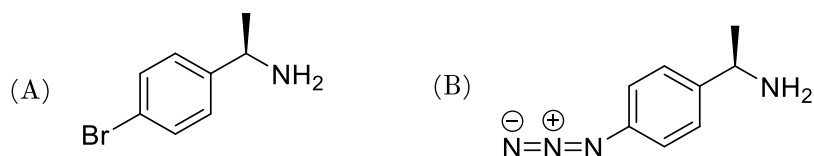
Fig. 6: (A) 4-bromo-(R)-(+)-α-Methylbenzylamine, (B) 4-azido-(R)-(+)-α-Methylbenzylamine

While monomers like R_{mba} form a helix-turn after a chain length of three[15], it is possible to forecast an amphiphilic structure with every third monomer being hydrophilic. *Fig.* 7 (A) depicts a homo peptoid with a chain length of 5 in top view. *Fig.* 7 (B) (top view) and *Fig.* 7 (C) (side view) show the amphiphilic structure of the heterogeneous peptoid with 12 residues. These co-polymers can be obtained with solid phase synthesis methods.
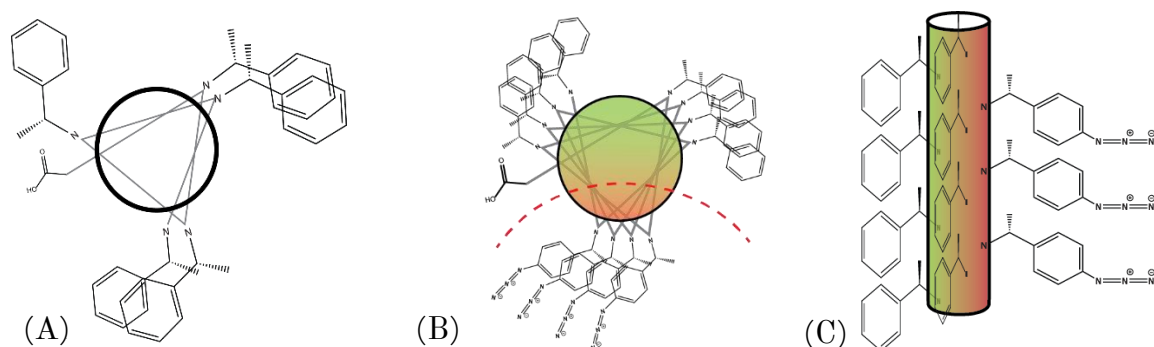
Fig. 7: (A) Top view pentamer R_{mba} (B) top view dodecamer amphiphilic hetero polypeptoid containing R_{mba} & AzR_{mba} (C) side view dodecamer amphiphilic hetero polypeptoid containing R_{mba} & AzR_{mba}

2.7. Solid-Phase Submonomer Synthesis

Solid-phase synthesis is carried out on a resin in contrast to solution techniques. Commonly used resins are *rink-amide* [*Fig.* 8] (A) or *2-chlorotritylchloride (2-CTC)* [*Fig.* 8] (B). The functional group is attached to a polystyrene carrier. The step-by-step polymerization starts on the chlorine of the 2-CTC and the amine on the rink amide resin, respectively. The advantage of the 2-CTC resin is its reusability.[16]

(A) 2-chlorotrityl chloride   (B) Rink amide
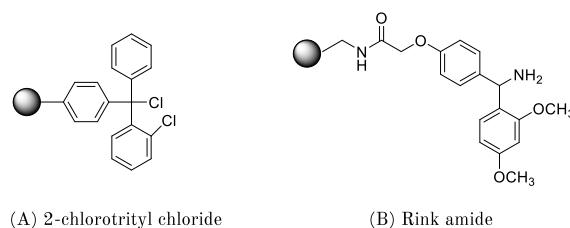
Fig. 8: (A) 2-CTC functional group (B) Rink amide functional group

The procedure is divided into five steps:

1) **Activation:** In contrast to the rink amide, the 2-CTC resin must be activated by an omega-amino acid before synthesis. Despite the additional step, it is readily used because of its reusability.

After activation, the elongation of the peptoid chain follows a two-step mechanism: Acetylation and the addition of the monomer.

2) **Acetylation:** Bromoacetic acid is used for acetylation since the terminal bromine group serves as a nucleophilic substitution partner. DIC facilitates this process. The acetyl-group serves as the backbone of the polypeptoid

3) **Monomer addition:** The *N*-substituted glycine is added. The choice of the monomers determines the side groups of the peptoid.

Steps two and three can be repeated until the peptoid reaches its desired length.

1) **Cleavage:** The product can be cleaved off the 2-CTC resin with a 1,1,1,3,3,3 Hexafluoroisopropanol (HFIP)/DCM[17] solution. Due to its low vapor pressure, the evaporation of the cleavage mixture HFIP/DCM after cleavage is straightforward. For rink amide tetrafluoro acid (TFA)/DMF solution is used.

2) **Reactivation:** Afterwards the 2-CTC resin can be reactivated using thionylchloride.[17] The rink amide must be discarded. In the method section, only the work with 2-CTC is described, since rink amide was not used.

2.7.1. Activation in DMF

The synthesis elongation starts on a primary amine. On the 2-CTC resin, the attachment of *fluorenylmethoxycarbonyl(Fmoc)-β-alanine* is necessary to generate a terminal amine. This process is catalyzed by *N,N,-diisopropylethylamine (DIPEA)*. After capping the remaining chloride-groups with MeOH, *Fmoc* is cleaved off with *piperidine* to expose the primary amine.
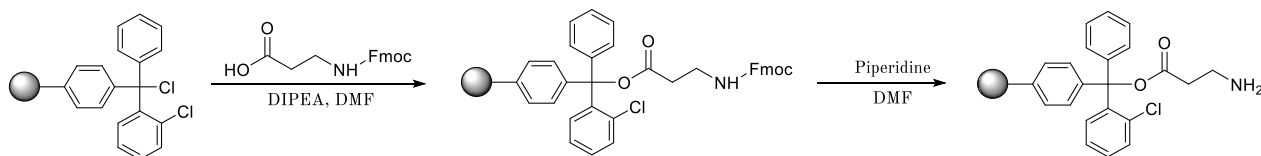
Fig. 9: Chemical reaction addition of beta-alanine to 2-CTC (incl. cleaving Fmoc group)

This way, the resin is activated and can be used for further modifications and synthesis.

2.7.2. Acetylation in DMF

The backbone is created by acetylation of the primary amine. Previous work has showed bromoacetic acid (BrHAc) to be an excellent acetylation agent since the terminal halogen group serves as an active group for further elongation. DIC activates the carboxyl group to facilitate the attachment to the primary amine. On the bromine the monomer can be attached.
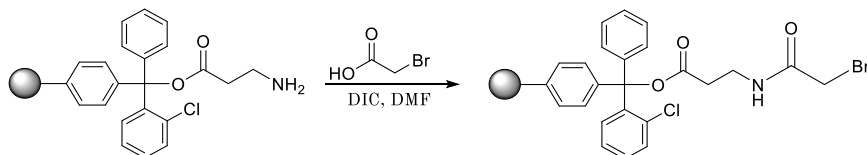
Fig. 10: Monomer addition in DMF (S_N^2-substitution)

During the monomer addition step, the monomer is added. The primary amino-group of the monomer attaches to the acetyl-group under the elimination of the bromine.
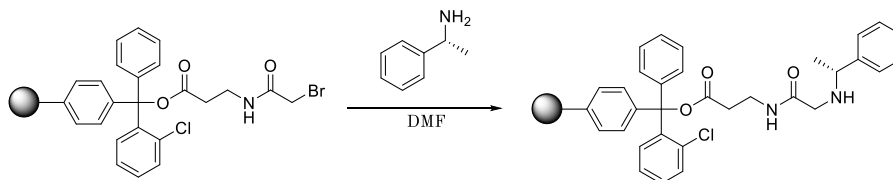
Fig. 11: Chemical reaction of nucleophilic substitution with the monomer

Cycling through the acetylation- and the S_N^2-step elongates the chain to its desired length. As previous works show, the incubation time must exceed at least 60 minutes due to the low reactivity of the process[9].
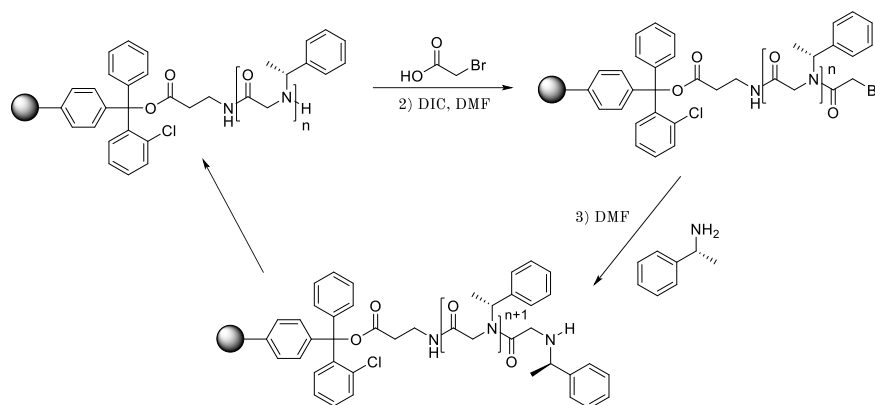
Fig. 12: Chemical Reaction of acetylation step & monomer addition

2.7.3.   Cleavage in DCM

After acquiring the desired length, the oligopeptoid product must be cleaved off the resin for further purification. A commonly used agent is 1, 1, 1, 3, 3, 3, Hexafluoroisopropanol (HFIP) in DCM. HFIP is easily removable due to its low vapor pressure and due to its volatile nature.
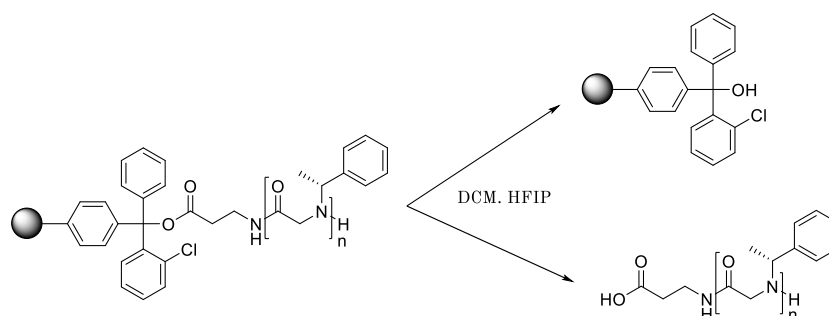
Fig. 13: Chemical reaction of product cleavage

2.7.4.   Regeneration of the resin in DCM

The 2-CTC resin can be recovered by adding *thionyl chloride* with the help of *pyridine*. The resin's terminal hydroxyl group gets restored to chloride making it reusable for further synthesis.
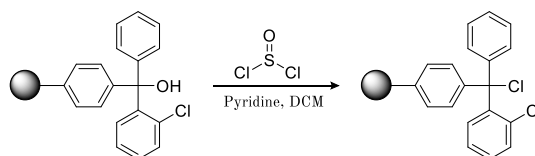
Fig. 14: Chemical reaction of resin recovery with thionyl chloride

Different chlorinating reagents are HCl, which is not suitable for the 2-CTC resin, which degrades when treated with acids, and acetyl chloride, which yields lower loading.[16]

3. Materials and Methods

3.1. Chemicals

3.2. Synthesis of the monomer 4-azido-(R)-(+)-α-Methylbenzylamine

The choice of the correct monomers in a sequence is the foundation of the proper function of the polypeptoid. For an amphiphilic oligopeptoid, a hydrophobic and a hydrophilic monomer must be chosen. Whereas (R)-(+)-α-methylbenzylamine R_{mba} is a candidate for a hydrophobic helix-forming monomer, the hydrophilic part can be a derivate of R_{mba} with a para-substituted active group. Active groups like azides offer a broad range of "click" coupling reactions to attach specific groups onto a molecule. Having azido groups incorporated into the oligomer, enables specific modification for further increasing hydrophilicity of the hydrophilic groups of the polypeptoid. 4-bromo-(R)-(+)-α-methylbenzylamine *(BrR_{mba})* serves as a precursor for 4-azido-(R)-(+)-α-methylbenzylamine *(AzR_{mba})* (product [1]). *AzR_{mba}* was synthesized by a modified protocol of Jacob Andersen et. al.[19] [*Fig.* 15]
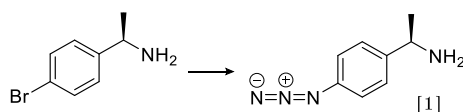
Fig. 15: Chemical reaction of 4-bromo-(R)-α-methylbenzylamine to 4-azido-(R)-α-methylbenzylamine (product [1])

CuBr (0,2 mmol) was added to a degassed *NaN₃* (4 mmol), *Na-Ascorbate* (0,1 mmol) and *trans-N,N′-Dimethylcyclohexane-1,2-diamine* (0,1 mmol) in 4 mL *EtOH:H₂O* [7:3] solution. Careful degassing and working under nitrogen are necessary to prevent oxidation of *CuBr*. Afterward, the a*ryl bromide* (2 mmol) was added to the reaction mixture and stirred at 100°C under reflux for 20 min.

To purify *AzR_{mba}* (product [1]), the reaction mix was extracted repeatedly with brine and ethyl acetate. The *AzR_{mba}* (product [1]) was captured in brine and transferred to an organic phase by adding EtAc three times. After pooling the 3 EtAc solutions, brine was added three times to extract impurities [*Fig.* 16].
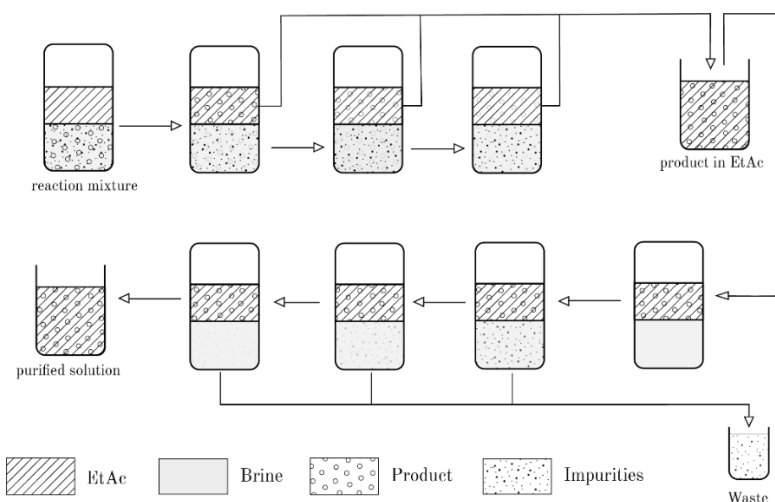
Fig. 16: Scheme of product purification with EtAc & Brine

The organic phase was separated and the solvent removed to isolate the product.

The aryl azide was purified by column chromatography using approx. 8 cm³ silica gel (60Å mesh 230 – 400). A ninhydrin solution (0,1 g *ninhydrin*, 500 µL a*cetic acid*, 100 mL *acetone*) was used to specifically stain the primary amine of the product. [**Fehler! Verweisquelle konnte nicht gefunden werden.**]
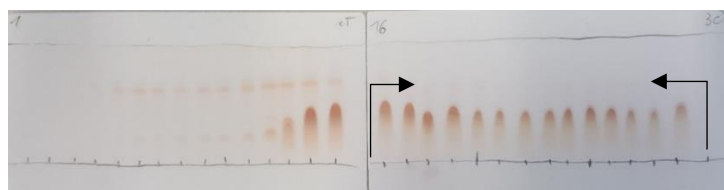
Fig. 17: TLC of fractions of size exclusion chromatography stained with ninhydrine, eluent: MeOH:Cl₃CH = 1:9

The combined (16-30) fractions were dried out and the purified AzR_{mba} (product [1]) could be isolated.

30 mg of AzR_{mba} (product [1]) was dissolved in 700 µL CDCl₃ and measured with ¹H-NMR. The spectrum showed the conversion to AzR_{mba} (product [1]) with 95 % efficiency.

3.3.   Solid Phase Submonomer Polypeptoid Synthesis

The synthesis was carried out in a 100 x 25 mm Ø column with a frit, twist-off cap and a valve [*Fig. 18*] (A). During all incubation steps, the column was placed sideways on a shaker (80 rpm) to assure sufficient mixing [*Fig. 18*] (B). Afterward, the liquid was drained by opening the valve [*Fig. 18*] (C) & (D) (the process was accelerated by flowing N₂).
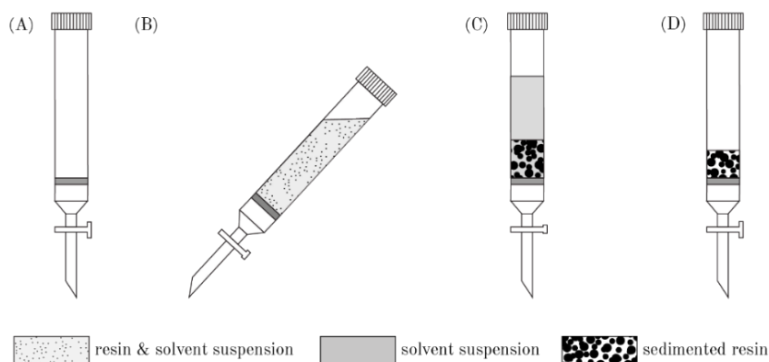
Fig. 18: *Scheme of column used (A) empty, (B) during* incubation, (C) before drainage, (D) after drainage

The chemicals in Table **1***: Chemicals, sum formula, properties, supplier and purity used for polypeptoid synthesis process.* were used for the monomer synthesis as received from the supplier when nothing else is explicitly stated in the protocols.

Table 1: Chemicals, sum formula, properties, supplier and purity used for polypeptoid synthesis process.

Polypeptoid synthesis				
Chemical	**Sum formula**	**Property**	**Supplier**	**Purity**
1,1,1,3,3,3,-Hexafluoro-2-propanol	$C_3H_2F_6O$	Liquid	ALDRICH	$\geq$99.0%
Bromo-(R)-(+)-α-methylbenzylamine (BrR_{mba})	$BrC_6H_4CH(CH_3)NH_2$	Liquid	ABCR	98%
Bromoacetic acid	$C_2H_3BrO_2$	Solid	ALDRICH	97%
Dichloromethane (DCM)	CH_2Cl_2	Liquid	SIGMA-ALDRICH	$\geq$99.5%
Dichloromethane *anhydrous* (DCM)	CH_2Cl_2	Liquid	SIGMA-ALDRICH	$\geq$99.8%
Diisopropyl ether	$(CH_3)_2CHOCH(CH_3)_2$	Liquid	Honeywell	99%
Diisopropylcarbodiimid (DIC)	$C_7H_{14}N_2$	Liquid	ALDRICH	99%
Fmoc-β-Ala-OH	$C_{18}H_{17}NO_4$	Powder	ALDRICH	$\geq$99.0%
Mathanol (MeOH)	CH_3OH	Liquid	SIGMA-ALDRICH	$\geq$99.8%
N,N-Diisopropylethylamine (DIPEA)	$C_8H_{19}N$	Liquid	SIGMA-ALDRICH	99,5%
N,N-Dimethylformamide *anhydrous* (DMF)	C_3H_7NO	Liquid	SIGMA-ALDRICH	99.8%
N,N-Dimethylformamide *puriss. p.a, ACS reagent* (DMF)	C_3H_7NO	Liquid	SIGMA-ALDRICH	99.8%
Piperidine	$C_5H_{11}N$	Liquide	SIGMA ALDRICH	99%
(R)-(+)-α-methylbenzylamine (R_{mba})	$C_6H_5CH(CH_3)NH_2$	Liquid	ALDRICH	98%

Thionyl chloride	SOCl₂	Liquid	Fluka	≥99.0%
RESIN	**Mesh**	**Property**	**Supplier**	**Substitution**
2-Chlorotritylchlorid resin	100-200	Resin	ROTH	1-1.5 mmol/g

3.3.1. Activation

The following protocol refers to 1000 mg *2-CTC* resin. According to the manufacturer, the resin is substituted with $1 - 1.5$ mmol/g active sites. All steps were conducted at room temperature.

Table 2: Procedure for activation of 2-CTC resin

swelling			
	Chemical(s)	**Amount**	**Incubation time**
I)	DCM	10 mL	10 min
II)	DCM : DMF = 2 : 1	10 mL	10 min
III)	DCM : DMF = 1 : 1	10 mL	10 min
loading			
I)	Fmoc-β-Alanine	0,250 g	10 min
	DIPEA	1,1 mL	
	DMF	10 mL	
wash			
I)	DMF	10 mL	10 min
II)	DMF	10 mL	10 min
III)	DMF	10 mL	$5 - 10$ min
capping			
I)	DCM : DIPEA : MetOH	$[10 + 0{,}6 + 1{,}2]$ mL	10 min
II)	DCM : DIPEA : MetOH	$[10 + 0{,}6 + 1{,}2]$ mL	10 min
III)	DCM : DIPEA : MetOH	$[10 + 0{,}6 + 1{,}2]$ mL	10 min
wash			
I)	DMF	10 mL	10 min
II)	DMF	10 mL	10 min
III)	DMF	10 mL	$5 - 10$ min
deprotect			
I)	Piperidine : DMF	$[2 + 6]$ mL (25% solution)	10 min
II)	Piperidine :DMF	$[2 + 6]$ mL (25% solution)	20 min
Wash			
I)	DMF	10 mL	10 min
II)	DMF	10 mL	10 min
III)	DMF	10 mL	5 - 10 min

According to Fayna Garcá-Martín et al., the capping step is not mandatory since the same action is performed by piperidine.[16]

3.3.2.   Acetylation

Table 3: Procedure of Acetylation

Acetylation			
	Chemical(s)	**Amount**	**Incubation time**
I)	BrHAc + DMF	10 eq	5 min
	DIC + DMF	9 eq	
Wash			
I)	DMF	10 mL	5 min
II)	DMF	10 mL	5 min
III)	DMF	10 mL	5 min

The BrHAc- and the DIC solution were stored separately as stock solutions and combined for the reaction-step. The stock solutions had double the concentration each because BrHAc- and the DIC solution were mixed 1:1. The reaction was conducted at room temperature. According to the manufacturer, acids harm the resin. Therefore, an adequate balance between volume, concentration and equivalence number of BrHAc must be adjusted. With the following equation, the amounts used for the synthesis can be calculated:

BrHAc amounts

$$amount\ [g] = \frac{(Amount\ Resin)\ [g] * (Substition\ lvl)\ \left[\frac{mmol}{g}\right] * M(BrHAc)\ \left[\frac{g}{mol}\right] * equivalences}{1000} \quad (1)$$

$M(BrHAc) = 139.0$ g/mol

DIC amounts

$$amount\ [g] = \frac{(Amount\ Resin)\ [g] * (Substition\ lvl)\ \left[\frac{mmol}{g}\right] * M(DIC)\ \left[\frac{g}{mol}\right]\ equivalences}{1000 * \rho(DIC)\ [\frac{g}{mL}]} \quad (2)$$

$M(DIC) \qquad = 126.2$ g/mol

$\rho(DIC) = 0.815$ g/mL

3.3.3. S_N^2-Substitution

Table 4: Procedure of monomer addition

SN$_2$- Substitution				
	Chemicals	**Amounts**	**Incubation time**	**temperature**
I)	Monomer : DMF	17 eq.	90 min	37°C
Wash				
I)	DMF	10 mL	5 min	RT
II)	DMF	10 mL	5 min	RT
III)	DMF	10 mL	5 min	RT

For the S_N^2-substitution, the concentration of the solution of the R_{mba} monomer and its

derivates should range from $1\,M - 2\,M$[9].

With the following equation, the amounts used for the synthesis can be calculated:

$$\frac{(\textit{Amount Resin})\,[g] * (\textit{Substition lvl})\left[\frac{\text{mmol}}{\text{g}}\right] * M(\textit{Monomer})\left[\frac{\text{g}}{\text{mol}}\right] \textit{equivalences}}{1000 * \rho(\textit{Monomer})\left[\frac{\text{g}}{\text{mL}}\right]} = \textit{amount}\,[\text{mL}] \quad (3)$$

M($Rmba$)	$= 121.18$ g/mol
ρ($Rmba$)	$= 0.952$ g/mL
M(Br$Rmba$)	$= 200.1$ g/mol
ρ(Br$Rmba$)	$= 1.39$ g/mL
M(Az$Rmba$)	$= 162.2$ g/mol
ρ(Az$Rmba$)	$=$ No data

3.3.4.   Cleavage & Precipitation

Table 5: Procedure of product cleavage

Washing step				
	Chemicals	**Amounts**	**Incubation time**	**temperature**
I)	DCM	10 mL	5 min	RT
II)	DCM	10 mL	5 min	RT
III)	DCM	10 mL	5 min	RT
cleave				
I)	HFIP : DCM	[2 + 8] mL (20% solution)	60 min	RT
II)	HFIP : DCM	[2 + 8] mL (20% solution)	30 min	RT
Washing step				
I)	DCM	10 mL	5 min	RT

The resin was treated twice with HFIP/DCM as summarized in Table 5, followed by pure

DCM to remove all the product from the column. The solution of the last washing step is

pooled as well. The combined fractions were dried. The oily remains were stirred for 10

minutes with diisopropylether, centrifuged (5000 rpm, 5 minutes) and dried in high

vacuum to yield the pure product. Despite the low vapor pressure, the product needs to

be dried excessively (24h at 0.1 mbar) and mechanically deagglomerated repetitively due

to trapped solvent between the molecules.

3.3.5.   Regeneration of the resin

Table 6: Procedure of resin recovery

Washing step				
	Chemicals	**Amounts**	**Incubation time**	**temperature**
I)	DCM	10 mL	5 min	RT
II)	DCM	10 mL	5 min	RT
III)	DCM	10 mL	5 min	RT
cleave				
I)	$SOCl_2$: Pyridine : DCM	1,2 eq : 2,4 eq	240 min	RT
Washing step				
I)	DMF	10 mL	5 min	RT
II)	DMF	10 mL	5 min	RT
III)	DMF	10 mL	5 min	RT

The resin was washed with DCM three times before treating it with thionyl chloride and pyridine. After the incubation time of at least 3 hours, the solvent was changed to DMF by washing the resin with DMF 3 times.

3.4.   MALDI-TOF-MS analysis

3.4.1.   General

In the course of the practical work, the matrix assisted laser desorption ionization – time of flight mass spectrometry (MALDI-TOF-MS) was proven to be the most convenient method to analyze the products of the synthesis. The principle of this method relies on the differences of velocities of various charged molecules in an evacuated electromagnetic field. As shown in Fig. 19, a laser shoots at the sample and releases the analytes. The molecules travel along a fixed distance until reaching a detector. Big molecules are slower than shorter molecules, given that they have the same net charge. Molecules with twice the charge fly exactly twice as fast. Two operation modes can be used:

1. In *positive mode*, a negative electromagnetic field is applied, so that positive ions are carried to the detector.

2. In *negative mode*, the electromagnetic field is negative, and anions can be detected.

To release the analytes a matrix is needed, which absorbs the energy of the laser. Furthermore, the matrix serves as an ion donor for neutral sample-molecules.
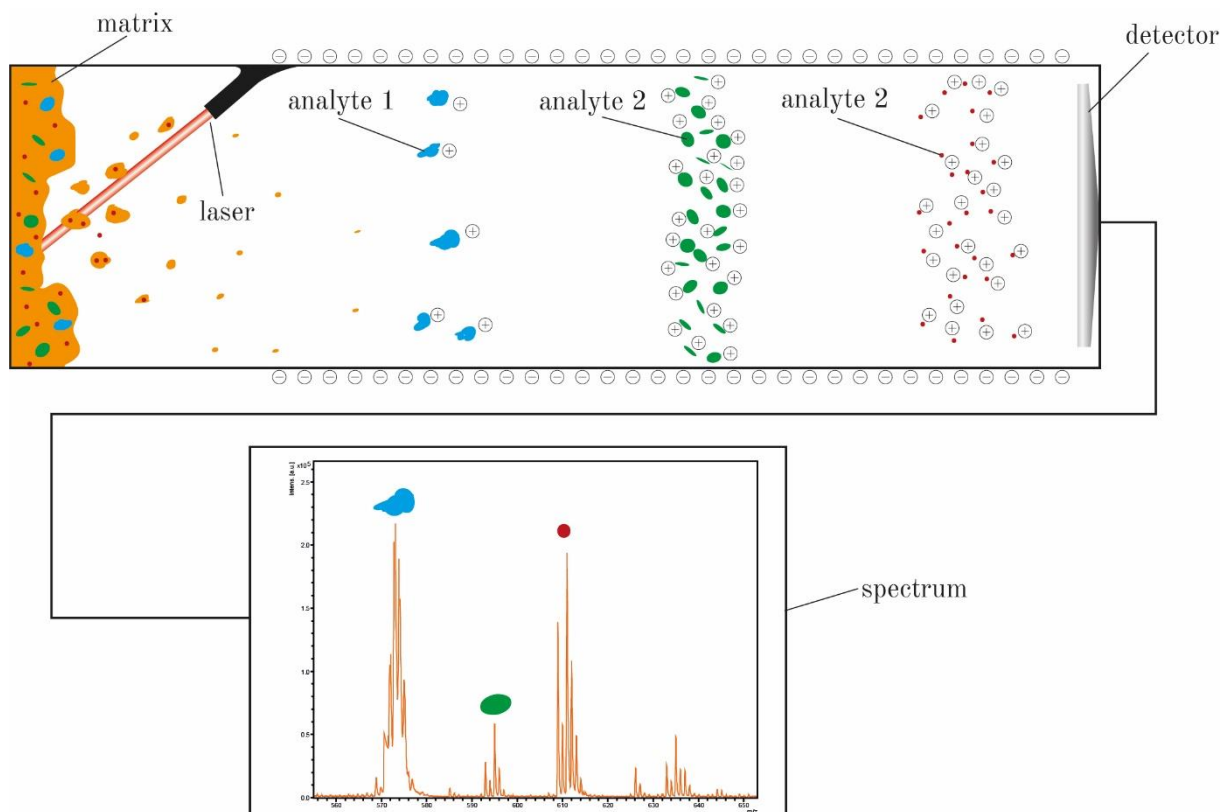
Fig. 19: Visualization of the mode of action of MALDI-TOF-MS: Yellow: Matrix, Blue: High molecular weight molecule, Green: Middle molecular weight molecule, Red: Low molecular weight molecule

In most cases, the analytes are neutral molecules. In positive mode the matrix transfers cations like hydrogen, sodium, potassium or ammonium to the product. This way the product can fly in the negative electromagnetic field. These cations are called *adducts*.

The product isn't visible as a single peak but as various peaks with a mass difference of 1 Δ m/z. This peak pattern derives from the isotopes of the atoms in the sample (The mass of a neutron is exactly 1 m/z). Smaller molecules have the most dominant peak at the exact mass like in the fictive molecule (A) (500 m/z) in Fig. 20. The larger the molecule, the higher the probability it contains atoms of different isotopes, causing the peak with the highest intensity to shift to the middle of the peak distribution of the isotopic pattern, as illustrated in the example of the fictive molecule (B) (2000 m/z) in Fig. 20.
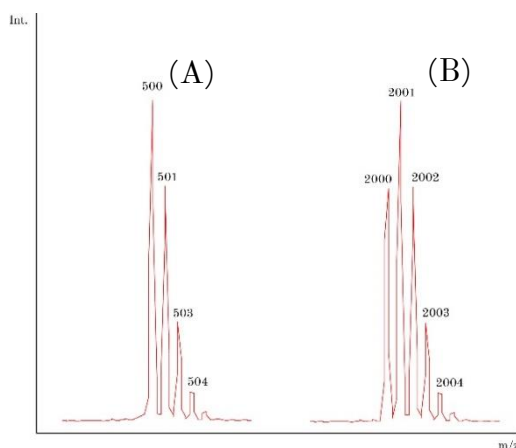
Fig. 20: Example of an isotopic peak distribution of a fictive molecule with low molecular weight (A) and higher molecular weight (B)

Fig. 21 shows a typical peak distribution of a MS spectrum. The exact mass of $m[C_{123}H_{139}N_{13}O_{14}]$ would be visible at 2022,1 m/z, but since this molecule has no net charge this exact mass-peak is not visible in the spectrum. However, the following adducts are observable:

- Hydrogen: $m[C_{123}H_{139}N_{13}O_{14}+H]^+ = 2023,1$ m/z
- Sodium: $m[C_{123}H_{139}N_{13}O_{14}+Na]^+ = 2045,1$ m/z
- Potassium: $m[C_{123}H_{139}N_{13}O_{14}+K]^+ = 2061,1$ m/z

$$m[C_{123}H_{139}N_{13}O_{14}]=2022,1 \text{ g/mol}$$
$$m[C_{123}H_{139}N_{13}O_{14}+H]^+=2023,1 \text{ g/mol}$$
$$m[C_{123}H_{139}N_{13}O_{14}+Na]^+=2025,1 \text{ g/mol}$$
$$m[C_{123}H_{139}N_{13}O_{14}+K]^+=2061,1 \text{ g/mol}$$
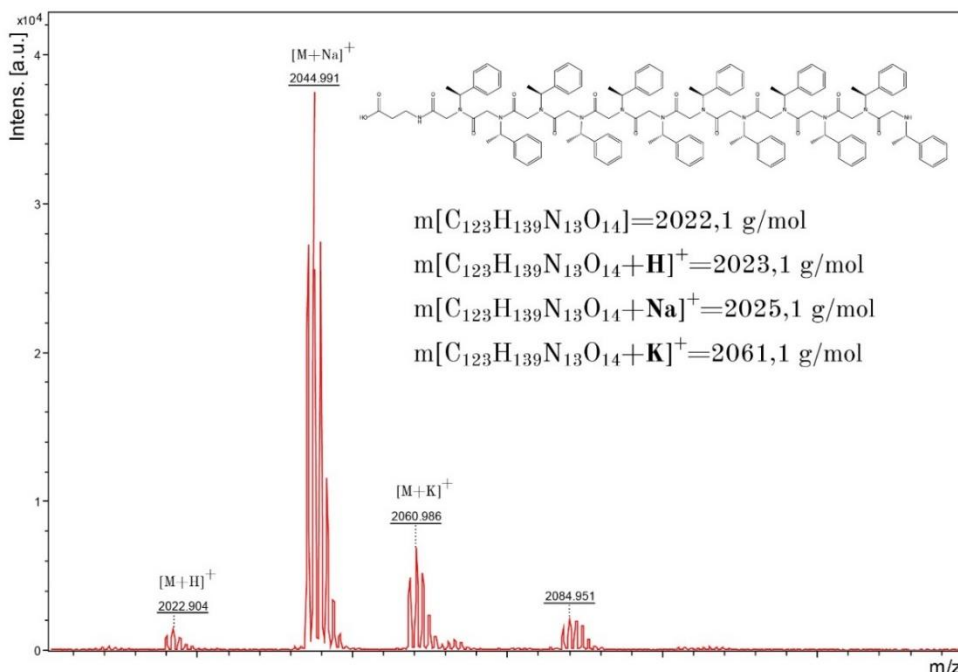
Fig. 21: Spectrum of a molecule with an exact mass of 2022.1 g/mol

The matrix and its composition used to obtain these spectrums plays a big role quality of the spectrum. The choice of the matrix is strongly dependent on the size of the molecule.

3.4.2.   The matrix

Many different matrices are used in peptide or peptoid analysis. In the practical work, we focused on three matrices:

1) 6-aza-2-thiothymine (ATT),

2) 2,5-dihydrocybenzoic acid (DHB)

3) α-cyano-4-hydrocycinnamic acid (ACH)

1) 6-aza-2-thiothymine (ATT)   2) 2,5-dihydroxybenzoic acid (DHB)   2) a-Cyano-4-hydroxycinnamic acid
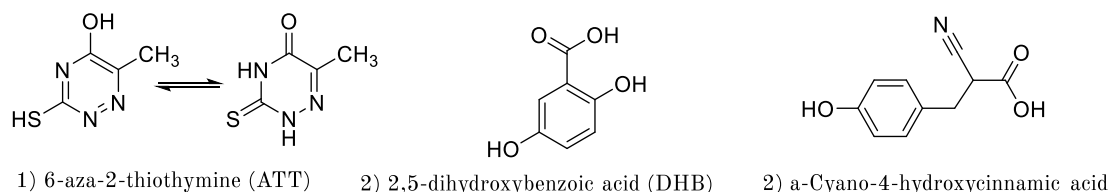
Fig. 22: Chemical structure of (A) ATT- (B) DHB- (C) ACH-matrix

The dry product was diluted with defined amounts of MeOH in order to determine exact concentrations, spotted on the MALDI-plate and dried in vacuum. The matrix is pipetted onto the dry sample and dried again in vacuum. The sample plate can now be brought into the MALDI-TOF mass spectrometer ready to be analyzed.

3.4.3.   Laser induced fragmentation technique (LIFT)

When determining the m/z in a MALDI-spectrum the mass peak alone is not a reliable information source about the presence of a sought molecule. The product can get fragmented and the m/z of the fragments in the spectrum can now be assigned to the theoretical weights of the fragments to avoid errors of coincidental mass-similarities. This exposes the fingerprint of the molecule. In the *laser induced fragmentation technique,* a high energy laser breaks apart the sample molecule and visualizes its fragments in the spectrum.
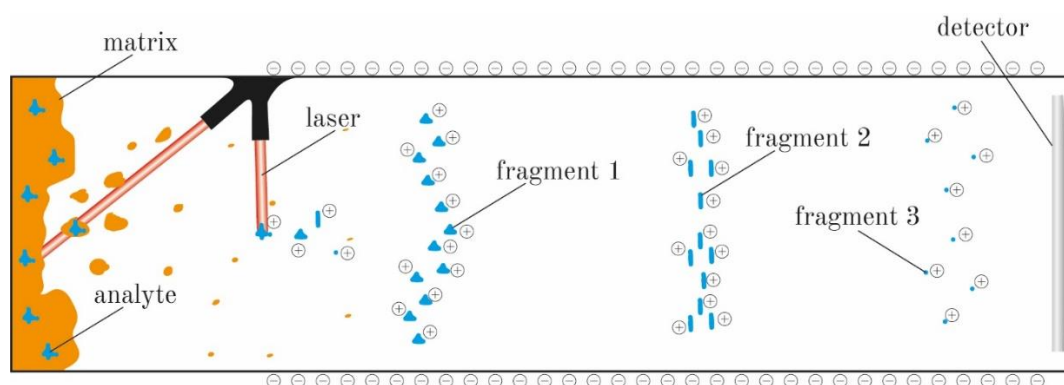

Fig. 23: Mode of action laser induced fragmentation technique

28

3.5. Reverse phase high performance liquid chromatography (RP-HPLC)

This separation process relies on the difference in hydrophobicity of the analytes. The sample is pushed through a column packed with a hydrophobic-resin on which C-18 chains are attached at high pressure. The higher the hydrophobicity, the longer the interaction with the resin, the longer the retention time. Polar molecules pass through the column with almost no interaction. Subsequently, a UV detector records the analytes which leave the column one after another. The samples are dissolved in methanol and injected.

3.1. Nuclear magnetic resonance (NMR)

NMR was used once to determine the efficiency of the conversion of the monomer bromo-(R)-(+)-α-methylbenzylamine *(BrR$_{mba}$)* to 4-azido-(R)-(+)-α-methylbenzylamine *(AzR$_{mba}$)*. This technique relies on the spin of the nuclei of hydrogen atoms in the sample. From the data is it observable which molecular neighbors each hydrogen has within the molecule. Each molecule has its own fingerprint, so that small changes deriving from altering molecular groups can be determined.

4. Results and Discussion

4.1. Synthesis of R_{mba} oligomers

Several factors can influence the synthesis. The effect of water on the efficiency of the synthesis is important to know if working under atmospheric exclusion is necessary. The concentration of bromoacetic acid is significant due to the acid labile resin. An incubation time must be found that assures relatively fast progress of the synthesis and reaching of the equilibrium of the reaction. An adequate length of the polypeptoid must be possible to acquire. Furthermore, it is crucial to know if the synthesis is still possible with alternating monomers.

A protocol for optimization of the overall yield was developed, based on previous works from our group[20] (Dipl. Ing. Marlene Egelseder). Different aspects such as the purity of the solvents working in pure N_2-atmosphere storing DIC & BrHAc-solutions were investigated separately. Furthermore, the possibility of capturing the monomer after the incubation-step and reuse it for the next monomer-addition step was tested. All experiments were conducted with the same protocol listed in "*3.2. Solid Phase Submonomer Polypeptoid Synthesis*" to maintain reproducibility. The synthesized products were cleaved off the resin, precipitated and dried under vacuum at least 24 hours in a flask of a known weight. The mass was determined by subtracting the weight of the flask from the total weight of the flask plus the product. The oligomers were synthesized with solid phase submonomer synthesis by using the concentrations and amounts of Table 7. The reaction conditions were kept according to Table 8.
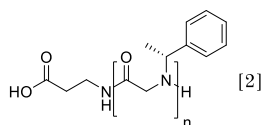
Fig. 24: Oligomer of R_{mba} (product[2])

Table 7: Amounts used for the synthesis of oligomers of R_{mba} on 2-CTC resin

	Equivalents	Stock concentration	Final concentration
BrHAc	10	1.62 M	0.81 M
DIC	9	1.78 M	0.89 M
R_{mba}	17	1.43 M	1.43 M

Table 8: Incubation conditions for the synthesis for the experiments in chapter 4.1. a) - d)

Incubation conditions	
Acetylation	45 min at room temperature
Monomer addition	90' at 37 °C

The protocol[20] assumes a substitution of the 2-CTC resin of 0.8 g/mmol. However, during the calculation of the yield, a substitution of 1.25 g/mmol was chosen, following the data of the manufacturer of the resin which is 1 – 1.5 g/mmol. The yields of the products were determined by the comparison of the theoretical mass-yield and the actual weight of the dry product. With equation (4) the yield can be calculated when measuring the weight of the dry product:

$$Yield\ [\%] = \frac{m(Product)[\text{mg}]}{M(Product)\ \left[\frac{\text{mg}}{\text{mmol}}\right] \cdot Resin\ Substitution\ \left[\frac{\text{mmol}}{\text{g}}\right] \cdot m(Resin)\ [\text{g}]} \cdot 100 \qquad (4)$$

At the following experiments in chapter 4.1.1. and 4.2.1. an error during the activation of the resin occurred. The amount of the deprotecting agent piperidine in the reaction was chosen too low. Only 25% of the reagent was used from the protocol. The error was systematic so that the results can be comparable. However, from experiment 4.2.2. onwards the correct amount of piperidine was used. These results are not comparable with the experiments where only 25% of the deprotecting agent piperidine was used.

4.1.1. DIC and BrHAc storage

At the activation step only 25% of the deprotecting agent piperidine was used. During the acetylation step BrHAc is added. To facilitate to mode of action DIC is added to the reaction mixture. To test the impact on the efficiency of the synthesis of storing the DIC and the BrHAc solution separately or in a mixture was tested.

A dimer of R_{mba} (M = 411,5 g/mol) was synthesized on 250 mg 2-CTC resin. DIC and BrHAc were stored together in one flask. The mass of the dry product yielded 16.5 mg.

$$Yield\ [\%] = \frac{16.5\ \text{mg}}{895.1\ \frac{\text{mg}}{\text{mmol}} \cdot 1.25\ \frac{\text{mmol}}{\text{g}} \cdot 0{,}250\ \text{g}} \cdot 100 = \mathbf{5.8}\ \%$$

For comparison pentamer of R_{mba} (M = 895,1 g/mol) was synthesized on 1000 mg resin. DIC and BrHAc were stored separately in two different beakers. The amounts required for one acetylation step were combined during the acetylation step in the reaction vessel. The mass of the dry product yielded 90 mg.

$$Yield\ [\%] = \frac{90\ \text{mg}}{895.1\ \frac{\text{mg}}{\text{mmol}} \cdot 1.25\ \frac{\text{mmol}}{\text{g}} \cdot 1\ \text{g}} \cdot 100 = \mathbf{8.04}\ \%$$

The increase in the yield from 5.8 % to 8.04 % can have various reasons. For example, during the precipitation step some amount of the product get lost. This makes it difficult to compare amounts which are already low, especially when more resin was used. Despite

the uncertainty of the meaningfulness, the data suggests that storing the BrHAc and DIC solution separately has a positive influence on the yield of the synthesis.

4.1.2.   The effect of water on the synthesis

4.1.2.1.   Anhydrous solvents

At the activation step only 25% of the deprotecting agent piperidine was used. Two types of purities of solvents were used to inspect the interference of water with solid phase submonomer synthesis. Normally the solvents used for the synthesis were:

DMF: 99.8% puriss. p.a., ACS reagent

DCM: 99.5%

A R_{mba}-dimer (M = 411,5 g/mol) on 1 g 2-CTC resin was conducted with anhydrous agents:

DMF: 99.8% anhydrous,

DCM: 99.8% anhydrous

The mass yield of the product was 14 mg. Using equation (4) a yield of 2.7% could be calculated. Comparing this result with the yield of experiment "4.1.1. DIC and BrHAc storage", no increase in yield can be observed. When working with non-anhydrous agents under atmosphere, the yield amounted 6-8 %. Having an overall yield of 2.7 % when working with anhydrous reagents suggests that water present in the solvents doesn't interfere with the synthesis.

4.1.2.2.   Anhydrous solvents under air exclusion (N2 flow)

At the activation step only 25% of the deprotecting agent piperidine was used. While working with anhydrous solvents, the synthesis of a pentamer of R_{mba} (M = 895,1 g/mol) was carried out under N_2-flow to ensure air exclusion to eliminate hygroscopic effects of the solvents. The mass-yield of the product was 117 mg. Using equation (4) a yield of 10.4 % could be calculated.

The yield of the synthesis increased from 2.7% from the experiment 4.1.2.1. "Anhydrous selvents" 4-fold to 10%.

However, if traces of water present in the non-anhydrous solvents would have interfered with the synthesis, it would not explain why the product yield of the experiment with anhydrous solvents under air decreases in comparison to the yield of the experiments where non-anhydrous solvents were used. The main problem of these experiments was

the low overall product yield. The data is comparable only to a certain extent. During the purification and product-transfer steps some amount of the product get lost. Even small amounts fall into weight when comparing the little weights of the products. The errors resulting from this experimental problem was detected after the experiments were conducted. From this experiment onwards the resin was deprotected sufficiently.

4.1.3.   Monomer recycling

Working with expensive monomers, it is important to know if it is possible to capture the supernatant of the monomer addition step and reuse it for the next one. This is possible due to the 17-fold excess in the reaction mixture. For that, a trimer of R_{mba} (M $= 572,7$ g/mol) was synthesized on 1 g resin. After each monomer addition step, the supernatant containing the monomer was captured. This solution was used again for the next monomer addition step. The mass-yield of the product was 323 mg. Using equation (4), a yield of 45.28 % could be calculated, assuming a substitution level of 1.25.

The data of the increase in mass yield, can be led back to the sufficient deprotection of the resin. A yield of 45.28% proves that by reusing the monomer it is possible to reduce the amount of monomer used. Still the reaction parameters must be tweaked to obtain higher yields.

4.2.   Mild acetylation conditions

According to the manufacturer, the 2-CTC resin is prone to degradation in extended contact with acids like BrHAc. To reduce resin hydrolysis there are two options:

 a.   the concentration of the bromoacetic acid could be reduced

 b.   the incubation time could be shortened.

The altered conditions were tested during the synthesis of a trimer of R_{mba} (product [3]) on 1000 mg 2-CTC resin. The concentration of BrHAc was reduced from 0.8 M to 0.4 M and the incubation time reduced from 45 to 5 min in the same experiment.


Fig. 25: Trimer of R_{mba} (product [3])

One Step					
	Amount	**DMF**	**Equivalents**	**Concentration stock**	**Final concentration**
BrHAc	0.56 mg	5 mL	5	0.8 M	0.4M
DIC	1.11 mL	3.89 mL	9	1.78 M	0.88 M
R_{mba}	1.73 mL	8.27 mL	17	1.43 M	1.43 M
Total					
	Amount	**DMF**	**Equivalents**	**Concentration stock**	**Final concentration**
BrHAc	1.78 mg	16 mL	5	0.8 M	0.4 M
DIC	3.57 mL	12.43 mL	9	1.76 M	0.88 M
R_{mba}	5.37 mL	25.63 mL	17	1.43 M	1.43 M

Table 10: Incubation conditions for the synthesis of the R_{mba} trimer (product [3])

Incubation conditions	
Acetylation	5 min at room temperature
Monomer addition	90 min at 37°C

Cleavage and purification steps were conducted according to the protocol "3.3.4. *aboveCleavage & Precipitation*".

From 1000 mg resin, 456 mg product could be harvested. Using equation (4), a yield of 63.7% can be calculated. By implementing both concepts – the reduction of the BrHAc-concentration and working with the shortened possible incubation-time of 5 min, the yield could be increased by 69.25%, compared to the yield of the established protocol which had a yield of 40%.

It can be concluded that the 2-CTC resin is indeed destroyed by bromoacetic acid over time and that the optimization of the acetylation step is important especially when the 2-CTC resin is reused.

The results of the experiments from chapter "4.1. Synthesis of R_{mba} oligomers" were strongly influenced by an error in the activation step of the resin. However, the efficiency of the synthesis was brought up to 63.7% yield by applying mild acetylation conditions and carefully activating the resin.

The R_{mba} trimer (product [3]) was analyzed with MALDI-TOF-MS, to assure that the product obtained from synthesis has the desired composition.

4.2.1.   MALDI-TOF-MS analysis of *the R_{mba}* trimer (product [3])

The R_{mba} trimer (product [3]) was observed with MALDI-TOF-MS in positive mode using the matrix *6-aza-2-thiothymin*e (ATT) [Fig. 26]. 1 µL of a 1 mg/mL of the R_{mba} trimer (product [3]) in MeOH solution was pipetted on the MALDI-plate. After drying

in vacuum, 1 μL of the ATT matrix-solution (3 mg/mL in ACN) was added and dried again. The exact mass of a R_{mba}-trimer is 572,30 m/z. The theoretical m/z peak pattern is plotted below:
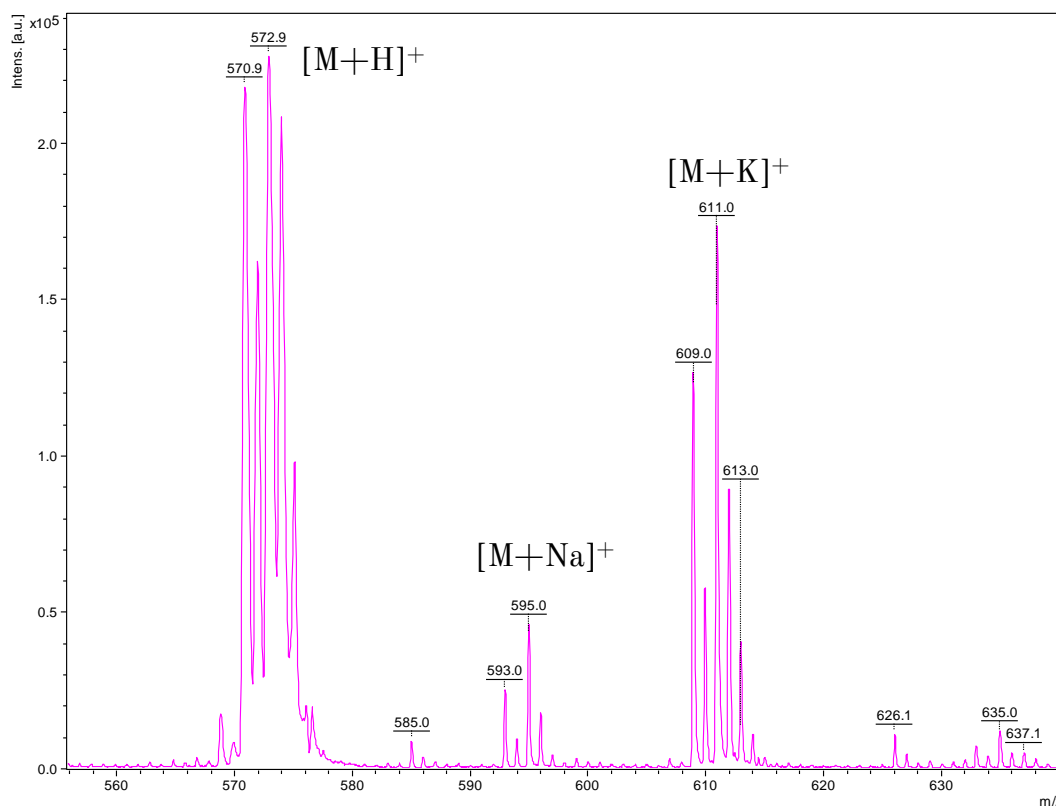

Fig. 26: MALDI-TOF-MS spectrum of R_{mba} trimer (product [3]) using ATT matrix

Table 11: Theoretical mass peaks of the Rmba trimer (product [3])

$[M+H]^+$		$[M+Na]^+$		$[M+K]^+$	
100%	573.30 m/z	100.0%	595.29 m/z	100.0%	611.26 m/z
35.7%	574.30 m/z	35.7%	596.29 m/z	35.7%	612.27 m/z
3.5%	575.31 m/z	6.2%	597.30 m/z	7.2%	613.26 m/z

The corresponding peaks for hydrogen (572.9 m/z), sodium (595.0 m/z) and potassium (611.0 m/z) adducts are observable with an accepted error of approx. -0,4 Δ m/z. Every product peak is accompanied by a trace peak at -2 Δ m/z. Further trace peaks can be found at -30, -35, -76 Δ m/z. The mass for the latter is lead back to subtracting one aromatic ring. No m/z peak is found when eliminating a second aromatic ring. According to this data only the terminal aromatic ring of the R_{mba} gets fragmented.
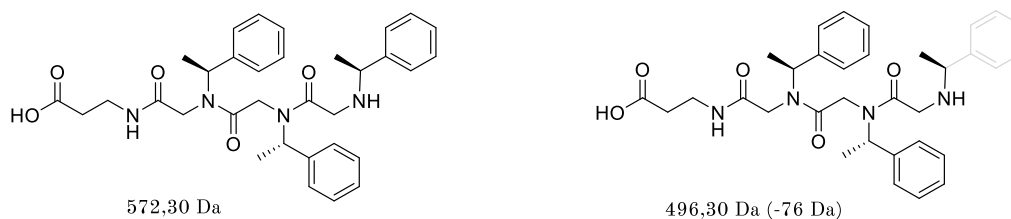
Fig. 27: Visualization of the loss of an aromatic ring of a trimer R_{mba}

Currently no explanation for the -2, -30 or -35 Δ m/z artefacts are proposed.

MALDI analysis did show that the overall synthesis yields the desired product. Several impurities (unknown composition) could be observed. Furthermore, it can be observed that shorter chain lengths of the peptoid are present, which suggests that the equilibrium of the monomer addition step is not 100% on the side of the incorporation of the monomer to the elongating polypeptoid. Measuring the sample with different matrices gives information on if the fragments derive from synthesis errors or the interaction with the matrix.

4.3. Comparison of different matrix-substances for MALDI-measurements of oligo-peptoids.

MALDI-TOF-MS is a commonly used technique to analyze peptide and peptoids. To gain more information about the oligopeptoid and its interaction with the matrices,

a. the influence of various matrices (ATT, DHB, ACH)

b. and fragmentation using LIFT

are tested.

For that, a pentamer of R_{mba} (product [4]) was synthesized on 1 g resin. The substitution factor was raised from 0.8 mmol/g to 1 mmol/g.
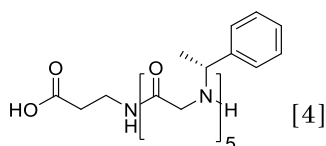

Fig. 28: Homo-polypeptoid R_{mba} x5 [4]

Table 12: Amounts used for the synthesis of oligopeptoid R_{mba} x5 (product [4]) on 1 g 2-CTC resin assuming a substitution factor of 1 g/mmol

One Step					
	Amount	**DMF**	**Equivalents**	**Stock concentration**	**Final concentration**
BrHAc	0.69 g	5 mL	5	1.0 M	0.5 M
DIC	1.39 mL	3.61 mL	9	2.2 M	1.1 M
R_{mba}	2.16 mL	7.84 mL	17	1.79 M	1.79 M
Total					
	Amount	**DMF**	**Equivalents**	**Stock concentration**	**Final concentration**
BrHAc	3.5 g	25.0 mL	5	1.0 M	0.5 M
DIC	7.0 mL	18 mL	9	2.2 M	1.1 M
R_{mba}	10.8 mL	39.2 mL	17	1.79 M	1.79 M

Table 13: Incubation conditions for the synthesis of R_{mba} x5 (product [4])

Incubation conditions	
Acetylation	5 min at room temperature
Monomer addition	90 min at 37°C

Cleavage and purification steps were conducted according to the protocol "3.3.4. *aboveCleavage & Precipitation*"

4.3.1.   MALDI-TOF-MS analysis of the R_{mba} pentamer (product [4]) using ATT matrix in positive mode

The first matrix to be observed it ATT. 1 µL of a 1 mg/mL of R_{mba} x5 (product [4]) in MeOH solution was pipetted on the MALDI-plate. After drying in vacuum, 1 µL of the ATT matrix-solution (3 mg/mL in ACN) was added and dried again. The sample was measured in positive mode.
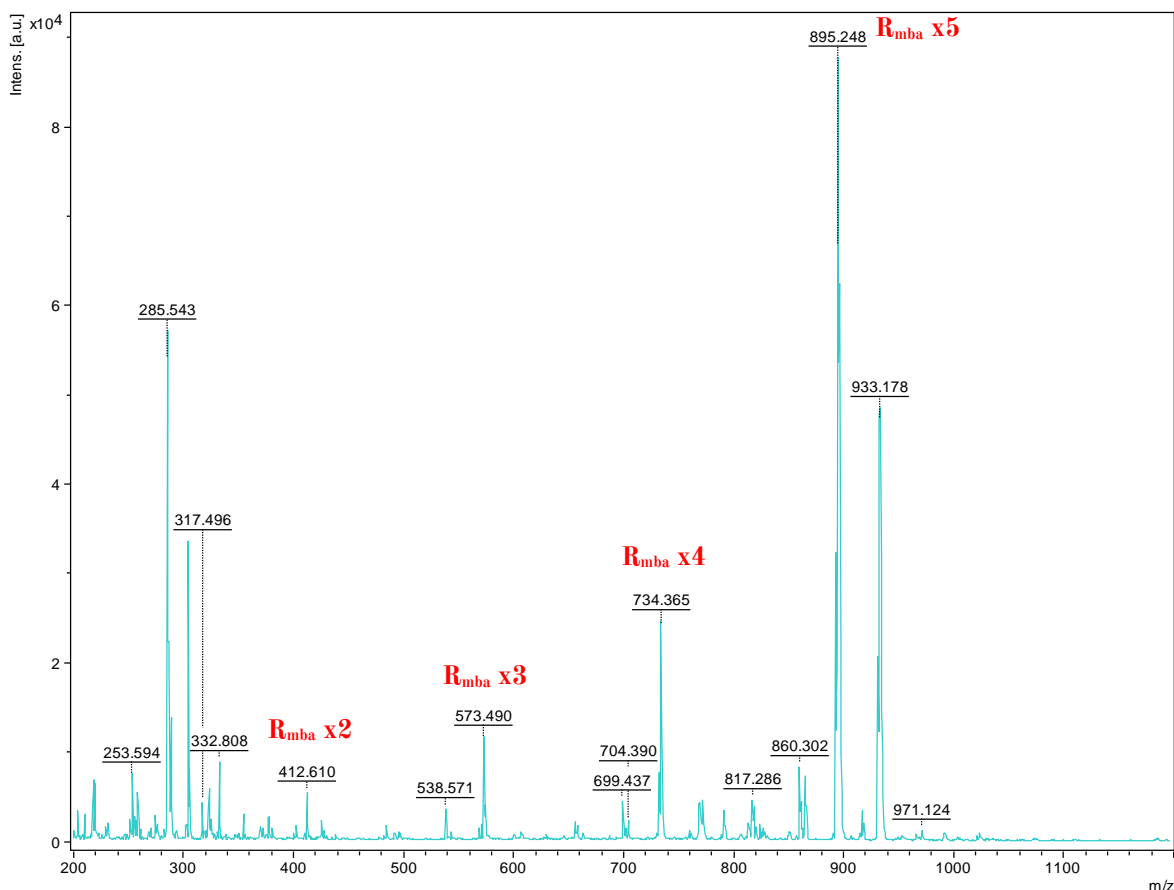
Fig. 29: MALDI-TOF-MS spectrum of the R_{mba} pentamer (product [4]) using ATT matrix

Table 14: Theoretical mass peaks of the R_{mba} pentamer (Product [4]) and shorter chain lengths

	$R_{mba,}$ x2	$R_{mba,}$ x3	$R_{mba,}$ x4	$R_{mba,}$ x5
[M+H]$^+$	412.2 m/z	573.3 m/z	734.4 m/z	895.5 m/z
[M+Na]$^+$	434.2 m/z	595.3 m/z	756.4 m/z	917.5 m/z
[M+K]$^+$	450.2 m/z	611.3 m/z	772.3 m/z	933.4 m/z

The MALDI data show the predicted product mass-peak at 895.25 m/z with an error of -0.25 m/z in its hydrogen and potassium adduct, respectively. Shorter chain lengths can be observed which either suggests synthesis errors or fragmentation during the MALDI-process. The -2 Δ m/z trace peak is present from R_{mba} x2 to R_{mba} x5 as depict in [Fig. 29]. Measuring the product using ATT-matrix reveals impurities and shorter chain lengths. Fig. 30 shows a zoomed in view on the product peak, where the -2 Δ m/z artefact is clearly visible.
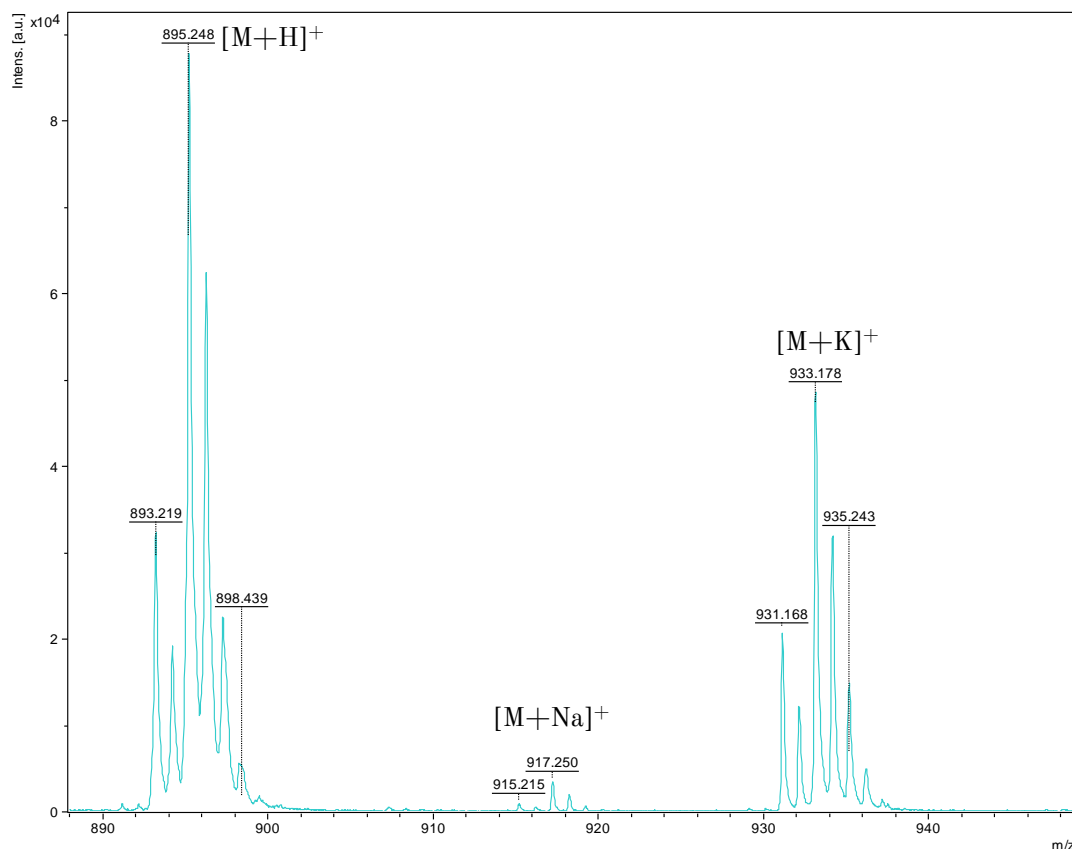
Fig. 30: MALDI-TOP-MS spectrum of the R_{mba} *pentamer (product [4]) (zoom in on product peak) using ATT matrix*

Due to investigations of Papac *et al.* it is known that the ATT matrix can cause fragmentation of sialised peptides.[21] ATT could also cause fragmentation of the oligopeptoid in that case. Measuring the same sample with a different matrix reveals if the trace peaks derive from the matrix or from synthesis errors.

4.3.2. MALDI-TOF-MS analysis of the R_{mba} pentamer (product [4]) using DHB-matrix

The matrix DHB was also tested for MALDI-TOF-MS measurement. 1 μL of a 1mg/mL of the R_{mba} x5 (product [4]) solution (in MeOH) was pipetted on the MALDI-plate. After drying in vacuum, 10 μL of the DHB matrix-solution (10 mg/mL in ACN) was added and dried again. The sample was measured in positive mode.
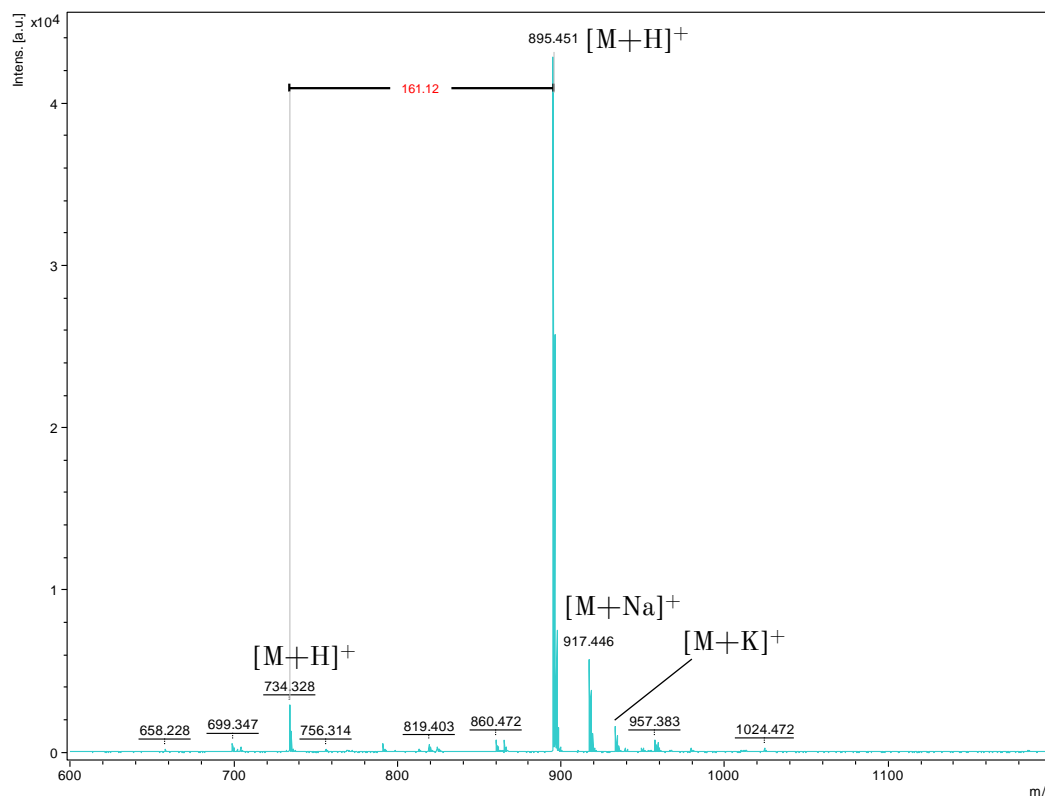
Fig. 31: MALDI-TOF-MS spectrum of of the R_{mba} *pentamer (product [4]) using DHB matrix*

The MALDI-TOF-MS spectrum shows the predicted mass peak in high intensity at 895.451 m/z with an error of -0.05 Δ m/z. The mass peak at 734.3 m/z corresponds to R_{mba} x4, which is an artefact of the monomer addition step which doesn't yield 100%. The product peak shows minimal signs of fragmentation. The comparison of the spectra from the product measured with ATT matrix [Fig. 29] and DHB matrix [Fig. 31] suggests that fragmentation is strongly matrix dependent. Below 600 m/z, no mass was found.
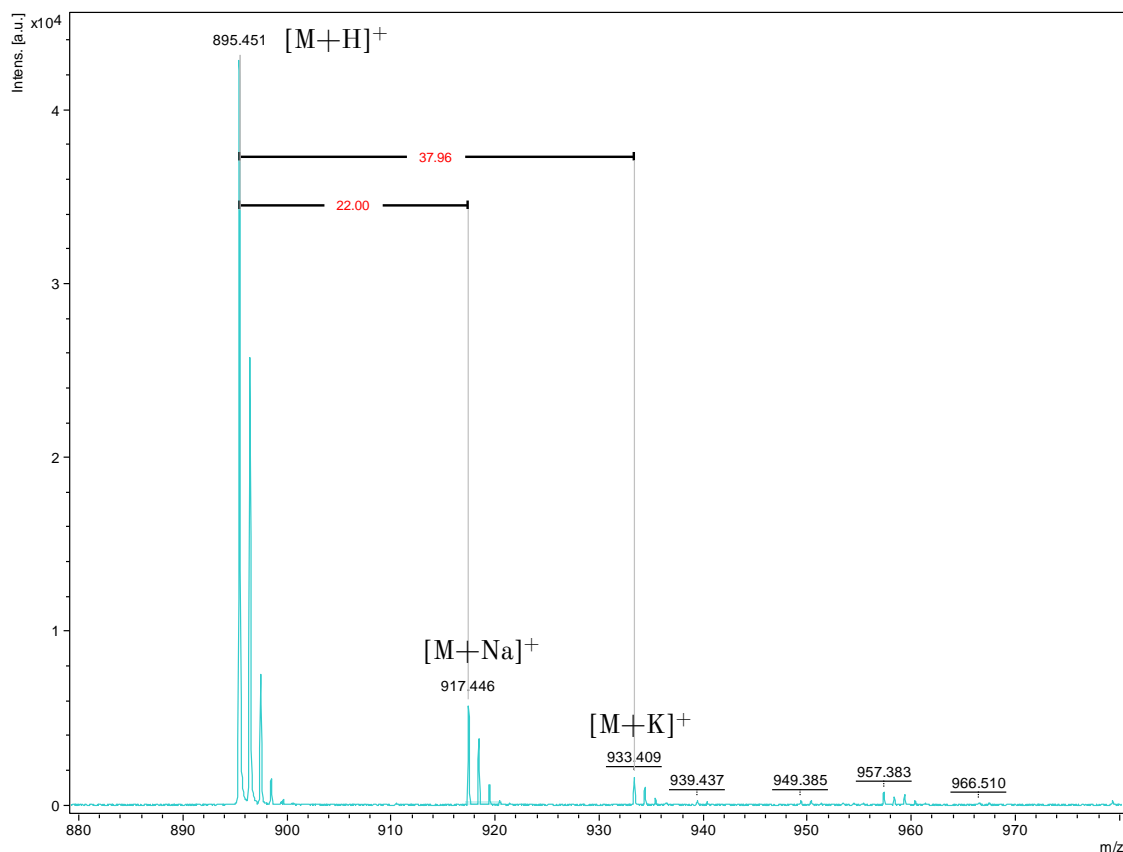
Fig. 32: MALDI-TOF-MS spectrum of the R_{mba} pentamer (product [4]) using DHB matrix (zoomed on product peak at 895 m/z)

A zoom in on the product peaks [Fig. 32] also show the normal isotopic peak distribution without a -2 Δ m/z trace peak. Hydrogen, sodium and potassium adducts are observable as predicted. The spectrum using DHB matrix suggests that the synthesis is efficient with very little errors and only little impurities unknown compositions in the sample.

4.3.3.   MALDI-TOF-MS LIFT (Laser Induced Fragmentation Technique) using DHB matrix

For further investigation upon the composition of the molecule, the R_{mba} x5 (product [4]) was analyzed with LIFT, which is a post-source decay technique to fragment the product molecule using DHB matrix. Furthermore, the data can be compared to the fragmentation pattern derived from the ATT – matrix. 1 μL of a 1 mg/mL R_{mba} x5 (product [4]) in MeOH solution was pipetted on the MALDI-plate. After drying in vacuum, 1 μL of the ATT matrix-solution (3 mg/mL in ACN) was added and dried again. The result is shown in [*Fig.* 33]
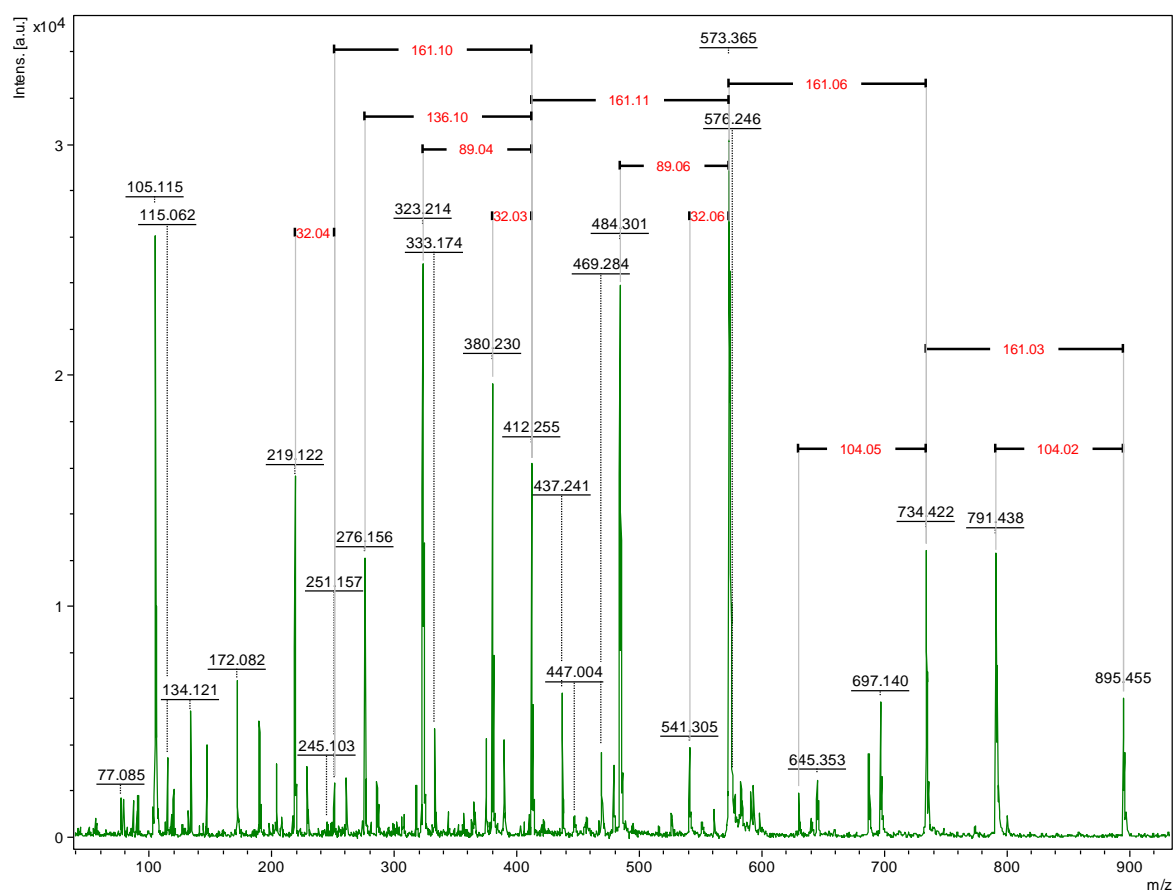
Fig. 33: MALDI-TOF-MS spectrum of of the R_{mba} pentamer (product [4]) using LIFT-technique and DHB matrix

The fragmentation pattern differs from the one which is caused by the ATT matrix. Fragmentation is not a chemical reaction; therefore, parts obtain charges due to the uneven distribution of electrons during the fragmentation process.
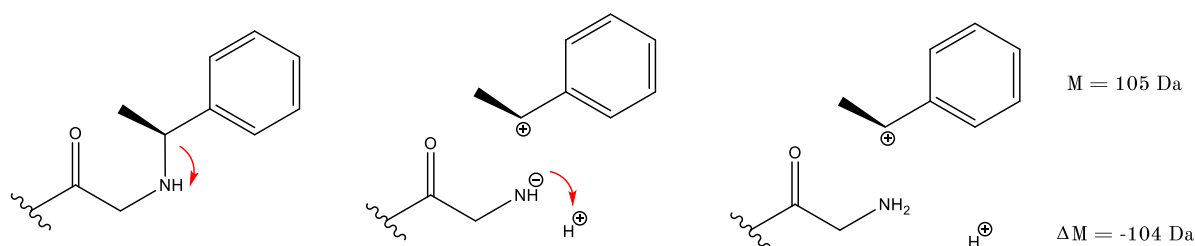

Fig. 34: Mode of action of the fragmentation

During the fragmentation, the electron moved to the nitrogen as the more electronegative atom, thereby charging it negatively. The nitrogen is rapidly protonated from the omnipresent hydrogen provided by the matrix, removing the negative charge on the amino group. In positive mode, the neutral molecule reaches the detector accompanied by an adduct. The loss in mass is -104 $\Delta m/z$. The positively charged ethylbenzene fragment

can be found at its exact mass (105 m/z). In **Fehler! Verweisquelle konnte nicht gefunden werden.**, every significant mass peak is explained via structural formula.


251.41 Da

645.34 Da

412.22 Da

484.26 Da

573.31 Da

323.18 Da

734.39 Da

162.09 Da

541.28 Da

437.22 Da

333.16 Da

229.09 Da

380.20 Da

276.13 Da

172.07 Da

687.35 Da

219.11 Da

115.05 Da
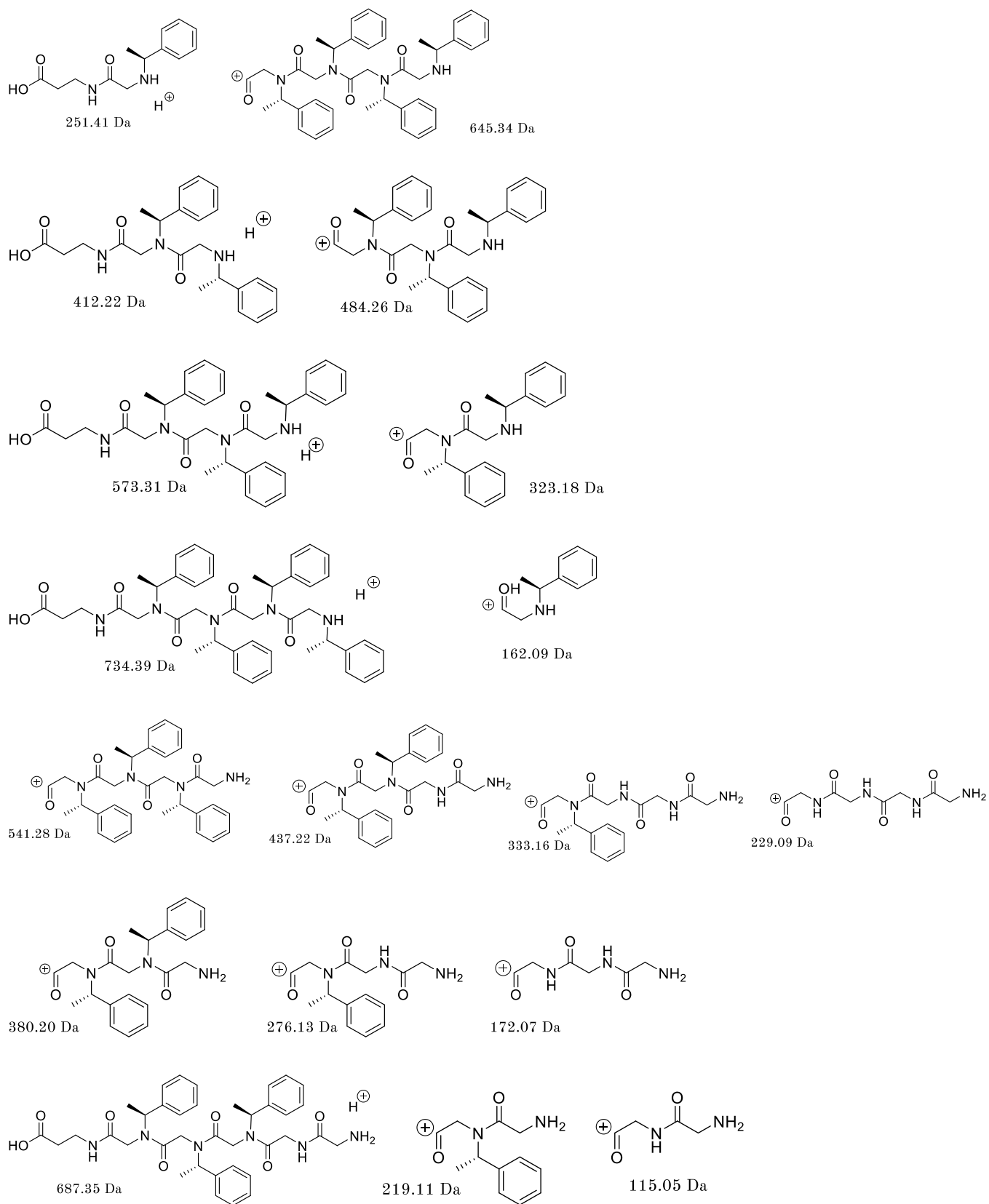
Fig. 35: Fragments found in: MALDI-TOF-MS of 5x R$_{mba}$ using LIFT-technique

For the peak at 679.14 m/z no explanation is currently available.

No agreement between the fragments resulting from the LIFT technique and the fragments caused by the ATT matrix is observed. This data shows that the ATT matrix should not be used while analyzing polypeptoids. The ATT matrix not only causes fragmentation of sialised peptides[21], but seemingly also of peptoids. These fragmentations cannot be imitated by a LIF-technique.

3.1.1.   MALDI-TOF-MS analysis of R_{mba} pentamer (product [4]) using ACH matrix in positive mode

A reason for the absence of the trace peaks present in the spectrum of the ATT matrix in comparison to the spectrum with the DHB matric can also be that the sample doesn't fly good enough with the DHB matrix. For this reason, a third matrix was used to verify that the whole product reaches the detector. A commonly used matrix for oligopeptide or -peptoid analysis with a molecular weight of 500 – 66000 g/mol is α-cyano-4-hydroxycinnamic acid. 1 µL of a 1 mg/mL of R_{mba} x5 (product [4]) in MeOH solution was pipetted on the MALDI-plate. After drying in vacuum, 1 µL of the ACH matrix-solution (3 mg/mL) was added and dried again. The results are shown in Figure [**Fehler! Verweisquelle konnte nicht gefunden werden.**]
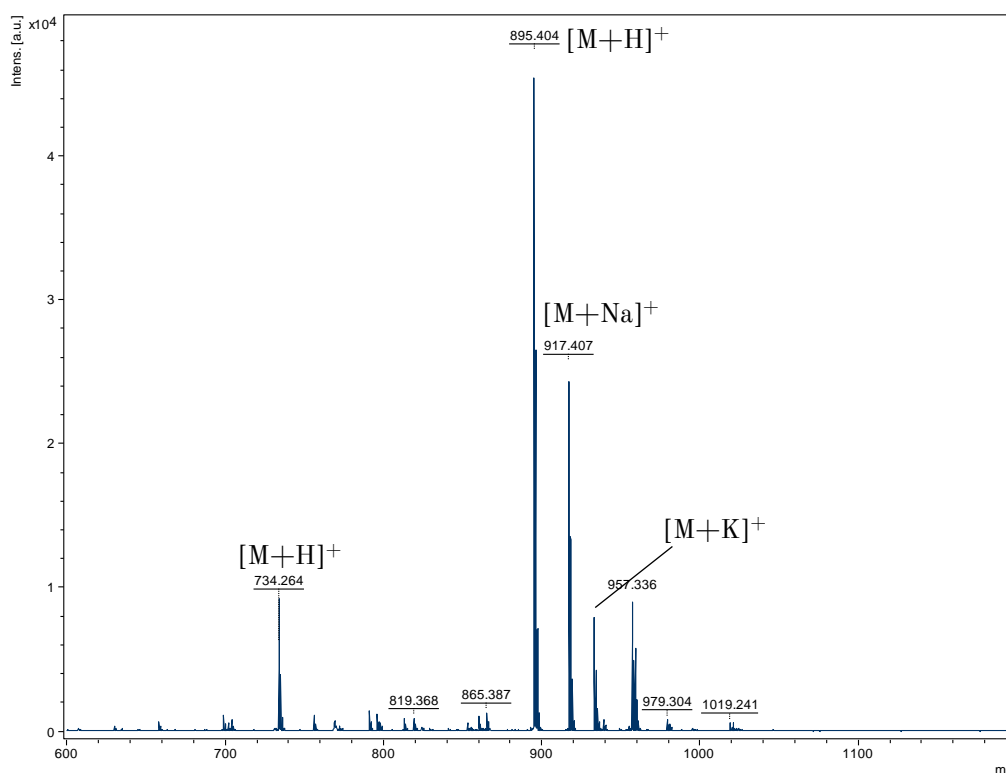

Fig. 36: MALDI-TOF-MS spectrum of the R_{mba} pentamer (product [4]) using DHB Matrix
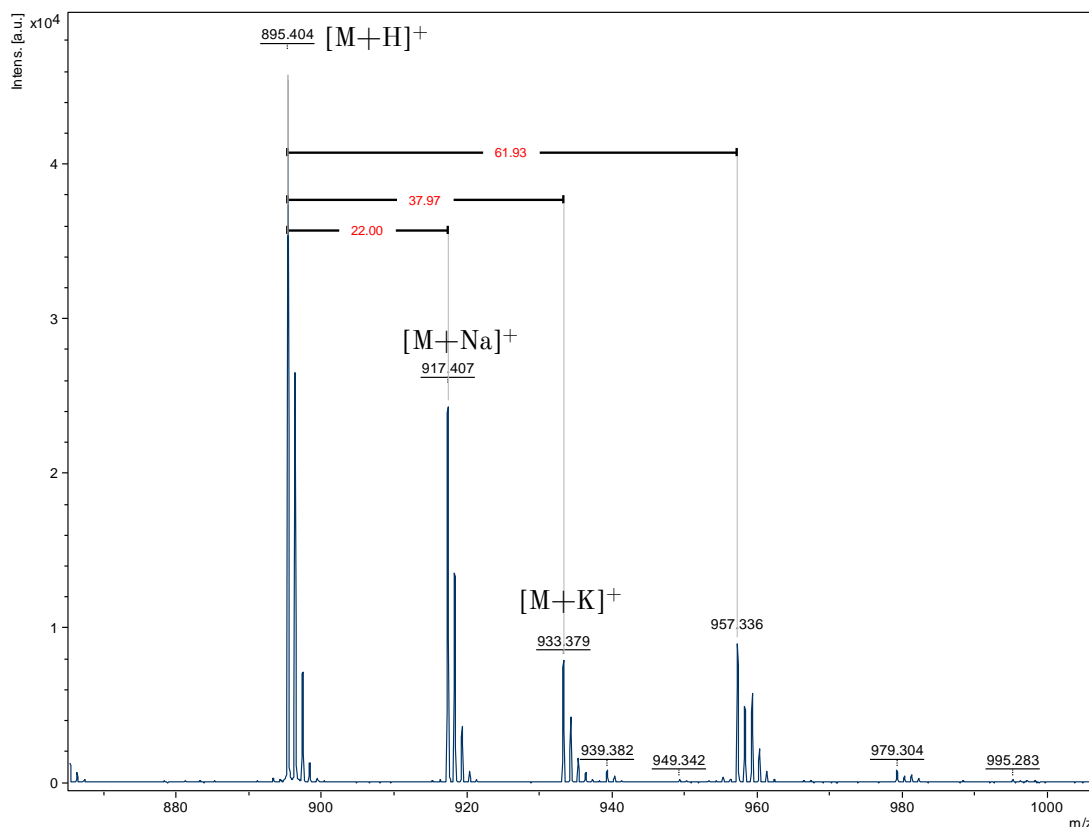
Fig. 37: MALDI-TOF-MS spectrum of the R_{mba} pentamer (product [4]) using DHB Matrix, zoomed in at product peek at 895.40 m/z

In the spectrum, the product-peak with its adduct $[M+H]^+ = 895.40$ m/z, $[M+Na]^+ = 917.41$ m/z $[M+K]^+ = 933.38$ m/z can be observed with an error of < 0.15 Δ m/z. Furthermore, a peak at 957.34 m/z is present which suggests another adduct with a mass of 62.33 m/z. No adduct with this mass is found in literature. In contrast to the MADLI-TOF-MS spectrum resulting from the measurement with the DHB matrix, the intensity of R_{mba} x4 is increased which either suggest fragmentation of the R_{mba} pentamer (product [4]) or that the R_{mba} x4 measured with DHB doesn't reach the detector. No significant mass below 700 m/z is found.

It appears that DHB has the least influence on creating trace peaks and presence of shorter chain lengths product fragmentation of the three matrices ATT, DHB & ACH. ACH gives rise to another unknown adduct peak at $+62.33$ Δ m/z and increases the intensity of R_{mba} x4. The spectrum with ATT matrix shows a significant amount of trace peaks and shorter chain lengths. This phenomenon could derive from fragmentation of the matrix or that the fragments themselves don't reach the MALDI-TOF-MS detector with ACH or DHB.

4.4. Using HPLC for determining the increase of hydrophobicity

The increase in hydrophobicity can be observed using reverse phase chromatography, with growing chain length when using hydrophobic monomers. Important for a synthesis where the monomer addition step doesn't yield 100% is the purification of the product from short chain lengths of the products. A pentamer with the monomer R_{mba} was synthesized on 1000 mg resin. Approximately 100 mg resin was removed after every monomer addition step and the last two acetylation steps:

1) R_{mba} x1   product [5]
2) R_{mba} x2   product [6]
3) R_{mba} x3   product [7]
4) R_{mba} x3 + Acetylated   product [8]
5) R_{mba} x4   product [9]
6) R_{mba} x4 + Acetylated   product [10]
7) R_{mba} x5   product [11]

[5] [6] [7] [9] [11]   [8] [10]
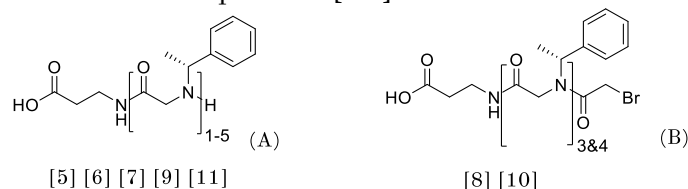
Fig. 38: (A) Homo-polypeptoid using R_{mba}; chain length: 1-5 [5][6][7][9][10](B) Acetylated homo-polypeptoid using R_{mba}; chain length: 3 and 4 [8][10]

Table 15: Amounts used for the synthesis of product [5] − [11] on 2-CTC resin

One Step					
	Amount	DMF	Equivalents	Concentration stock	Final concentration
BrHAc	0.69 g	5 mL	5	1.0 M	0.5 M
DIC	1.39 mL	3.61 mL	9	2.2 M	1.1 M
R_{mba}	2.16 mL	7.84	17	1.79 M	1.79 M
Total					
	Amount	DMF	Equivalents	Concentration	Concentration
BrHAc	3.5 g	25.0 mL	5	1.0 M	0.5 M
DIC	7.0 mL	18 mL	9	2.2 M	1.1 M
R_{mba}	10.8 mL	39.2 mL	17	1.79 M	1.79 M

Table 16: Incubation conditions for the synthesis of products 5-11

Incubation conditions	
Acetylation	5' at room temperature
Monomer addition	90' at 37°C

Products [7] − [11] were cleaved and purified according to "3.3.4. *aboveCleavage & Precipitation*", dissolved in MeOH (1 mg/ mL MeOH) and analyzed with RP-HPLC.

46

HPLC parameters

Resin: silica C18

Solvent A: H$_2$O

Solvent B: ACN

Linear gradient: 2% - 100% B

Runtime: 120 min

Detector wavelength: 214nm
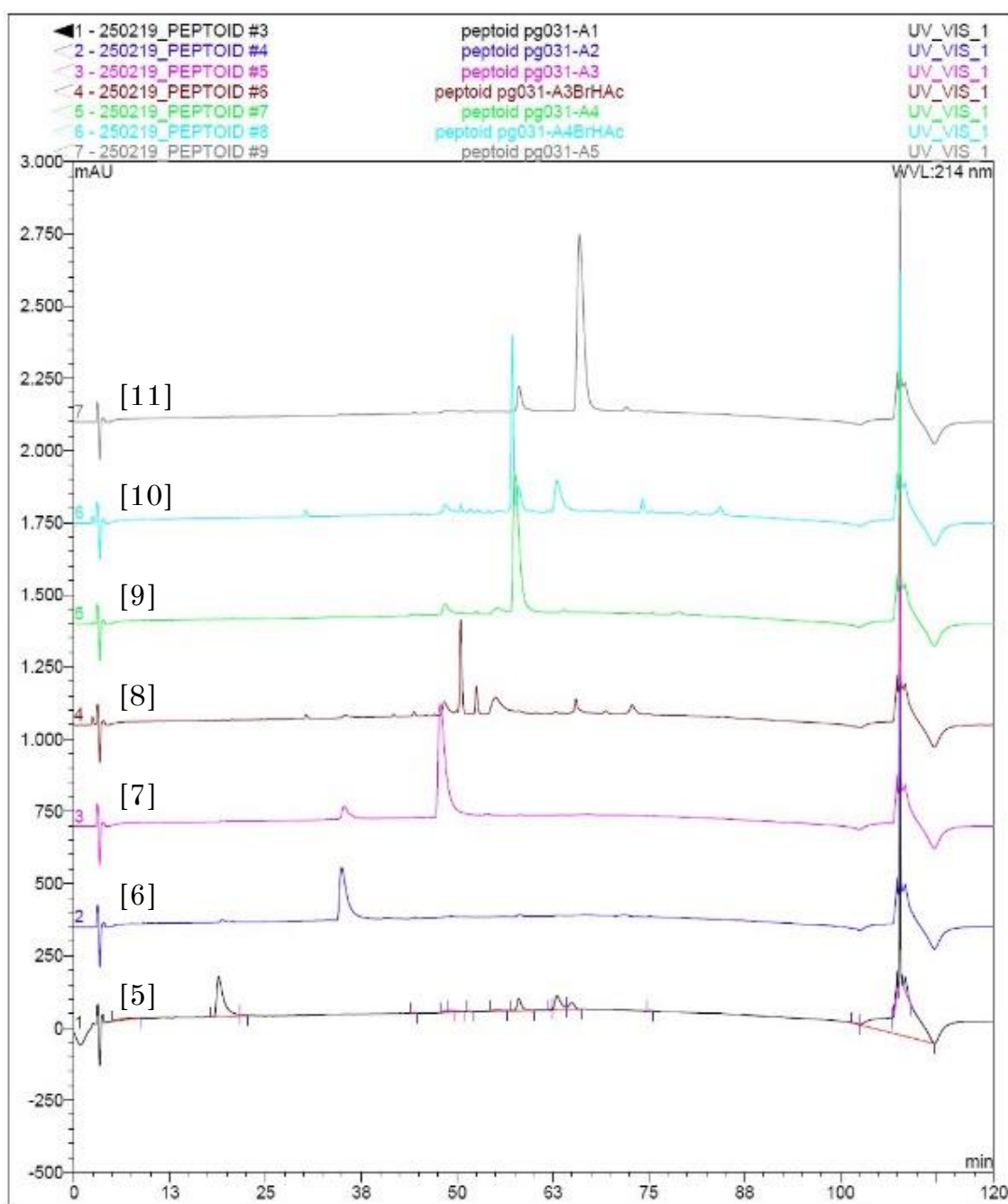
Fig. 39: C18 RP- HPLC spectrum of $R_{mba} x1 - R_{mba} x5$

Table 17: Retention times of $R_{mba} x1 - R_{mba} x5$

	Product	Retention time
[5]	R_{mba} x1	19 min 30 sec
[6]	R_{mba} x2	35 min 25 sec
[7]	R_{mba} x3	48 min 25 sec
[8]	R_{mba} x3 (acetylated)	50 min 30 sec
[9]	R_{mba} x4	57 min 50 sec
[10]	R_{mba} x4 (acetylated)	63 min 00 sec
[11]	R_{mba} x5	66 min 07 sec

The spectrum at 280 nm shows no signal despite that aromatic rings absorb at this wavelength.[22] The strongest peak intensity could be observed at 214 nm. As expected, the hydrophobicity and hence the retention time increases as well, with increasing chain length of the product with the monomer R_{mba}. The difference in retention time is reduced with growing chain length. According to this data it is possible to separate products with different chain length to purify the product with this method. At a specific length, separation will not be possible with these parameters since the difference in retention time will be too short. The difference in retention time from R_{mba} x1 and R_{mba} x2 is approximately 16 min. The difference in retention time from R_{mba} x4 and R_{mba} x5 is approximately 9 min. We expect insufficient separation at a chain length of around R_{mba} x40 − x50. After that the retention times of two subsequently chain lengths are almost identical and so separation can be observed.

4.5. Synthesis of polypeptoids (R_{mba} Dodecamer) with longer chains

The oligopeptoid must exceed a specific length to span through cell-membranes. Membranes of prokaryotes are typically 4 nm thick[23]. A dodecamer, with 40 sp^3 bonds present and an average bond length of approx. 150 pm[7] results in a total length of 6 nm. The synthesis of the peptoid using the monomer R_{mba} (Product [12]) was conducted on 1000 mg freshly loaded & deprotected resin. The volume of DMF and the amounts of BrHAc & DIC were adjusted to reach the preferred equivalence numbers of 10 and 9 respectively.
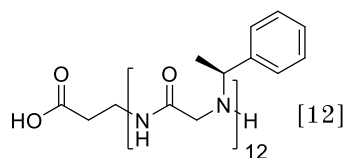
Fig. 40: Structural formula Dodecamer of R_{mba} [12]

Table 18: Amounts used for the synthesis of R_{mba} x12 (product [12]) on 1000 mg 2-CTC resin (substitution level of 1 mmol/g)

One Step					
	Amount	**DMF**	**Equivalents**	**Stock concentration**	**Final concentration**
BrHAc	1.39 mg	10 mL	10	1.0 M	0.5 M
DIC	1.39 mL	8.61 mL	9	1.1 M	0.55 M
R_{mba}	2.16 mL	7.84 mL	17	1.79 M	1.79 M
Total					
	Amount	**DMF**	**Equivalents**	**Stock concentration**	**Final concentration**
BrHAc	7.09 mg	51.0 mL	10	1.0 M	0.5 M
DIC	7.11 mL	43.9 mL	9	1.1 M	0.55 M
R_{mba}	11.04 mL	40.0 mL	17	1.79 M	1.79 M

Table 19: Incubation conditions for the synthesis of R_{mba} x12 (product [12])

Incubation conditions	
Acetylation	5' at room temperature
Monomer addition	90' at 37°C

The polypeptoid R_{mba} x12 (product [12]) were cleaved and purified according to "3.3.4. *aboveCleavage & Precipitation*"

Theoretical mass-yield: 2023.5 mg

Practical mass-yield: 1380 mg

Following equation (4) and assuming a substitution level of 1 mmol/g, a yield of 68.21% was calculated. Due to monomer addition efficiency below 100%, shorter chain lengths of the product accumulate which lead to meaningless yield-data, considering different molar weights in the sample. A purification step is important to determine the exact mass-yield. Preparative reversed phase HPLC serves as an adequate method.

4.5.1. MALDI-TOF-MS of the dodecamer using ATT matrix

To further analyze the ratios of shorter chain length in comparison to the product, the sample was measured with MALDI-TOF-MS. 1 µL of a 1mg/mL R_{mba} x12 (product [12]) in MeOH solution was pipetted on the MALDI-plate. After drying in vacuum, 1 µL of the ATT matrix-solution (3 mg/mL in CAN) was added and dried again. The sample was measured in positive mode. A strong fragmentation can be observed as shown in

[Fig. 41]. The mass difference of 161 Δ m/z derives from the fragmentation of one N-substituted glycine.
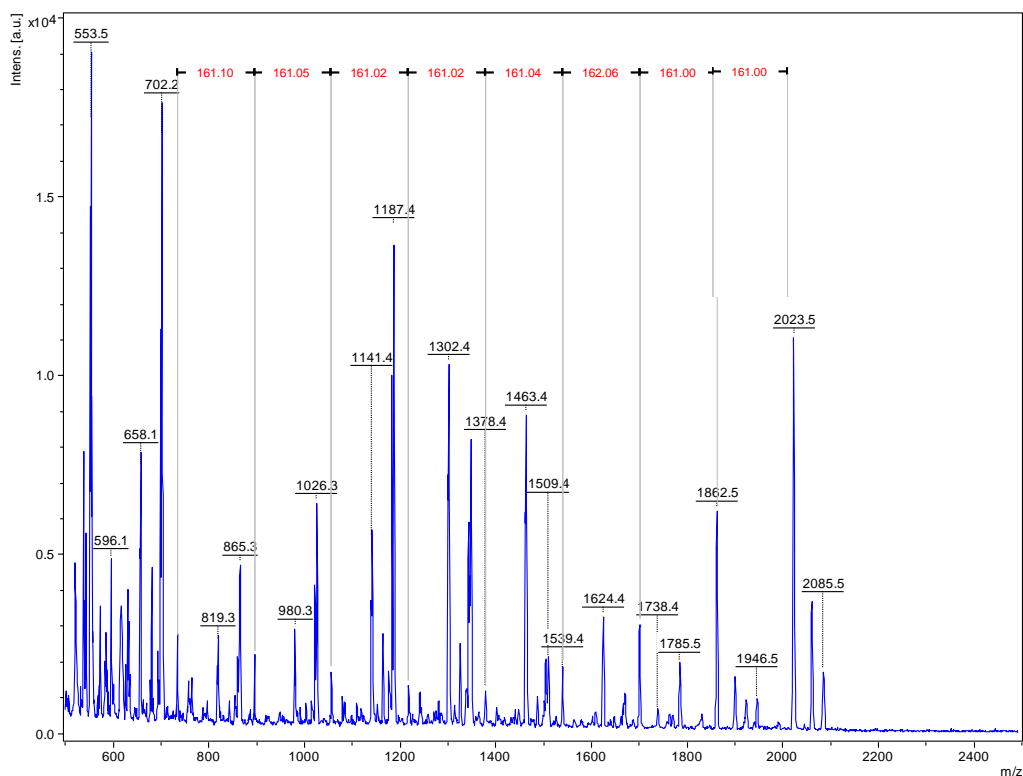

*Fig. 41: MALDI-TOF-MS spectrum of R_{mba} x12 (product [12]) measured with ATT Matrix*
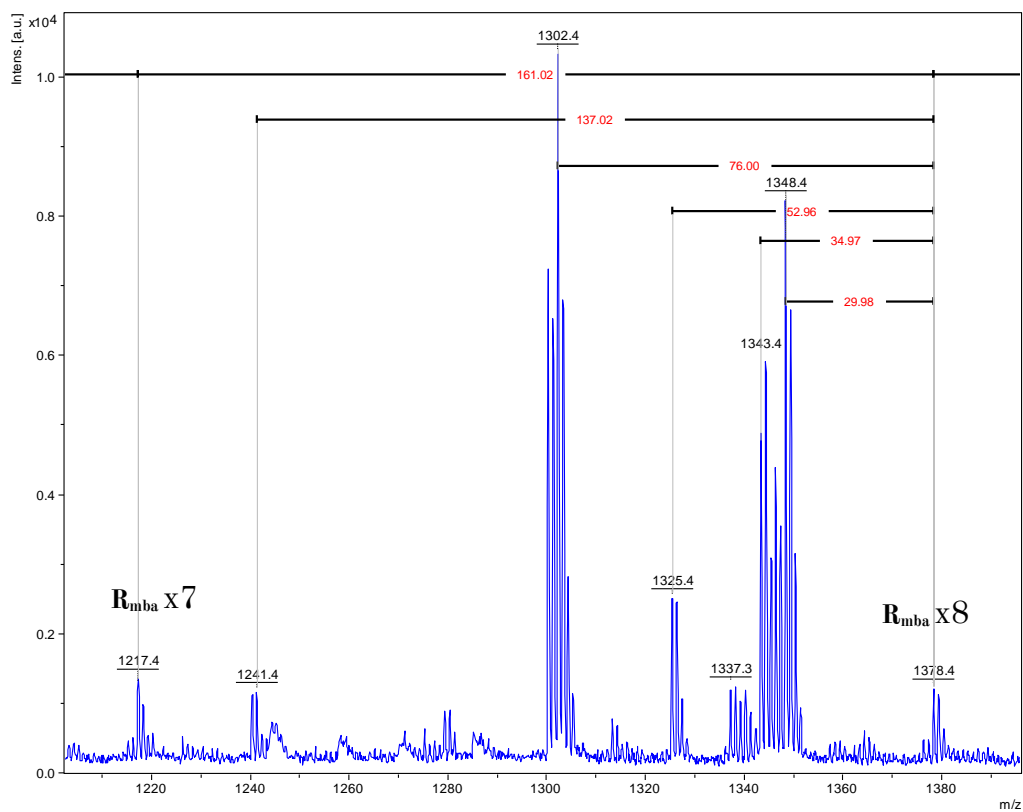
Fig. 42: MALDI-TOF-MS spectrum of R_{mba} x12 (product [12]) (zoom in on R_{mba} x7- R_{mba} x8 fragment) measured with ATT Matrix

Zooming in on the m/z range between R_{mba} x7 & R_{mba} x8 [Fig. 42] the following trace peaks are observable:

- -30 Δ m/z
- -35 Δ m/z
- -76 Δ m/z
- -137 Δ m/z

These trace peaks are observable from the tetramer to the dodecamer. When plotting the peak intensity on a graph, a Poisson distribution of the trace peaks -30 Δ m/z [**Fehler! Verweisquelle konnte nicht gefunden werden.** blue] & - 76 Δ m/z [**Fehler! Verweisquelle konnte nicht gefunden werden.** grey] becomes visible. This distribution can only derive from fragmentation rather than synthesis errors. Accumulating synthesis errors don't follow statistical curves like a Poisson distribution. In the range of the mass-peak for R_{mba} x12 almost no fragments are present. The exact mass from R_{mba} x5 to R_{mba} x12 follows a normal exponential curve [**Fehler! Verweisquelle konnte nicht gefunden werden.** orange] as predicted for a synthesis.
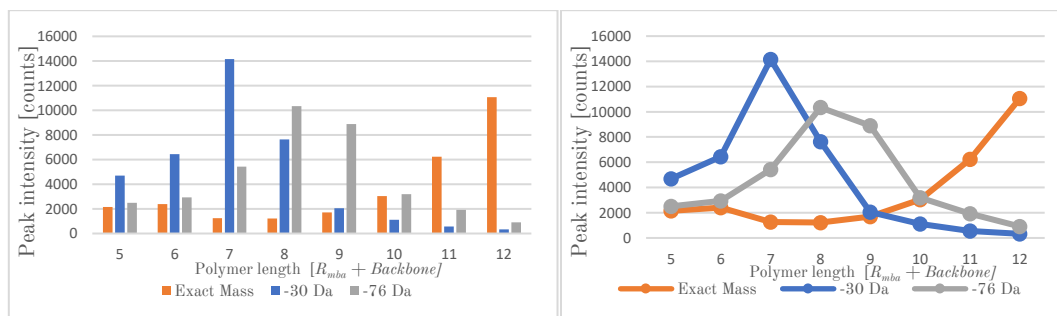
Fig. 43: trend of trace peaks over fragments R_{mba} x5 to Rmba x12 (left: Bar-diagram, right: Line-diagram)

During previous measurements, the exact m/z of the product at its shorter chain lengths was accompanied by a -2 Δ m/z trace peak. In this example only the -76 Δ m/z fragment peak showed this behavior. The exact mass of the product peaks for R_{mba} x5 to R_{mba} x12 follow a normal isotopic peak pattern without the -2 Δ m/z trace peak. As demonstrated above, the ATT matrix has a strong influence on the sample so that measurements with a different matrix are necessary.

4.5.2. MALDI-TOF-MS of the dodecamer using DHB matrix

As previous experiments have shown, ATT causes fragmentation of the product. The sample was measured again with DHB matrix. 1 µL of a 1 mg/mL R_{mba} x12 (product

[12]) in MeOH solution was pipetted on the MALDI-plate. After drying in vacuum, 1 μL of the DHB matrix-solution (10 mg/mL) was added and dried again. The sample was measured in positive mode.
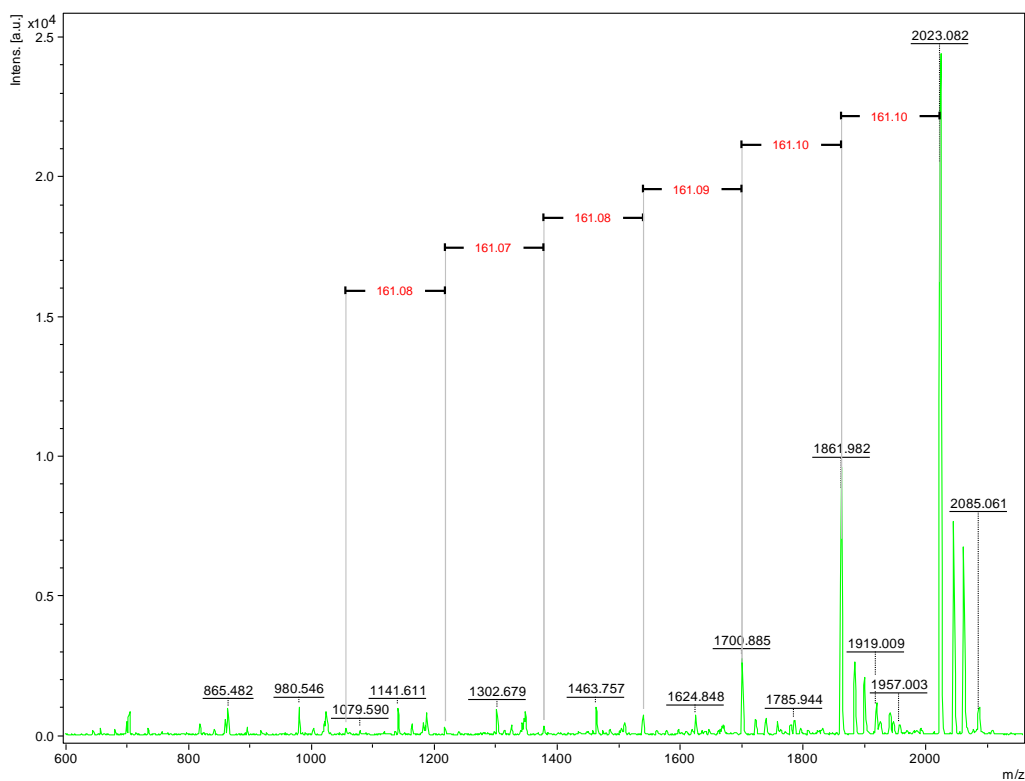

*Fig. 44: MALDI-TOF-MS spectrum of R_{mba} x12 (product [12]) using DHB Matrix*

$[M+H]^+$
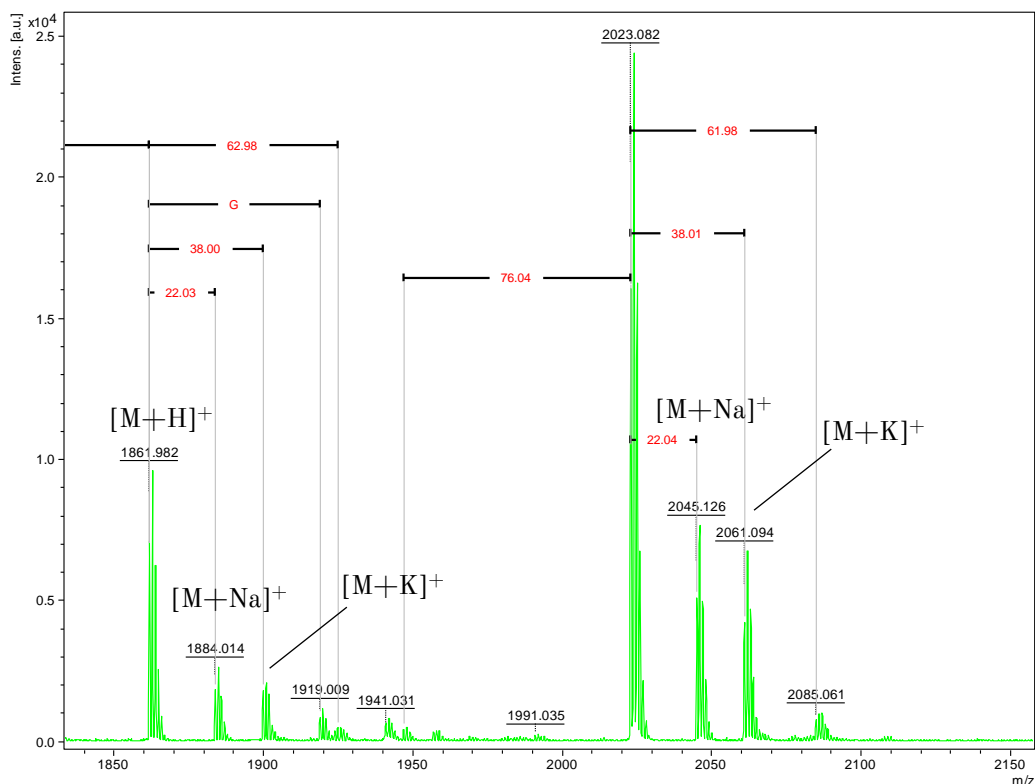
Fig. 45: MALDI-TOF-MS spectrum of R_{mba} x12 (product [12]) using DHB Matrix (zoom in on product peak at 2023.06 m/z)

The predicted m/z peaks for the product are observable at m/z = 2023.082 with an error of -0.02 Δ m/z as seen in Fig. 44 and Fig. 45. The sodium and potassium adduct are present. No significant fragmentation occurs. The synthesis inefficiency becomes visible as shorter chain lengths of the product are visible with a mass difference of 161 Δ m/z. The -76 Δ m/z trace peak is still visible, meaning that ATT only enhances the formation of this by-product and not causing it.

4.5.3.   MALDI-TOF-MS of the dodecamer using ACH matrix (+ sodium excess)

During a measurement with sodium excess, the adduct peak is shifted to the sodium peak by adding sodium acetate (NaHAc). With this sodium excess, a shift in the spectrum from +1 (hydrogen) and +39 Δ m/z (potassium) to +22 Δ m/z (sodium) from the exact mass is induced to create one dominant peak. 1 µL of a 1 mg/mL R_{mba} x12 (product [12]) in MeOH solution was pipetted on the MALDI-plate. After drying in vacuum, 1 µL of NaHAc (20 mM) is added and dried. Afterward, the ACH matrix-solution (3 mg/mL) is added and dried again.
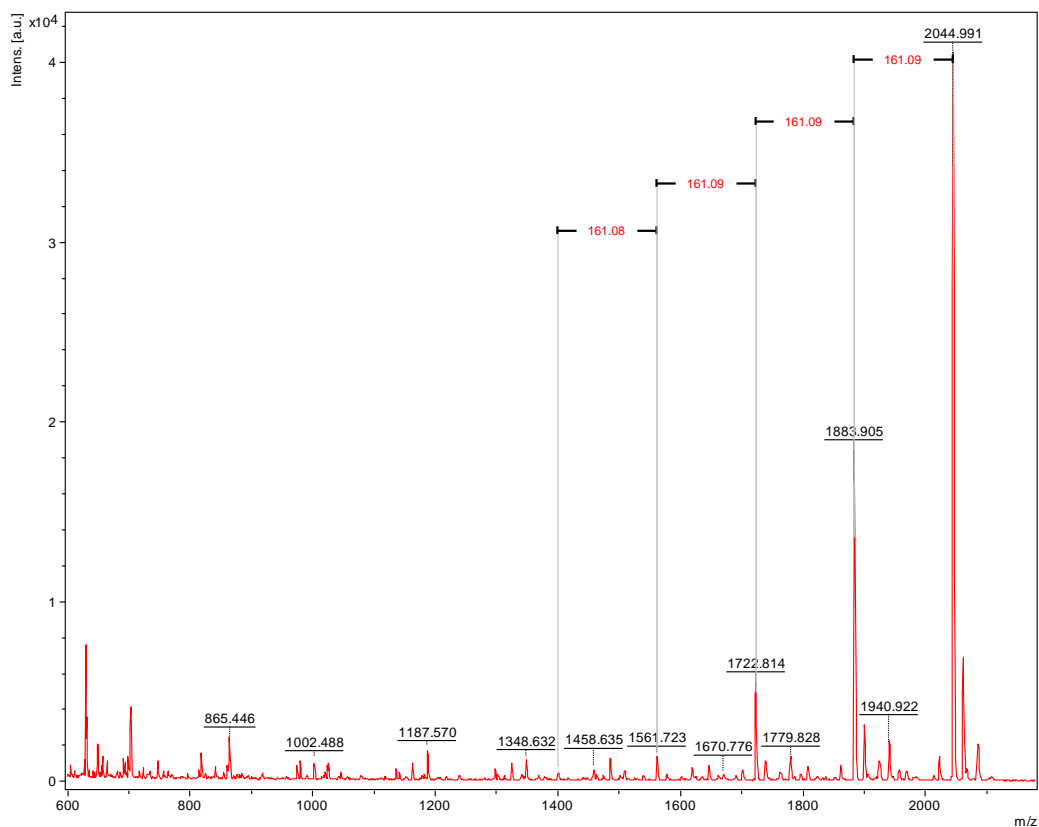
Fig. 46: MALDI-TOF-MS spectrum of the R_{mba} dodecamer (product [12]) using ACH-matrix + Sodium excess
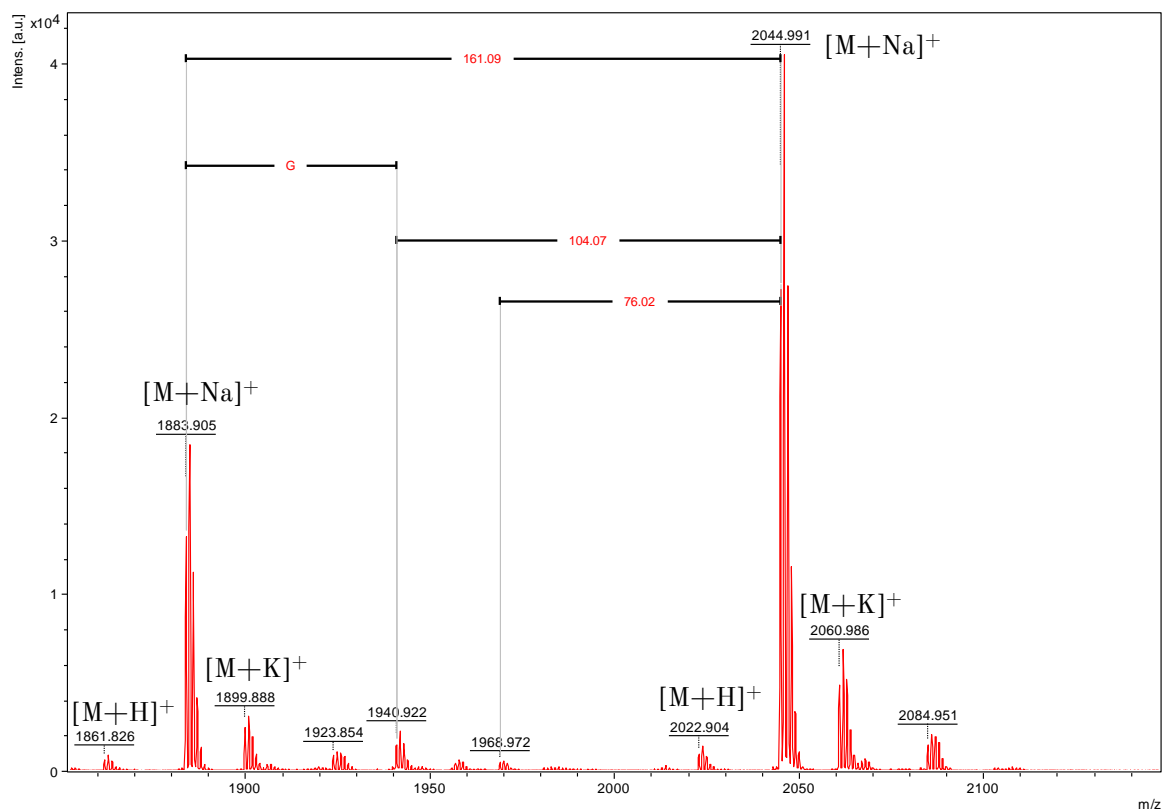

Fig. 47: MALDI-TOF-MS spectrum of the R_{mba} dodecamer (product [12]) using ACH-matrix + Sodium excess (zoom in on product peak at m/z = 2044.99)

The spectrum contains the predicted m/z product peaks at its sodium adduct at 2044.99 m/z with an error of 0.01 Δ m/z *as* seen in Fig. 46 and Fig. 47. Shorter chain lengths of the product are present in the sample, due to the fact that the yield of each monomer addition is less than 100%. Only negligible trace peaks are observed upon zooming in on the product peak position. The difference of -104 Δ m/z results from fragmentation shown in **Fehler! Verweisquelle konnte nicht gefunden werden.**. The loss of the side-group of the *N*-substituted glycine results in a difference of -57 Δ m/z, which is the mass of an incorporated glycine (denoted with the letter G) visualized in Fig. 48.
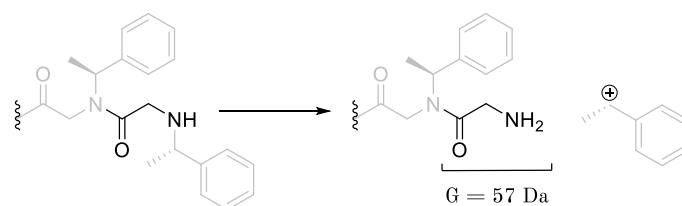

Fig. 48: Visualization of glycine, incorporated into a oligopeptoid

4.6. Cross-reaction of alternating hydrophilic and hydrophobic monomers

To create amphiphilic helices, the synthesis of a polypeptoid with alternating hydrophobic and hydrophilic monomers must be possible. The para-substituted halogen derivate was used to demonstrate the synthesis of amphiphilic oligomers. The synthesis of the sequence $[R_{mba} - BrR_{mba}]_2$ was conducted on 500 mg freshly loaded and activated 2-CTC resin.
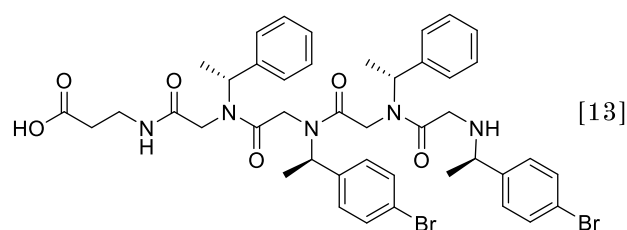

Fig. 49: Hetero-polypeptoid with the sequence $[R_{mba} - BrR_{mba}]_2$ (product [13])

The BrR_{mba} monomer solution was captured after the first monomer addition step and reused at the second one. In the previous experiments, the amount of the bromoacetic acid was halved to reach the low concentration, hence the equivalence number was halved as well. By adjusting the volume and increasing the amount of bromoacetic acid, the equivalence number was raised to 10.

Table 20: Amounts used for the synthesis of [R_{mba} - BrR_{mba}]₂ (product [13]) on 500 mg 2-CTC resin (substitution level 1 mmol/g)

One Step					
	Amount	**DMF**	**Equivalents**	**Concentration stock**	**Final concentration**
BrHAc	0.69 g	6 mL	10	0.84 M	0.42 M
DIC	0.70 mL	5.3 mL	9	0.92 M	0.46 M
R_{mba}	1.08 mL	4.92 mL	17	1.49 M	1.49 M
BrR_{mba}	1.3 mL	5.7 mL	18	1.14 M	1.14 M
Total					
	Amount	**DMF**	**Equivalents**	**Concentration stock**	**Final concentration**
BrHAc	2.89 g	25 mL	10	0.84 M	0.42 M
DIC	2.90 mL	22.1 mL	9	0.92 M	0.46 M
R_{mba}	2.34 mL	10.66 mL	17	1.49 M	1.49 M
BrR_{mba}	1.3 mL	5.7 mL	18	1.14 M	1.14 M

Table 21: Incubation conditions during synthesis of [R_{mba} - BrR_{mba}]₂ (product [13])

Incubation conditions	
Acetylation	5' at room temperature
Monomer addition	90' at 37°C

The oligopeptoid (product [13]) was cleaved and purified according to "3.3.4. aboveCleavage & Precipitation"

The mass yield of the harvested product amounted 375 mg. With equation (4) assuming a substitution factor of 1 mmol/g and a molar mass of M(Product[5]) = 889.2 g/mol a mass-yield of 84.06% was calculated. This increase in yield suggest derives from the raise of the equivalence number. To make a statement about the composition of the product harvested from the resin, mass spectrometry analysis is necessary.

4.6.1. MALDI-TOF-MS analysis of [R_{mba} - BrR_{mba}]₂ (product [13])

[R_{mba} - BrR_{mba}]₂ (product [13]) was analyzed with MALDI-TOF-MS to examine the purity of the product. 1 µL of a 1mg/mL [R_{mba} - BrR_{mba}]₂ (product [13]) in MeOH solution was pipetted on the MALDI-plate. After drying in vacuum, 1 µL of the DHB matrix-solution (10 mg/mL) was added and dried again. The sample was measured in positive mode.

The MALDI-TOF-MS spectrum shows the product peak at 892.25 m/z with an error of 0.05 Δ m/z. The sodium adducts are dominant in contrast to the hydrogen and the potassium peaks. Very few impurities are visible. The peak distribution visible in Fig. 50 derives from the element bromine which occurs in nature in two different isotopes:

1) 79 *m/z* ~50 %
2) 81 *m/z* ~50 %

which result in the -2 Δ m/z peak pattern. This -2 Δ m/z artefact is not comparable with the trace peak resulting from the measurement with ATT matrix.
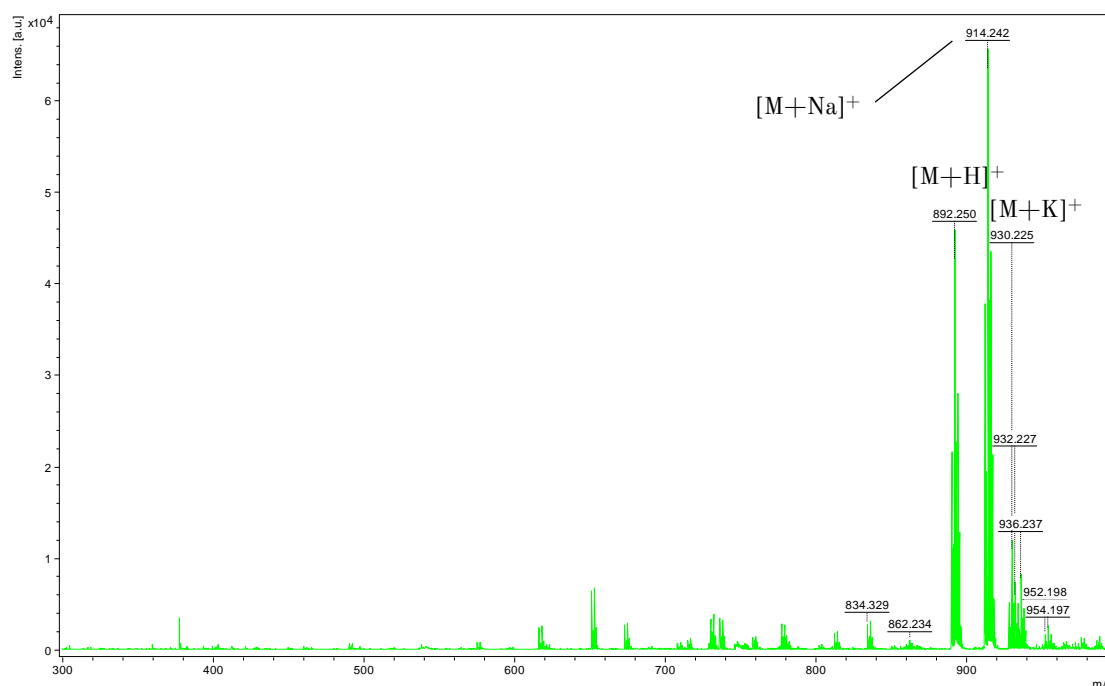

*Fig. 50: MALDI-TOF-MS spectrum of the oligopeptoid (product [13]) using DHB matrix*
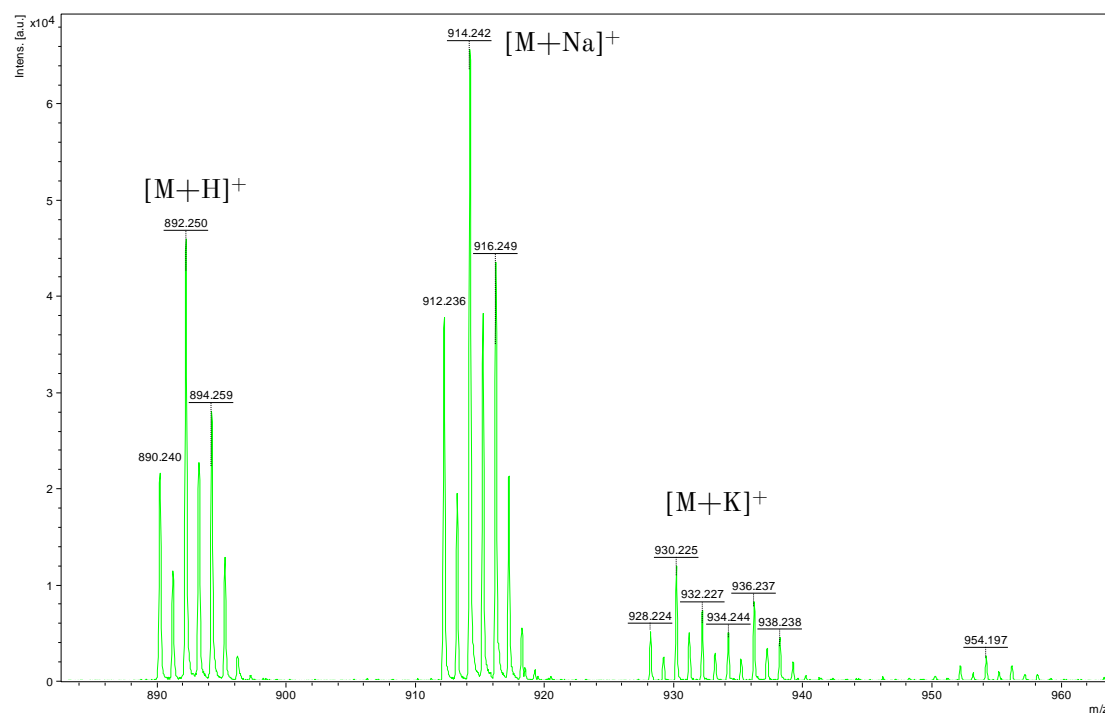
Fig. 51: MALDI-TOF-MS spectrum the oligopeptoid (product [13]) using DHB matrix (zoom in on product peak at 914.24 m/z)

According to this data it is possible to synthesize an oligo-peptoid with alternating a hydrophobic and hydrophilic monomer respectively. The yield shows that it is possible to reuse the monomer solution after capturing the supernatant of the monomer addition

step and still obtain high yields. The low amount of impurities that were present could be eliminated using preparative HPLC.

4.7. Cross-reaction of alternating hydrophilic and hydrophobic monomers

Halogens are commonly used modification groups. However, incubation conditions needed for altering halogens into different active groups can be harsh. In the case of modifying BrR_{mba} to AzR_{mba} high temperatures are reached which could destroy the peptoid. For this reason, the synthesis-step of the monomer AzR_{mba} from BrR_{mba} is necessary before incorporation in the oligo peptoid. The monomer was synthesized according the manual "*3.1. Synthesis of the monomer 4-azido-(R)-(+)-α-Methylbenzylamine (product [1])*". The synthesis of a dodecamer with the sequence [R_{mba} - R_{mba} - AzR_{mba}]$_4$ was conducted on 250 mg freshly loaded 2-CTC resin:
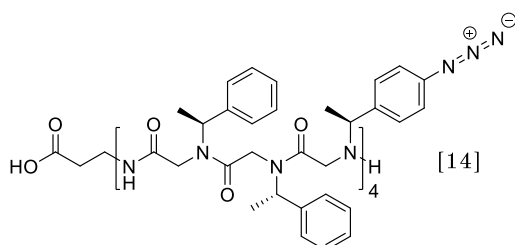

*Fig. 52: Hetero-polypeptoid dodecamer with the sequence [*Rmba* - *Rmba* - *AzRmba*]4 (product [14])*

The supernatant of the monomer addition step containing AzR_{mba} was captured and reused for the following monomer addition step.

Table 22: Amounts used for the synthesis of [R_{mba} - R_{mba} - AzR_{mba}]4 (product [14]) on 250 mg 2-CTC resin assuming a substitution level of 1.25

One Step					
	Amount	**DMF**	**Equivalents**	**Concentration stock**	**Final Concentration**
BrHAc	0.43 mg	3 mL	10	1.04 M	0.52 M
DIC	0.43 mL	2.56 mL	9	1.16 M	0.58 M
R$_{mba}$	0.68 mL	3.32 mL	17	1.40 M	1.40 M
AzR$_{mba}$	1.00 g	3.99 mL	14	1.23 M	1.23 M
Total					
	Amount	**DMF**	**Equivalents**	**Concentration stock**	**Final Concentration**
BrHAc	5.36 g	37 mL	10	1.04 M	0.52 M
DIC	5.37 mL	31.63 mL	9	1.16 M	0.58 M
R$_{mba}$	5.58 mL	27.42 mL	17	1.40 M	1.40 M
AzR$_{mba}$	1.00 g	3.99 mL	14	1.23 M	1.23 M

Table 23: Incubation conditions during the synthesis of [R_{mba} - R_{mba} - AzR_{mba}]4 (product [14])

Incubation conditions	
Acetylation	5' at room temperature
Monomer addition	90' at 37°C

[R_{mba} − R_{mba} − AzR_{mba}]₄ (product [14] was cleaved and purified according to "3.2.4. Cleavage & Precipitation." The mass yield of the product amounted to 250 mg from a theoretical yield of 546,26 mg assuming a substitution level of 0.8 g/mmol and a molar mass of M(product [14])=2186.1 g/mol. A yield of 45,77 % could be calculated with equation (4). A yield of >80% is expected with the established protocol. The low yield suggests that errors occurred during the synthesis. The sample has to be further investigated by MALDI-TOF-MS.

4.7.1. MALDI-TOF-MS analysis of $[R_{mba}$ - R_{mba} - $AzR_{mba}]_4$ (product [14]) using ATT matrix

To obtain information of the composition of the product harvested from the molecule MALDI-TOF-MS analysis of the $[R_{mba}$ - R_{mba} - $AzR_{mba}]_4$ (product [14]) was conducted. 1 µL of a 1 mg/mL $[R_{mba}$ - R_{mba} - $AzR_{mba}]_4$ (product [14]) in MeOH solution was pipetted on the MALDI-plate. After drying in vacuum, 1 µL of the ATT matrix-solution (3 mg/mL in ACN) was added and dried again. The sample was measured in positive mode. The theoretical mass peak for $[R_{mba}$ - R_{mba} - $AzR_{mba}]_4$ (product [14]) at 2186.1 m/z is absent, as shown in Fig. 53.
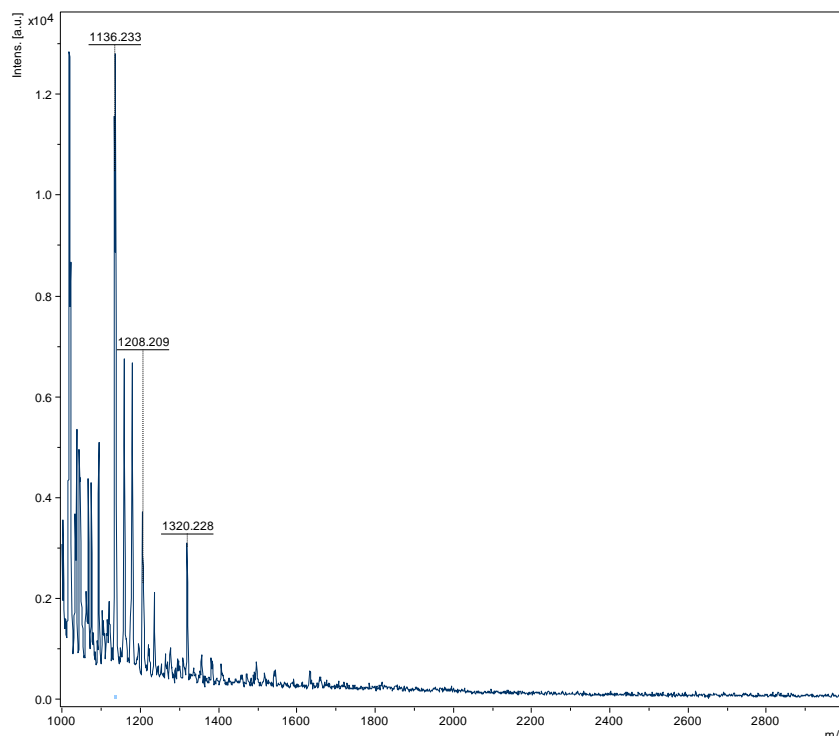

Fig. 53: MALDI-TOF-MS spectrum of [Rmba - Rmba - AzRmba]4 (product [14]) using ATT matrix
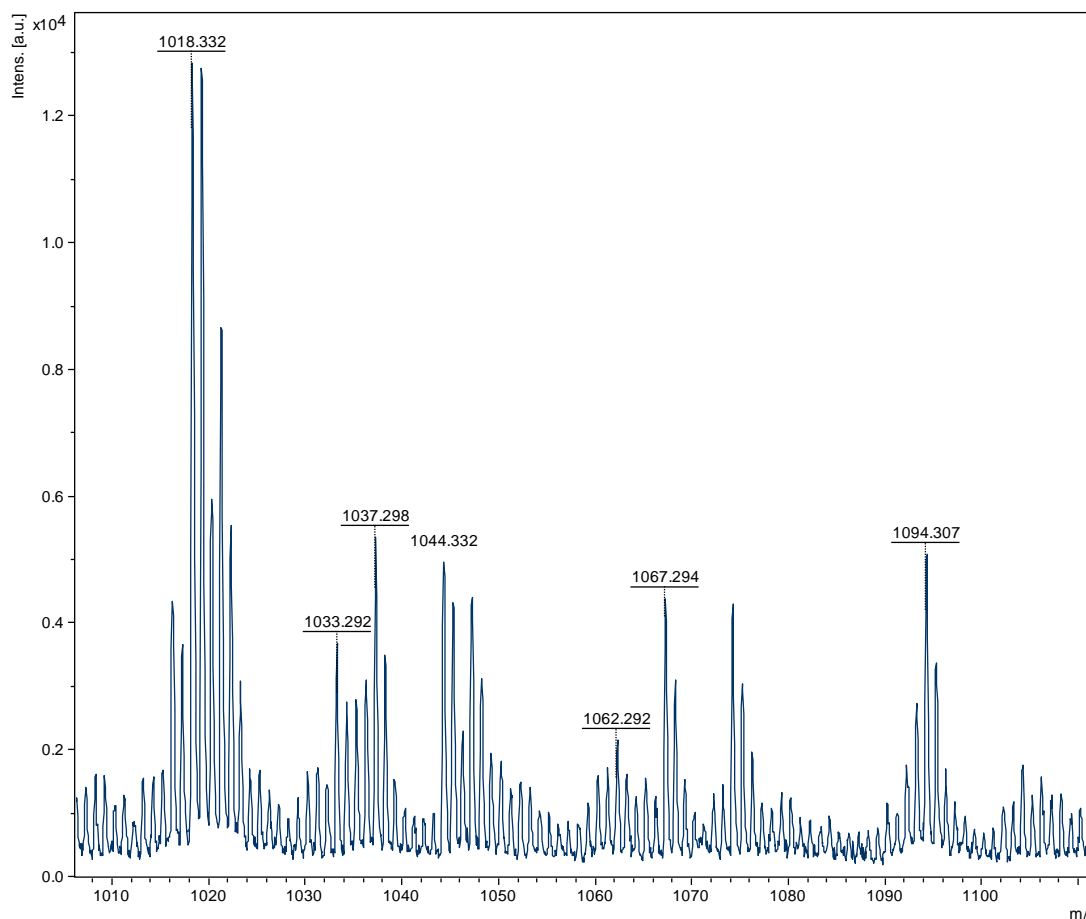
*Fig. 54: MALDI-TOF-MS spectrum of [Rₘba - Rₘba - AzRₘba]₄ (product [14]) using ATT matrix (zoom in on Peak 1080 m/z)*

As seen in Fig. 54 a mass-peak at 1018.5 m/z is present. It can be explained with a peptoid with the sequence $[R_{mba}]_2 - [AzR_{mba}]_3$ [Fig. 55]. This suggests that adding R_{mba} onto an acetylated AzR_{mba} is not possible. Even though, sodium and potassium adducts are missing in the spectrum. Nevertheless the -2 Δ m/z fingerprint is observable. Assuming the molecule in Fig. 55 has formed, the low dry mass harvested from the resin would be explainable, since the molar mass is lower as well.
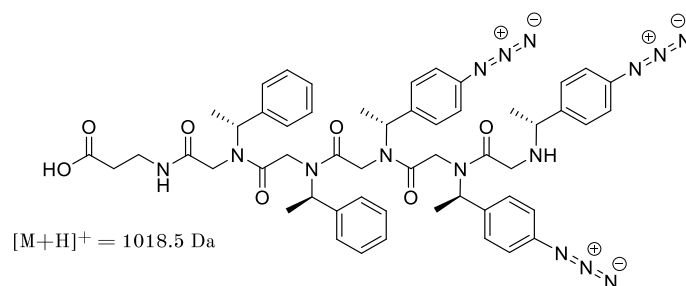

*Fig. 55: Structure formula of [Rₘba]₂ − [AzRₘba]₃*
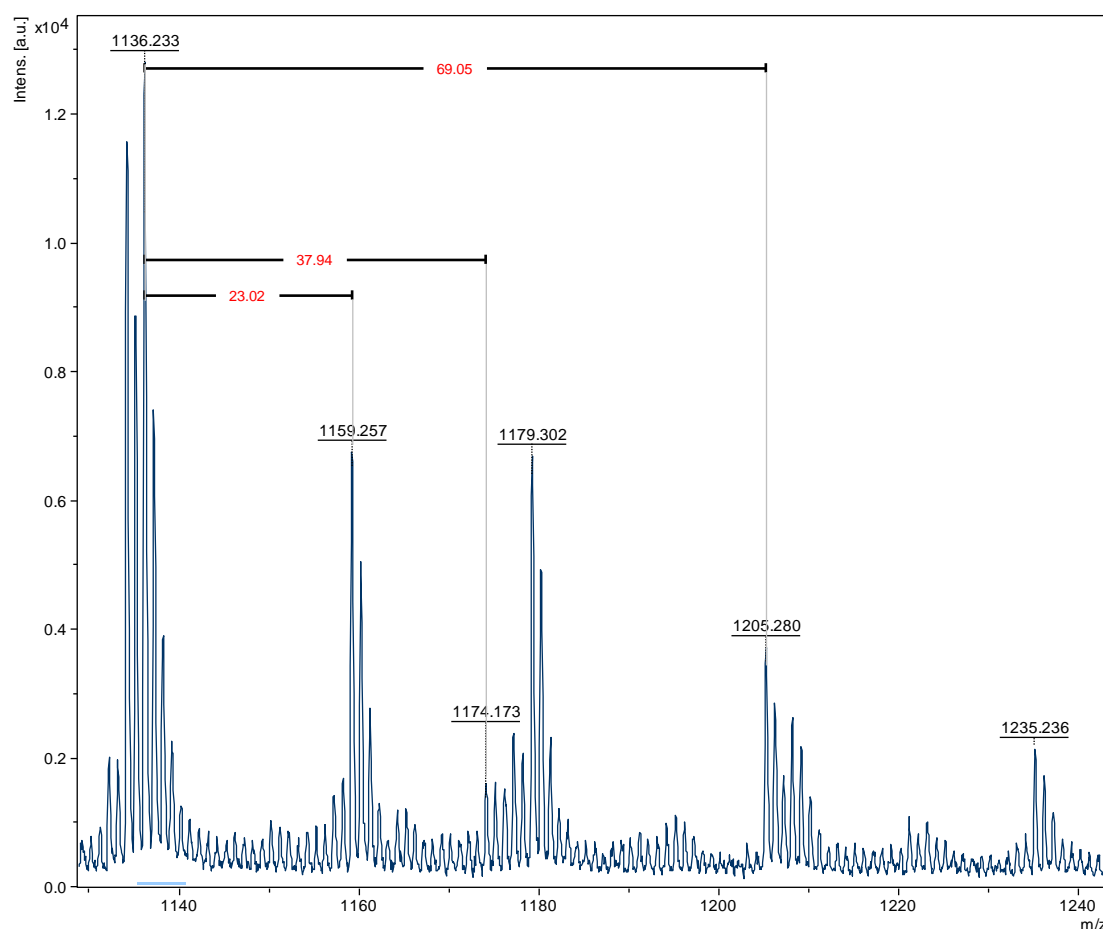
Fig. 56: MALDI-TOF-MS spectrum of [R_{mba} - R_{mba} - AzR_{mba}]$_4$ (product [14]) using ATT matrix (zoom in on peak 1136 m/z)

In Fig. 56 a peak at 1136 m/z is observable, which is accompanied by a sodium and a potassium adduct and the -2 Δ m/z trace peak, respectively. No combination of educts leads to this mass. Synthesizing a homo-polypeptoid with 12 blocks is possible as previous experiments showed. According to the MALDI spectrum the synthesis of the oligopeptoid [R_{mba} - R_{mba} - AzR_{mba}]$_4$ did not work due to the lack of the existence of the mass peak in the spectrum. It is unclear why the synthesis did not work. It was proven in previous experiments that the synthesis of hetero polypeptoids with BrR_{mba} and R_{mba} is possible with relatively high yield. In contrast, a hetero-polypeptoid with the monomer AzR_{mba} and R_{mba} couldn't be synthesized. This experiment shows that reactive groups of the monomers have an influence on the outcome of the synthesis.

4.7.2.   MALDI-TOF-MS analysis of the oligopeptoid (product [14]) using DHB matrix

The oligopeptoid (product [14]) was measured again using DHB matrix, to give a broader view on the sample. 1 μL of a 1 mg/mL [R_{mba} - R_{mba} - AzR_{mba}]$_4$ (product [14])

61

solution was pipetted on the MALDI-plate. After drying in vacuum, 1 μL of the DHB matrix-solution (10 mg/mL in ACN) was added and dried. The sample was measured in positive mode.
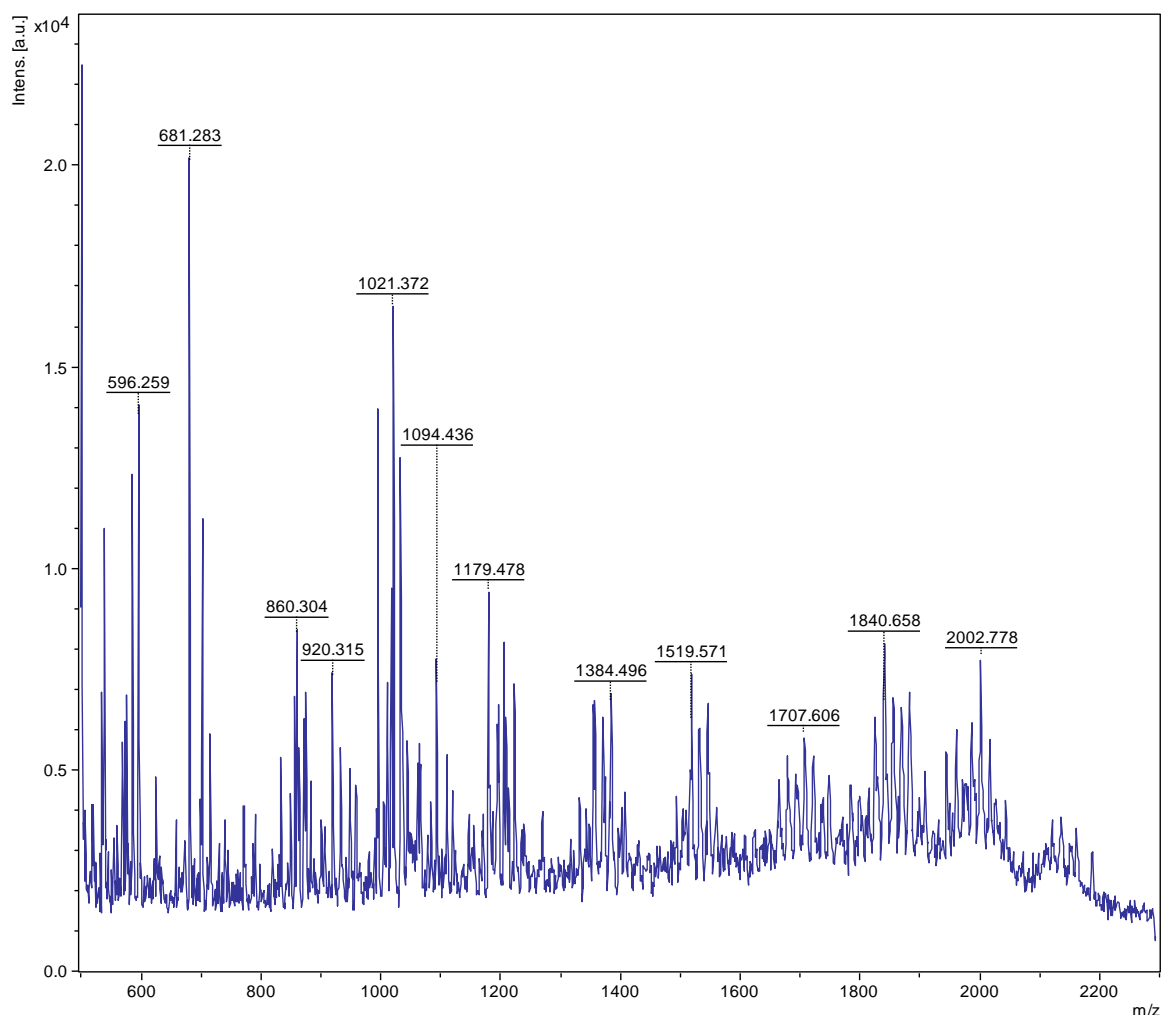

Fig. 57: MALDI-TOF-MS spectrum of [R_{mba} - R_{mba} - AzR_{mba}]$_4$ (product [14]) using DHB matrix

The m/z peak for [R_{mba} - R_{mba} - AzR_{mba}]$_4$ (product [14]) at 2186.1 m/z at is absent as well. The peaks found in this spectrum can't be explained with any combination of the educts. The peak at 1018.33 m/z visible in the spectrum ATT [Fig. 53] from the proposed structure in Fig. 55 is absent. The spectra of the measurements with ATT and DHB, respectively, only show similarities in the peak at 1179.48 m/z. The product is strongly matrix dependent.

4.8. Resin recovery

The advantage of the 2-CTC resin is its reusability. The active groups can be reactivated after cleaving the product from the resin. A trimer of R_{mba} was synthesized on 1000 mg of the same reactivated 2-CTC resin successively.
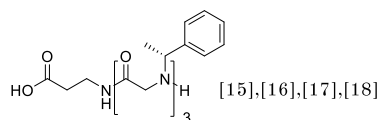

Fig. 58: Structure formula of R_{mba} trimer (product [15] – [18])

Table 24: Amounts used for one synthesis of a trimer of R_{mba} (product [15] – product [18])

One Step					
	Amount	**DMF**	**Equivalents**	**Concentration stock**	**Final concentration**
BrHAc	1.11 mg	5 mL	10	1.6 M	0.4 M
DIC	1.11 mL	3.89 mL	9	1.78 M	0.88 M
R_{mba}	1.73 mL	8.27 mL	17	1.43 M	1.43 M
Total					
	Amount	**DMF**	**Equivalents**	**Concentration stock**	**Final concentration**
BrHAc	3.6 mg	16 mL	10	0.8 M	0.8 M
DIC	3.6 mL	12.43 mL	9	1.76 M	0.88 M
R_{mba}	5.37 mL	25.63 mL	17	1.43 M	1.43 M

After the cleavage and purification according to "3.2.4. Cleavage & Precipitation." The resin was recovered. Using the following amounts and incubation conditions.

Table 25: Amounts used and incubation conditions for the reactivation of the 2-CTC resin

One Step					
	Amount	**DMF**	**Equivalents**	**Incubation temperature**	**Incubation time**
Thionylchloride	130 μL	9.58 mL	1.2	RT	240 min
Pyridine	290 μL		2.4		

The following amounts could be harvested from the resin:

Table 26: mass yield of the products harvested from 1000 mg 2-CTC resin

Sample Name	No. of recovery steps	Mass-yield
product [15]	0	323 mg
product [16]	1	256 mg
product [17]	2	114 mg
product [18]	3	48 mg

A significant loss of yield could be observed when recovering the resin and using it again for synthesis. The recovery step could be insufficient, or the acid-labile resin gets destroyed during the acetylation step. The samples were measured with MALDI-TOF-MS to obtain information about the composition of the product. 1 μL of 1 mg/mL R_{mba} trimers (product [15] - product [17]) in MeOH solution were pipetted on the MALDI-

plate. After drying in vacuum, 1 μL of the ATT matrix-solution (3 mg/mL in ACN) were added and dried again. The samples were measured in positive mode.
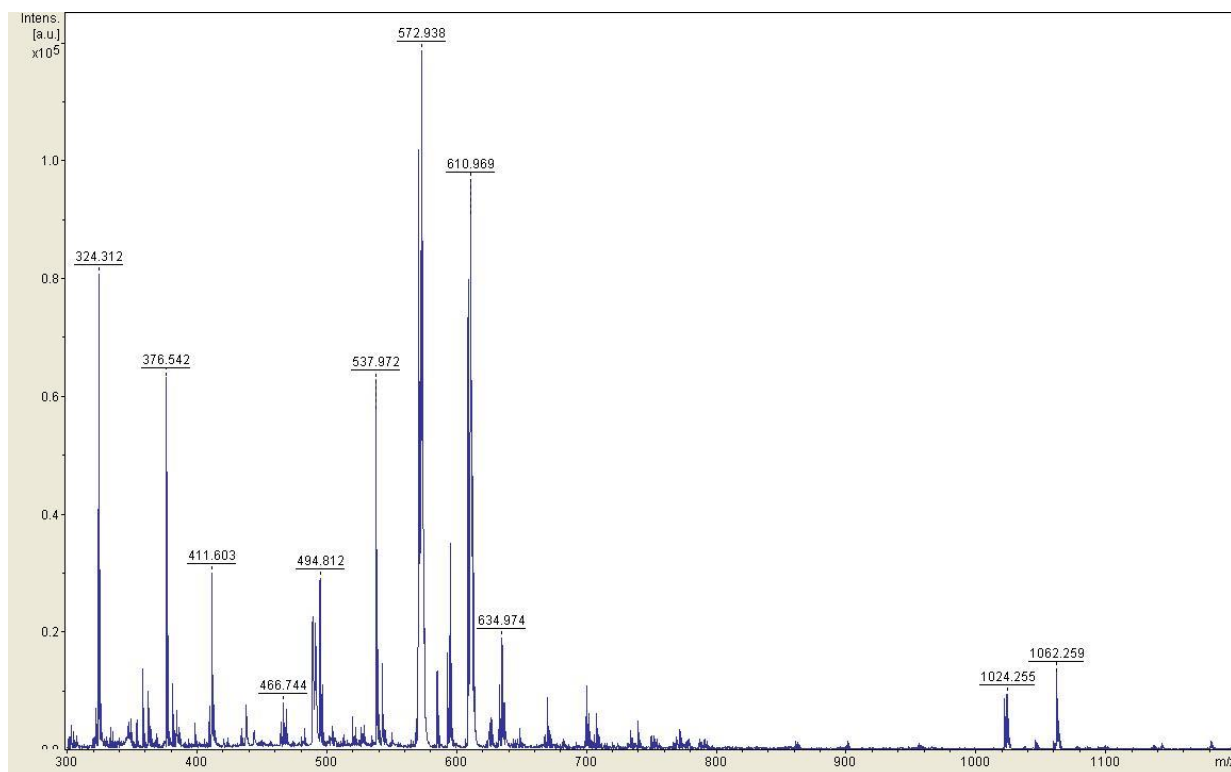

Fig. 59: MALDI-TOF-MS spectrum of R_{mba} trimer (product [15]) on fresh 2-CTC resin with ATT matrix
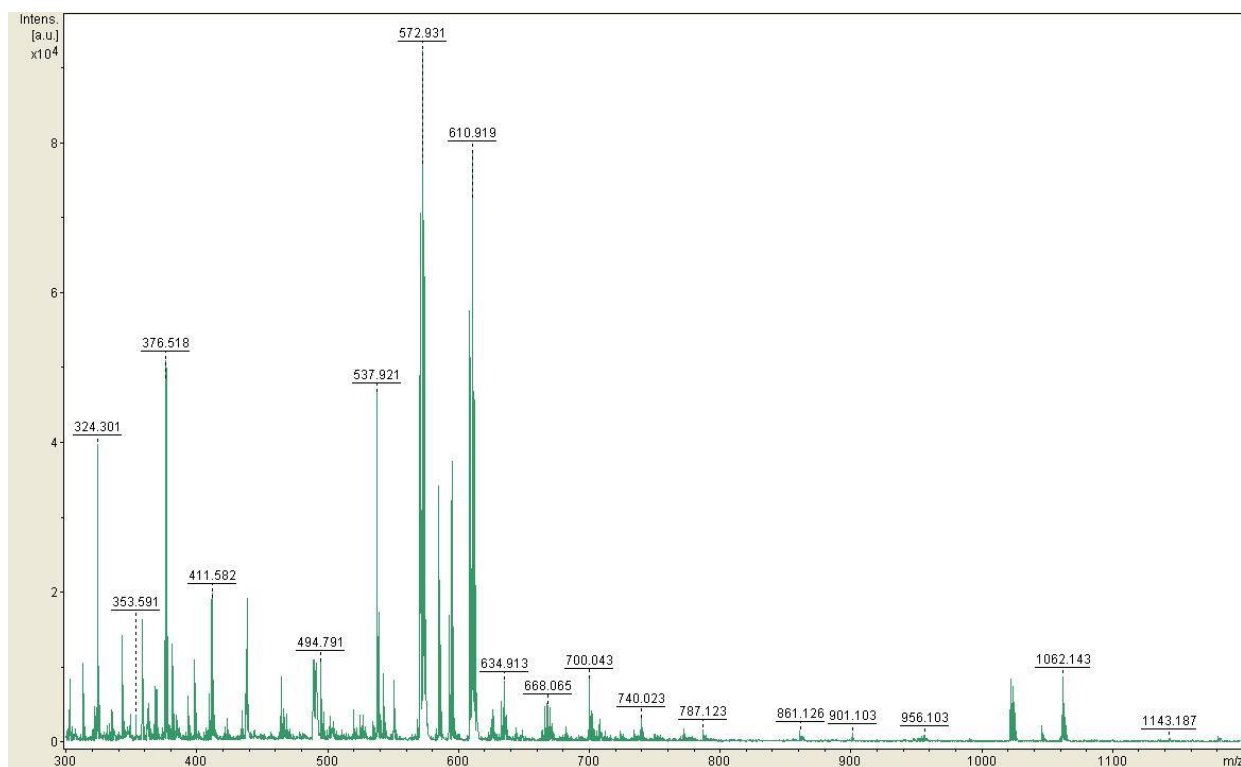

Fig. 60: MALDI-TOF-MS spectrum of R_{mba} trimer (product [16]) on one time reactivated 2-CTC resin with ATT matrix
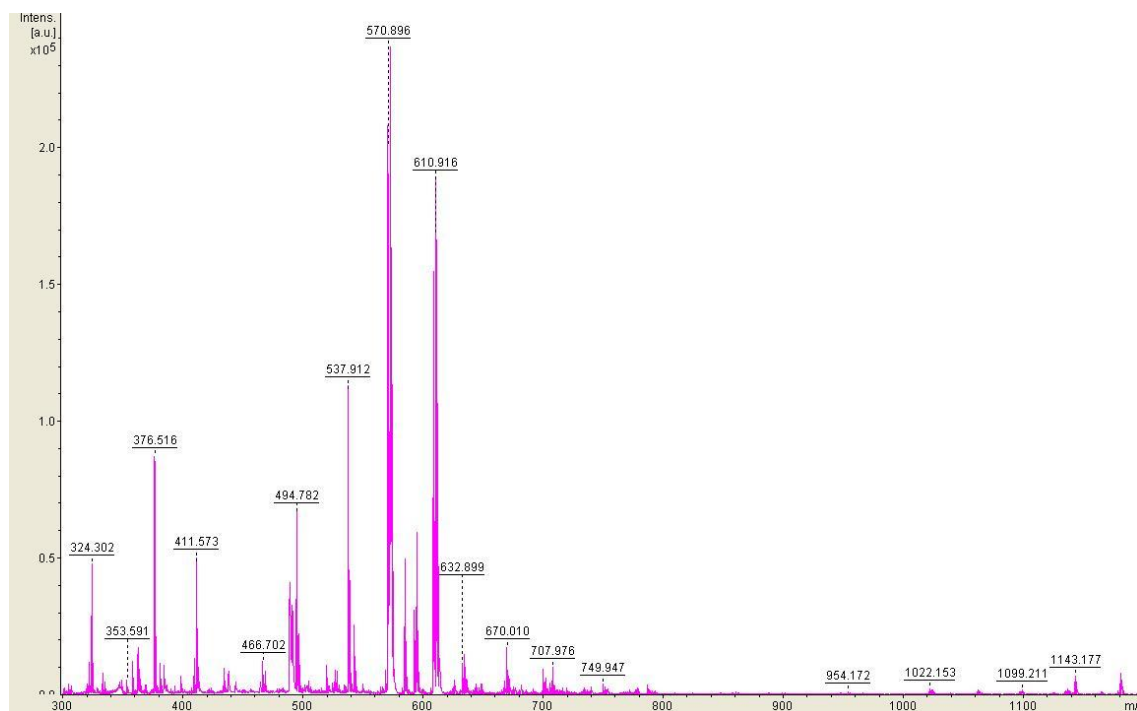
Fig. 61: MALDI-TOF-MS spectrum of R$_{mba}$ trimer (product [17]) on two times reactivated 2-CTC resin with ATT matrix

The product peak visible in Fig. 59, Fig. 60 and Fig. 61 (theoretical m/z = 572.7) is present with an error of ~0.2 Δ m/z. The peak at 324.3 m/z decreases in intensity over the course of the reactivation steps. When dividing the ratio of the intensity of the peaks 324 m/z and the product peak at 572 m/z with the loss in mass-yield, a similar value is obtained. This peak can only derive from the cleavage step since excessive washing of the resin during synthesis is done, making it impossible to have significant amounts of residues from previous steps inside the sample.

Table 27: Comparison of product from recovered resin to yield with respect of the mass peak 324 m/z

| Sample Name	No. of recovery steps	Mass-yield	proportion	Int. Peak 324 m/z	Int. Peak 572 m/z	Ratio 324 : 572 m/z	Ratio between samples
product [15]	0	323 mg		1.3	2.1	62 %	
product [16]	1	256 mg	**79%**	4	9	44 %	**71 %**
product [17]	2	114 mg	**45%**	0.5	2.4	21 %	**47 %**
product [18]	3	48 mg	**42%**	??	??	??	??

To investigate which solute is responsible for the occurrence of the cleavage of the mass 324 m/z, the resin was treated with the solutes used in the reaction at room temperature for 7 days. The supernatants were dried. 1 μL of a 1 mg/mL the product solutions (in MeOH) were pipetted on the MALDI-plate. After drying in vacuum, 1 μL of the ATT

matrix-solution (3 mg/mL in ACN) was added on every sample and dried again. The samples were measured in positive mode. The substances used during synthesis were BrHAc (in DMF), BrHAc + DIC (in DMF), DCM, HFIP (in DCM) and DMF. In Table 28 the chemicals, solvents, concentration and colors of the supernatant and resin are shown.

Table 28: Solution, Solvent, Concentration, color of resin and supernatant and color of supernatant

Chemical	BrHAc	BrHAc + DIC	DCM	HFIP	DMF
Solvent	in DMF	in DMF		in DCM	
concentration	0.8 M	0.8 M BrHAc; 0.8 M DIC		25 % (v/v)	
Color resin & supernatant					
Color supernatant					
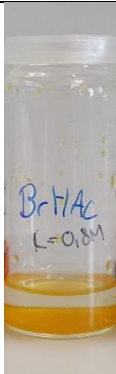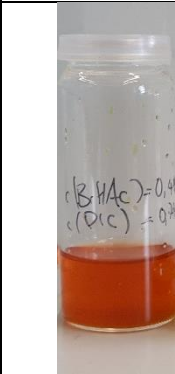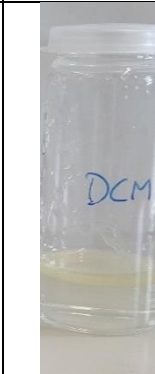
MALDI-TOF-MS spectrums ([Fig. 64], [Fig. 65], [Fig. 66], [Fig. 67], [Fig. 68]) show that the mass 324 m/z is present in every sample even when only treated with DMF, to which the resin is chemically inert. The spectra of the treatments with DMF, DCM and the cleavage solution (DCM + HFIP) resemble each other, meaning no reaction took place. This suggests that the peak distribution observed in the spectra derived from the ATT matrix. The spectra of the BrHAc treatment resembles the spectra with DMF treatment in the 285, 304 and the 323 m/z peak. The peak at 285 m/z can be explained with the matrix building disulfide bonds with itself as in *Fig.* 62.
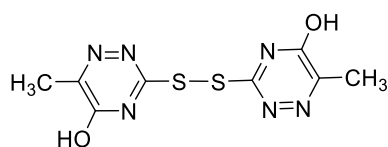
$$[M+H]^+ = 285.02 \ \text{Da}$$

Fig. 62: Chemical structure of disulfide bonding of ATT-matrix

However, the mass error with 0.7 Δ m/z is comparatively high and no adducts with sodium or potassium can be found. The spectrum of the resin treatment with BrHAc + DIC in DMF solution has only one similar peak (410 m/z) with the derived spectrum from the resin treatment with DMF. The intensity of this peak is very low in the spectra of the DMF treatment. Furthermore, a peak at 313.76 m/z is present in the BrHAc + DIC treatment. The H$^+$ adduct of the functional group of 2-CTC [Fig. 63] has a m/z ratio of 313.06. Neither a sodium nor the potassium peak of this mass adduct can be found.
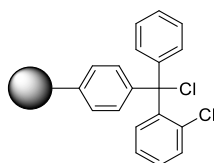
Fig. 63: Chemical Structure of 2-CTC resin
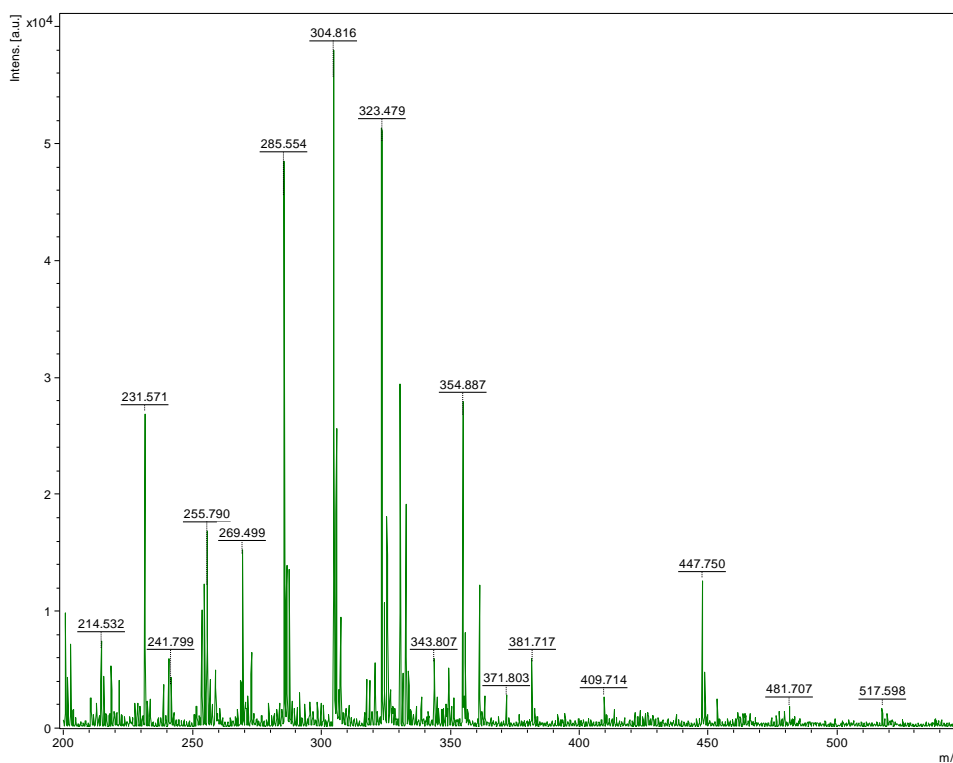
Fig. 64: MALDI-TOF-MS spectrum of supernatant after treatment of 2-CTC resin with BrHAc using ATT-matrix

67
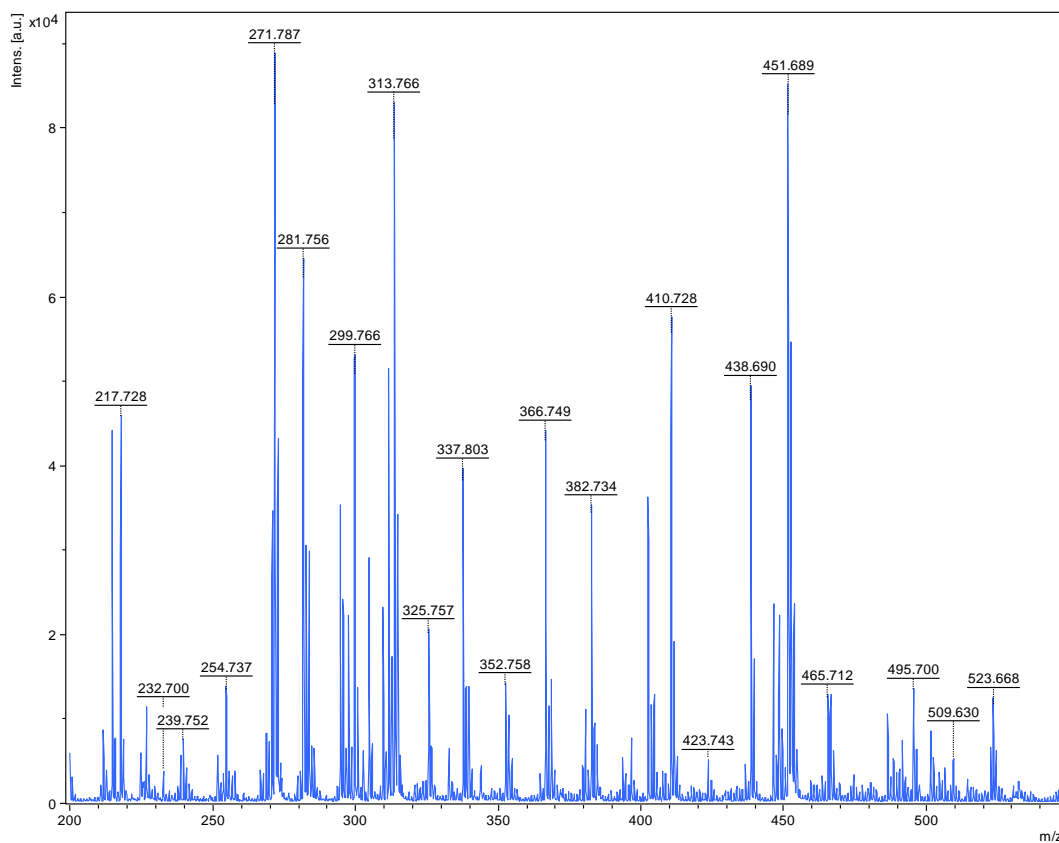
Fig. 65: MALDI-TOF-MS spectrum of supernatant after treatment of 2-CTC resin with BrHAc and DIC using ATT-matrix
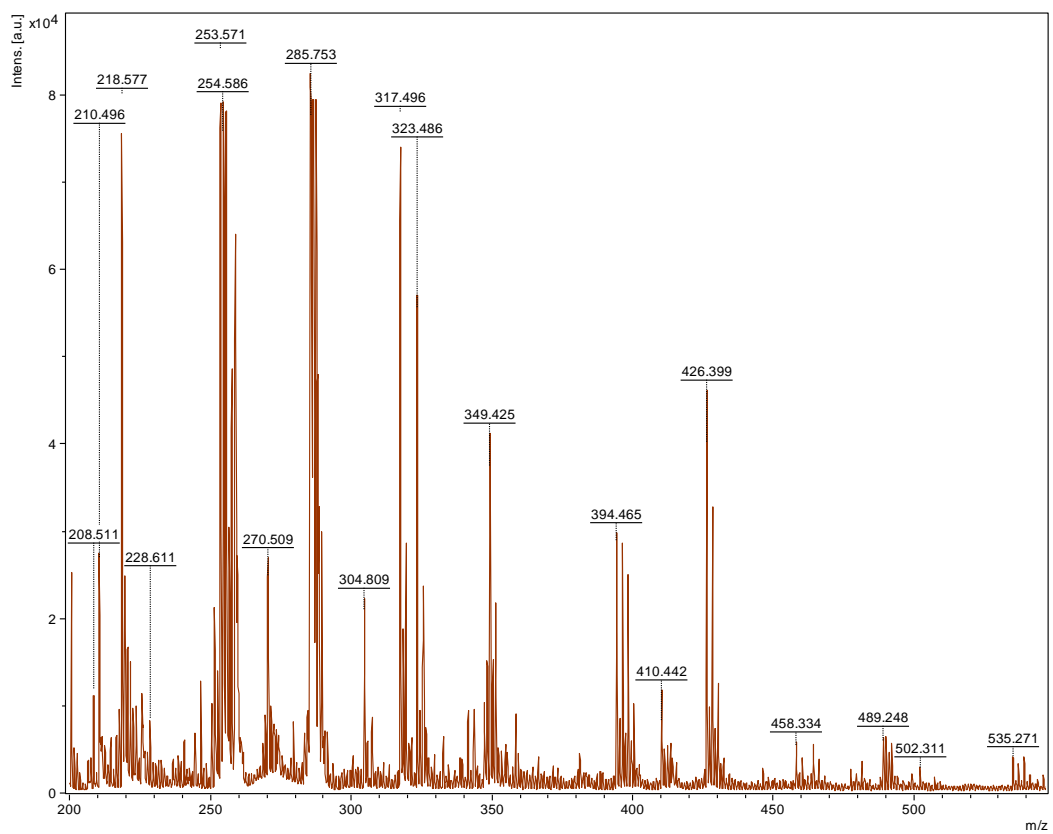
Fig. 66: MALDI-TOF-MS spectrum of supernatant after treatment of 2-CTC resin with DCM using ATT-matrix

68
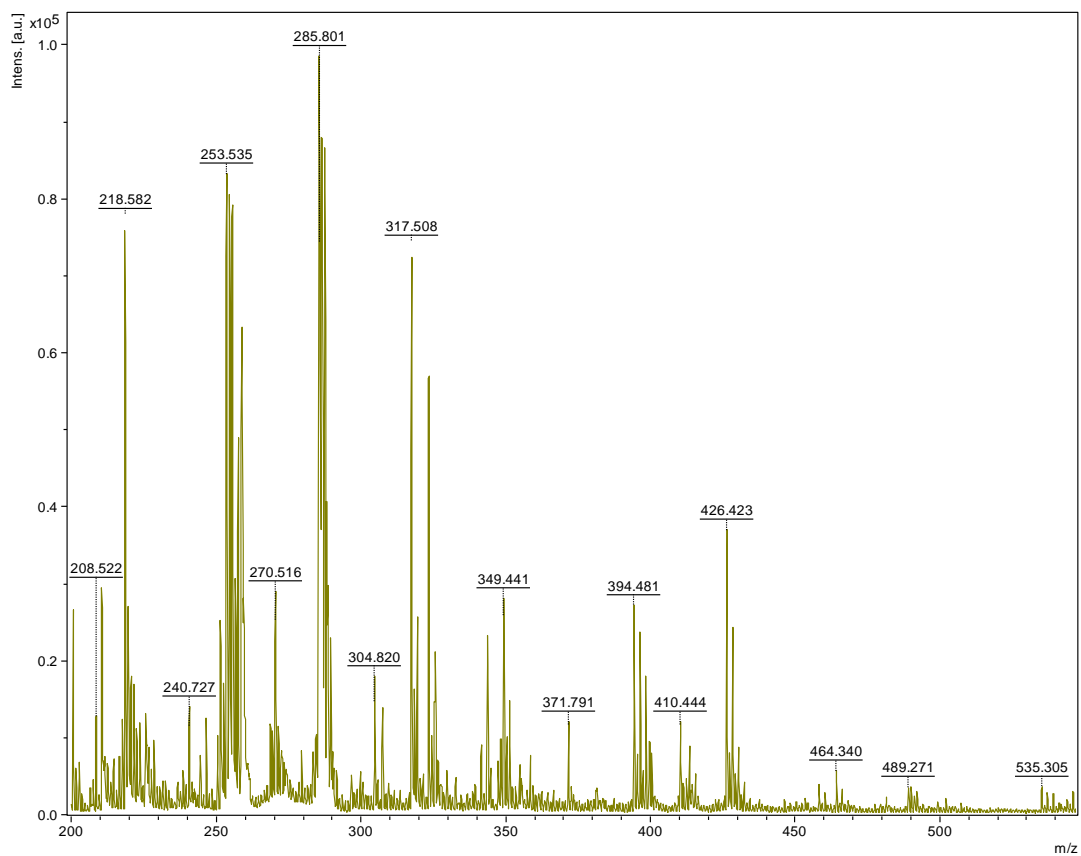
Fig. 67: MALDI-TOF-MS spectrum of supernatant after treatment of 2-CTC resin with 25% HFIP in DCM using ATT-matrix
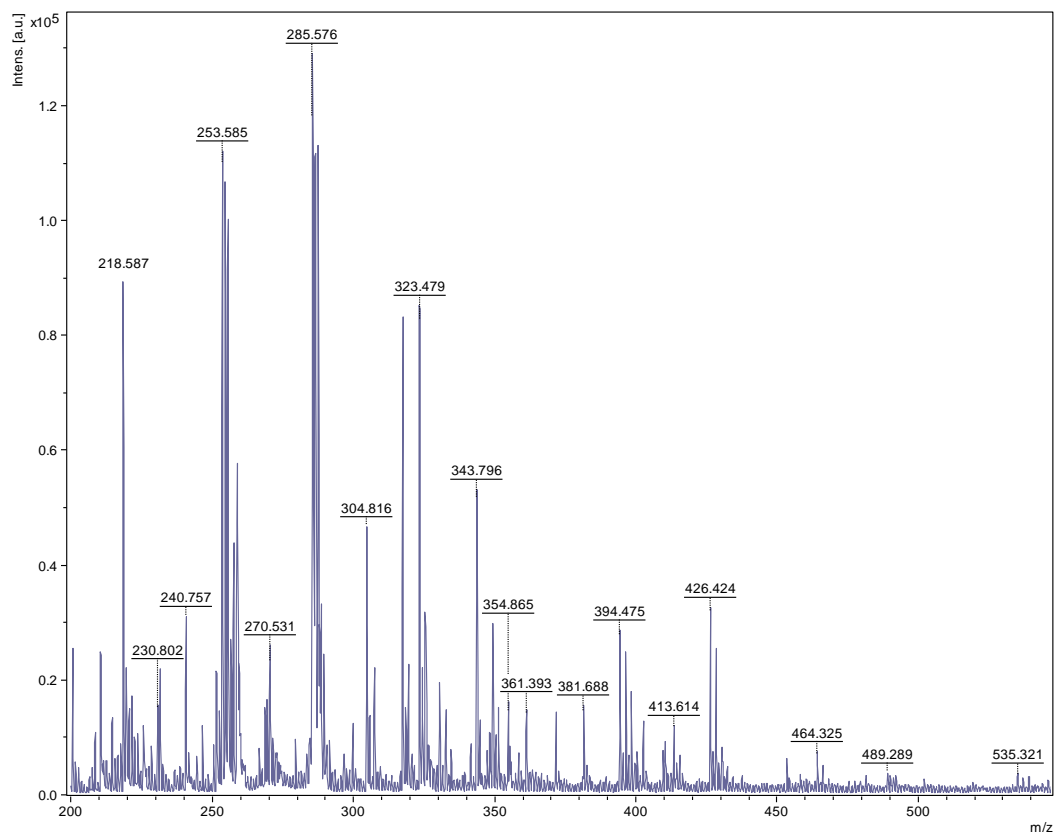

Fig. 68: MALDI-TOF-MS spectrum of supernatant after treatment of 2-CTC resin with DMF using ATT-matrix

As predicted, the treatments with bromoacetic acid show signs of degradation of the resin with the functional group of 2-CTC being present. The MALDI results show that the peak at 325 m/z stands in no correlation with the HFIP cleavage solution since this peak is found in every spectrum. The peak at 325 m/z could derive from the ATT matrix itself. However, no alteration or derivate of the ATT molecule lead to a mass in a close range to 325 m/z. In conclusion the data shows that the foundation of reusing the resin is the usage of low acetylation conditions. Otherwise the resin degrades over time and low yields are the consequence.

5. Conclusion

5.1. Optimization of the synthesis protocol

We showed that with optimized parameters, an oligo-peptoid up to a chain length of 12 can be synthesized with a mass yield of ~60 %. Trimers were synthesized with a yield of 63.7%. At the end of the work yields up to 84% were achieved. By reducing the concentration of BrHAc & incubation time during the acetylation step the yield was increased by 69,06%. We improved the protocol with regard to reaction volume, equivalence numbers of the ingredients and the concentration of the synthesis parameters from 40% overall yield to 84%. In table 22, the conditions resulting in the highest yields in the course of the practical work for oligo-peptoid synthesis are listed.

Table 29: Optimal synthesis conditions for oligo peptoids

	Amount	DMF	Equivalents	Stock concentration	End concentration	Incubation time	Incubation temp.
BrHAc	0.69 g	6 mL	10	0.84 M	0.42 M	5 Minutes	RT
DIC	0.70 mL	5.3 mL	9	0.92 M	0.46 M		
R_{mba}	1.08 mL	5.38 mL	17	1.49 M	1.49 M	90 Minutes	37 °C
BrR_{mba}	1.3 mL	5.7 mL	18	1.14 M	1.14 M	90 Minutes	37 °C

We observed that capturing the monomer solution after the incubation step and reusing it for the next monomer addition step did not affect the overall yield.

MALDI-TOF-MS data proved that a hetero oligo-peptoid could be synthesized with alternating R_{mba} and BrR_{mba} with a chain-length of at least 4. The mass yield amounted to 84%. Further elongation must be tested.

MALDI analysis of a hetero oligo-peptoid with alternating R_{mba} and AzR_{mba} showed no result. According to this data it is not possible to add R_{mba} on an acetylated AzR_{mba}.

The low yield of synthesis on recycled resin could be traced back to resin destruction due to extensive acid treatment.

5.2. MALDI-TOF-MS analysis

With positive mode MALDI-TOF-MS analysis the composition of the product can be determined. However, the results are strongly matrix dependent. DHB showed the least

amount of fragmentation during measurement. Applying LIFT on a pentamer of R_{mba} the fragments could be investigated and assigned. The spectrum using the ACH matrix showed negligible fragmentation, similar to the results using the DHB matrix. In contrast, the intensity of the mass peaks of shorter chain lengths of the peptoid is increased. Using the ATT matrix, many trace peaks and shorter chain length peaks of the product could be observed. The following fragments were observed in the spectrum when using the ATT matrix:

1) -2 Δ m/z
2) -30 Δ m/z
3) -35 Δ m/z
4) -76 Δ m/z

Only the loss in mass of 76 Δ m/z can be explained with the fragmentation of the terminal aromatic ring as [Fig. 27] depicts. No explanation could be found for the -2, -30 and -35 Δ m/z.

The MALDI-TOF-MS analysis showed the possibility of the synthesis of oligo-peptoids ranging from 3 to 12 blocks of R_{mba}. According to the data, it is necessary to purify the product from shorter chain lengths due to the fact that the equilibrium of the monomer addition is not 100% on the side of incorporation. Further, we observed that the alternating incorporation of AzR_{mba} and R_{mba} was not possible in contrast to BrR_{mba} and R_{mba}. Comparing the three matrixes ATT, ACH and DHB, the latter showed neglectable signs of fragmentation and trace peaks. With ATT matrix, strong fragmentation of the product occurred, despite the low incubation time. The analysis of the sample was strongly matrix dependent.

5.3. Purification

Due to yields below 100% during every monomer addition step, shorter chain lengths of the product are present in the sample after synthesis as shown by the MALDI data. A convenient method to purify the product is reversed phase HPLC. We showed that with increasing chain-length the hydrophobicity hence the retention time increases. We determined the retention times of a monomer to a pentamer. With preparative C18-RP-HPLC purification of the product is possible.

5.4. Final remark

The solid phase submonomer synthesis proved to be an excellent tool to create hetero polypeptoids with a controlled sequence. The goal of improving the overall yield of the synthesis was reached by adjusting the synthesis parameters especially during the acetylation step. The achievement of synthesizing a hetero polypeptoid with an alternating hydrophobic and hydrophilic monomer, sets the foundation for the research of amphiphilic polypeptoid helices with longer chain lengths and its effect on bacterial cell membranes. With MALDI-TOF-MS it is possible to analyze the product and its artefacts and HPLC allows to separate the different chain lengths to yield a purified product. In the future further experiments upon modifications of the bromine within the oligopeptoid must be conducted to enhance hydrophilic properties. A big challenge in the future will be the design of the correct sequence and polarity differences of the polypeptoid to specifically target prokaryotic cell membranes.

6. References

1. Alexander Fleming, *On the Antibacterial Action of Cultures of a Penicillium, with Special Reference to their Use in the Isolation of B. influenzæ,* Br J Exp Pathol **1929 Jun**; 10(3): 26-236

2. Mariya Lobanovska, Giulia Pilla, *Penicillin's Discovery and Antibiotic Resistance: Lessons for the Future? Y*ale J Biol Med. **2017 Mar**; 90 (1): 135–145.

3. David van Duin, David Paterson, *Multidrug Resistant Bacteria in the Community: Trends and Lessons Learned.* Infect Dis Clin North Am. **2016** Jun; 30(2): 377–390. DOI: 10.1016/j.idc.2016.02.004

4. Jun Chen, Su-Min Guan, Wei Sun and Han Fu, *Melittin, the Major Pain-Producing Substance of Bee Venom*, Xi'an, China, Neurosci Bull. **2016 Jun**; 32(3): 265–272. DOI: 10.1007/s12264-016-0024-y

5. Tim Skern, *Exploring Protein Structure: Principles and Practise* **2018** Jul Box 3.2. (33)

6. Geert van den Bogaart, Jeanette Vela´squez Guzma´n, Jacek T. Mika, and Bert Poolman, *On the Mechanism of Pore Formation by Melittin*, Groningen, J Biol Chem. **2008 Dec**; 283(49): 33854–33857. Doi: 10.1074/jbc.M805171200

7. *Fox, Marye Anne; Whitesell, James K. (1995).* Organische Chemie: Grundlagen, Mechanismen, Bioorganische Anwendungen. Springer. *ISBN 978-3-86025-249-9. **2003***

8. David Whitford, *Proteins Structure and Function* **2013** Apr

9. Helen Tran, Sarah L. Gael, Michael D. Connolly, Ronald N. Zuckermann, *Solid-phase Submonomer Synthesis of Peptoid Polymers and their Self Assembly into Highly-Ordered Nanosheets,* J. J Vis Exp. **2011 Nov** 2;(57): e3373. DOI: 10.3791/3373.

10. Emily C. Davidson, Adrianne M. Rosales, Anastasia L. Patterson, Boris Russ, Beihang Yu, Ronald N. Zuckermann and Rachel A. Segalman, *Impact of Helical Chain Shape in Sequence-Defined Polymers on Polypeptoid Block Copolymer Self-Assembly*, California, United States, Macromolecules **2018**, 51, 5, 2089-2098. DOI: 10.1021/acs.macromol.8b00055

11. Tracy J. Sanborn, Cindy W. Wu, Ronald N. Zuckermann, Annelise E. Barron, *Extreme stability of helices formed by water-soluble poly-N-substituted glycines (polypeptoids) with α-chiral side chains*, California, United States, Biopolymers **2002 Jan**, 63(1):12-20. DOI: 10.1002/bip.1058

12. Miller, S. M., Simon, R. J., Ng, S., Zuckermann, R. N., Kerr, J. M., & Moos, W. H. (1994). *Proteolytic studies of homologous peptide and N-substituted glycine peptoid oligomers.* Bioorganic & Medicinal Chemistry Letters, 4(22), 2657–2662. doi:10.1016/s0960-894x(01)80691-0

13. Tan, N. C.; Yu, P.; Kwon, Y. U.; Kodadek, T. *High-Throughput Evaluation of Relative Cell Permeability between Peptoids and Peptides*. B Bioorg Med Chem. 2008 Jun 1; 16(11): 5853–5861. DOI: 10.1016/j.bmc.2008.04.074

14. Gangloff N, Fetsch C, Luxenhofer R. *Polypeptoids by living ring-opening polymerization of N-substituted N-carboxyanhydrides from solid supports.* Macromol Rapid Commun. **2013 Jun** 25;34(12):997-1001. DOI: 10.1002/marc.201300269

15. Adrianne M. Rosales, Hannah K. Murnen, Steven R. Kline, Ronald N. Zuckermann and Rachel A. Segalman, *Determination of the persistence length of helical and non-helical polypeptoids in solution*, Berkeley, CA, Soft Matter, *2012*; 8, 3673-3680; DOI: 10.1039/C2SM07092H

16. Fayna Garcá-Martin, Núria Bayó-Puxan,Luis J. Cruz, James C. Bohling and Fernando Albericio, *Chlorotrityl Chloride (CTC) Resin as a Reusable Carboxyl Protecting Group,* Barcelona, Spain, QCS, **2007 March;** No. 10, 1027 – 1035 DOI: 10.1002/qsar.200720015

17. Bollhagen, R., Schmiedberger, M., Barlos, K., & Grell, E. *A new reagent for the cleavage of fully protected peptides synthesised on 2-chlorotrityl chloride resin.* Journal of the Chemical Society, Chemical Communications, **1994** 2559-2560. DOI: doi.org/10.1039/C39940002559

18. Matthaia Ieronymaki, Maria Eleni Androutsou, Anna Pantelia, Irene Friligou,1,2 Molly Crisp, Kirsty High, Kirsty Penkman, Dimitrios Gatos, Theodore Tselios, *Use of the 2-Chlorotrityl Chloride Resin for Microwave-Assisted Solid Phase Peptide Synthesis,* Biopolymers **2015**; 104(5): 506-14. DOI: 10.1002/bip.22710

19. Jacob Andersen, Ulf Madsen, Fredrik Björkling, Xifu Liang, *Rapid Synthesis of Aryl Azides from Aryl Halides under Mild Conditions*, Denmark, Synlett 2005(14): 2209-2213. DOI: 10.1055/s-2005-872248

20. Marlene Egelseder, Erik Reimhult, Ronald Zirbs, *Synthesis of polypeptoid architectures as nanoparticles shells*, Vienna, Austria, **2018,** 15

21. Papac DI, Wong A, Jones AJS. *Analysis of acidic oligosaccharides and glycopeptides by matrix assisted laser desorption/ionization time-of-flight mass spectrometry.* Anal. Chem. ***1996***, (68)18: 3215-3223.

22. Paul Held Ph. D., Senior Scientist, Applications Dept., BioTek Instruments, Inc. *Peptide and Amino Acid Quantification Using UV Fluorescence in Synergy HT Multi-Mode Microplate Reader*

23. Kuchel, Philip W., & Gregory B. Ralston. *Theory and Problems of Biochemistry.* New York: Schaum's Outline/McGraw-Hill, **1988**: 7.

7. Appendix

Table 30: Molar weights of all products that were targeted by synthesis steps of a polypeptoid containing the monomer R_{mba}

	Molar weight [g/mol]	[M+H]$^+$ [g/mol]	[M+Na]$^+$ [g/mol]	[M+K]$^+$ [g/mol]
R_{mba} x1	**250,3**	**251,30**	**273,3**	**289,3**
R_{mba} x1 (Acetlyated)	371,2	372,25	394,25	410,25
R_{mba} x2	**411,5**	**412,50**	**434,5**	**450,5**
R_{mba} x2 (Acetlyated)	532,4	533,45	555,448	571,448
R_{mba} x3	**572,7**	**573,70**	**595,7**	**611,7**
R_{mba} x3 (Acetlyated)	693,6	694,65	716,648	732,648
R_{mba} x4	**733,9**	**734,90**	**756,9**	**772,9**
R_{mba} x4 (Acetlyated)	854,8	855,85	877,848	893,848
R_{mba} x5	**895,1**	**896,10**	**918,1**	**934,1**
R_{mba} x5 (Acetlyated)	1016,0	1017,05	1039,048	1055,048
R_{mba} x6	**1056,3**	**1057,30**	**1079,3**	**1095,3**
R_{mba} x6 (Acetlyated)	1177,2	1178,25	1200,248	1216,248
R_{mba} x7	**1217,5**	**1218,50**	**1240,5**	**1256,5**
R_{mba} x7 (Acetlyated)	1338,4	1339,45	1361,448	1377,448
R_{mba} x8	**1378,7**	**1379,70**	**1401,7**	**1417,7**
R_{mba} x8 (Acetlyated)	1499,6	1500,65	1522,648	1538,648
R_{mba} x9	**1539,9**	**1540,90**	**1562,9**	**1578,9**
R_{mba} x9 (Acetlyated)	1660,8	1661,85	1683,848	1699,848
R_{mba} x10	**1701,1**	**1702,10**	**1724,1**	**1740,1**
R_{mba} x10 (Acetlyated)	1822,0	1823,05	1845,048	1861,048
R_{mba} x11	**1862,3**	**1863,30**	**1885,3**	**1901,3**
R_{mba} x11 (Acetlyated)	1983,2	1984,25	2006,248	2022,248
R_{mba} x12	**2023,5**	**2024,50**	**2046,5**	**2062,5**